Development and Characterization of Carbon Nanotubes (CNTs) and Silicon Carbide (SiC) Reinforced Al-based Nanocomposites

BY

KACHALLA ABDULLAHI GUJBA

A Thesis Presented to the

DEANSHIP OF GRADUATE STUDIES

KING FAHD UNIVERSITY OF PETROLEUM & MINERALS

DHAHRAN, SAUDI ARABIA

In Partial Fulfillment of the
Requirements for the Degree of

MASTER OF SCIENCE

In

MECHANICAL ENGINEERING

MARCH 2012

KING FAHD UNIVERSITY OF PETROLEUM & MINERALS

DHAHRAN 31261, SAUDI ARABIA

DEANSHIP OF GRADUATE STUDIES

This thesis, written by **Kachalla Abdullahi Gujba** under the direction of his thesis advisor and approved by his thesis committee, has been presented to and accepted by the Dean of Graduate Studies, in partial fulfillment of the requirements for the degree of **MASTER OF SCIENCE IN MECHANICAL ENGINEERING**.

Thesis Committee

Dr. Nasser Al-Aqeeli (Advisor)

Dr. Tahar Laoui (Member)

Dr. Saheb Nouari (Member)

Dr. Amro M. Al- Qutub
(Department Chairman)

Dr. Salam A. Zummo
(Dean of Graduate Studies)

16/4/12

Date

DEDICATION

Dedicated

to my beloved parents, brothers, sisters and well-wishers.

ACKNOWLEDGMENT

All praise and thanks are due to my Lord, ALLAH SUBHAN WA TAALA, for giving me the health, knowledge and patience to complete this work. I acknowledge the financial support given by King Fahd University of Petroleum and Minerals-KFUPM/ Center of Excellence in Nanotechnology-CENT during my graduate studies.

My sincerest gratitude goes to my advisor Dr Nasser Al-Aqeeli and co-advisors/committee members Dr. Saheb Nouari and Dr Tahar Laoui who guided me with their dedicated attention, expertise, and knowledge throughout this research. I am also grateful to Dr Abbas Hakeem for his constructive guidance and support. Thanks are also due to the department's Chairman Dr. Amro Qutub and staff members of the department who helped me directly or indirectly.

Special thanks are due to my colleagues in the Mechanical Engineering Department, for their aid and support. Thanks are also due to all my friends for their support and encouragement.

My heartfelt gratitude is given to my beloved father, mother, uncles, aunts, brothers and sisters who always support me with their love, patience, encouragement and constant prayers. I would like to thank my grandmother and all members of my family in Nigeria for their emotional and moral support throughout my study.

TABLE OF CONTENT

LIST OF FIGURES

LIST OF TABLES

LIST OF ABBREVIATIONS/ NOMENCLATURE

Al	Aluminum
Al-Si	Aluminum – Silicon
Ar	Argon
BPR	Ball-to-Powder Ratio
CIP	Cold Isostatic Pressing
CS	Conventional Sintering
ECAE	Equal channel angular extrusion
EDS	Energy Dispersive Spectroscopy
HIP	Hot Isostatic Pressing
Hv	Vickers' Hardness
hr	hour
KJ	Kilo Joules
KN	Kilo Newton
MA	Mechanical Alloying
Mg	Magnesium
Mins	Minutes
MM	Mechanical Milling
MMCs	Metal Matrix Composites
MPa	Mega Pascal
MWCNTs	Multiwall Carbon Nanotubes
nm	Nanometer
PM	Powder Metallurgy
PCA	Process Control Agent
PSA	Particle Size Analyzer
SEM	Scanning Electron Microscope

SiC	Silicon Carbide
SPS	Spark Plasma Sintering
SWCNTs	Single wall Carbon Nanotubes
TEM	Transmission Electron Microscope
TPa	Tera Pascal
UTS	Ultimate Tensile Strength
wt.%	Weight Percent
XRD	X-Ray Diffraction

THESIS ABSTRACT (ENGLISH)

Name **Kachalla Abdullahi Gujba**

Title **Development and Characterization of Carbon Nanotubes (CNTs) And Silicon Carbide (SiC) Reinforced Al-based Nanocomposites.**

Department **Mechanical Engineering**

Date **12-03-2012**

Composites are engineered materials developed from constituent materials; matrix and reinforcements, to attain synergistic behavior at the micro and macroscopic level which are different from the individual materials. The high specific strength, low weight, excellent chemical resistance and fatigue endurance makes these composites superior than other materials despite anisotropic behaviors. Metal matrix composites (MMCs) have excellent physical and mechanical properties and alumium (Al) alloy composites have gained considerable interest and are used in multiple industries including: aerospace, structural and automotive. The aim of this research work is to develop an advanced Al-based nanocomposites reinforced with Carbon nanotubes (CNTs) and silicon carbide particulates (SiCp) nanophases using mechanical alloying and advanced consolidation procedure (Non-conventional) i.e. Spark Plasma Sintering (SPS) using two types of aluminum alloys (Al-7Si-0.3mg and Al-12Si-0.3Mg). Different concentrations of SiC_p and CNTs were added and ball milled for different milling periods under controlled atmosphere to study the effect of milling time and the distribution of the second phases. Characterization techniques were used to investigate the morphology of the as received monolithic and milled powder using Field Emission Scanning Electron Microscope (FESEM), Energy Dispersive Spectroscopy (EDS), X-Ray Mapping, X-Ray Diffraction (XRD) and Particle Size Analyses (PSA). The results revealed that the addition of high concentrations of SiC_p and CNTs in both alloys aided in refining the structure of the resulting powder further as the reinforcement particles acted like a grinding agent. Good distribution of reinforcing particles was observed from SEM and no compositional fluctuations were observed from the EDS. Some degree of agglomerations was observed despite the ethyl alcohol sonication effect of the CNTs before ball milling. From the XRD; continuous reduction in crystallite size and increase in internal strains were observed as milling progressed with increase in wt.% reinforcement due to the severe plastic deformation. Al/SiC and Al/CNTs were successfully consolidated by the SPS at sintering temperatures of 400, 450 and 500°C with SiC at 5, 12 and 20wt% and 0.5wt%CNT milled for 20hrs and 3 hrs respectively. It was obtained that sintering temperature of 500°C was the most suitable as the densification achieved for SiC reinforced sample was above 98% and 100% for unreinforced sample. The hardness increased with increasing SiC content from 0, 5 to 12 wt% i.e 68, 82, 85 respectively. At 20%wt of SiC a slight decrease in the hardness was observed i.e. 70 which might be attributed to high wt.% SiC, a similar trend was observed for the other alloy studied. For CNT reinforced samples, the hardness and densification increased significantly and 100% densification was obtained at 500ºC, a hardness value from 68 to 82 was achieved from 0 to 0.5wt%CNT with a similar trend to the other alloy of interest. Conclusively, sintering of both alloys at 500ºC and above is the most suitable, the use of SiCp and CNTs as reinforcements improved the hardness, 12wt% SiC showed better hardness values than 20wt% SiC at all three temperatures and the Al alloy containing higher Si in its alloying elements showed better hardness values using the same reinforcement and sintering parameters.

MASTER OF SCIENCE DEGREE

KING FAHD UNIVERSITY OF PETROLEUM AND MINERALS, SAUDI ARABIA.

THESIS ABSTRACT (ARABIC)

الاسم: عبدالله كشالا كاجبا

الموضوع: تحسين تصنيعي وتشخيص للأنابيب الكربونية و كربيد السليكا كمعززات متناهية الصغر للألمونيوم.

القسم: الهندسة الميكانيكية.

التاريخ: 12-03-2012

تعد المواد المركبة أحد أهم المواد الهندسية والتي تصنع إما على طريقة المصفوفات أو بالتعزيز من أجل الحصول على مواصفات فائقة الفوة على المستوي المتناهي في الصغر لم بكن بالإمكان الحصول عليه بإتخدام كل مادة منفصلة على حدا.

الصلابة وخفة الوزن والمقاومة للتفاعلات الكيميائية بالإضافة إلى قوة التحمل للقوى المتغيرة حتى على المدى البعيد يجعل من هذه المواد محل جذب نظرا للمواصفات فائقة التميز مقارنة بغيرها من المواد. تمتلك مصفوفات المعادن المركبة خصائص ميكانيكية وفيزيائية متميزة وكذلك معدن الألمونيوم المركب أصبح محل إهتمام بالغ خصوصا في القطاع الصناعي مثل صاعة مركبات الفضاء ووسائل النقل المختلفة.

الهدف من هذا المشروع البحثي هو تحسين تصنيع مركب معدن الألمونيوم من خلال إضافة Carbon nanotubes (CNTs) and silicon carbide particulates (SiCp) بأحجام متناهية الصغر بإستخدام التعدين الميكانيكي وطرق متقدمة تساهم في دمج وتماسك المركبات مثل : Spark Plasma Sintering (SPS) لمعدنين من الألمونيوم هما (Al-7Si-0.3Mg and Al-12Si-0.3Mg) بنسب مختلفة تم إضافة كلا من SiC_p and CNTs إلى آلة الطحن لفترات زمنية مختلفة تحت محيط متحكم فيه كل ذلك من أجل دراسة أثر كلا من الفترة الزمنية في عملية الطحن وتوزيع المادة المضافة.تم إختبار وتحليل النتائج بإستخدام تقنيات دقيقة ومتقدمة من اجل دراستها والوصول إلى نتائج علمية دقيقة وصحيحة وهذه الأجهزة مثل:

Field Emission Scanning Electron Microscope (FESEM), Energy Dispersive Spectroscopy(EDS), X-Ray Mapping, X-Ray Diffraction(XRD) and Particle Size Analyses(PSA)

النتائج أظهرت أن إضافة كلا من SiC_p and CNTs بكميات كبيرة في كلا المعدنين يساعد في تحسين بناء البودرة الناتجة وكأن هذه المواد المعززة تعمل كعامل صنفرة داخل المادة الأساسية. كذلك التوزيع الجيد لجسيمات المادة المعززة شوهدت من خلال المجهر الإلكتروني وليس هناك تباين تركيبي من خلال ما شوهد بواسطة). هناك درجة من التجمع بغض النظر عن أثر مادة إثيل الكحول المضافة خلال طحن CNTs ومن خلال الأشعة السينية تم مشاهدة النقصان في الحجم البلوري وزيادة في الإنفعال الداخلي كلما زادت النسبة الوزنية للمواد المعززة بسبب التشوه البلاستيكي الكبير.

نسبة Al/SiC و Al/CNTs تم دمجهم بنجاح من خلال SPS عند درجات حرارة مختلفة (400, 450, 500) ل SiC بنسب وزنية مختلفة (5,12,20,0.5) و الكربون نانو تيوب طحنت لمدة 20 ساعة و3 ساعات على التوالي. تم الوصول إلى أن التسخين إلى 500 درجة مئوية هي أفضل درجة حرارة نظرا لإمكانية تكثيف المادة إلى 98% للمواد المعززة SiCو100% للموتد غير المعززة . عند إضافة 20% من ال SiC هناك إنخفاض قليل في الصلابة.

كذلك الصلابة والكثافة في زيادة عند إضافة CNTs فتم الحصول على 100% من الكثافة عند 500 درجة مئوية. فقيمة الصلابة زادت من 68 إلى 82 عند إضافة الكاربون بنسبة مابين 0 إلى 0.5 نسبة وزنية.

ختاما التسخين لكلا المعدنين عند درجة 500 مئوية وأعلى يعتبر هو الخيار الأنسب والأفضل كذلك إستخدام SiCp و CNTs كمواد معززة تحسن بشكل ملحوظ صلابة المادة كذلك بالنسبة للمعادن الألمونيوم التي تحتوي على نسبة أعلى من Si تظهر صلابة أعلى عند نفس المعزز وعوامل التسخين.

درجة الماجستير

جامعة الملك فهد للبترول والمعادن، المملكة العربية السعودية

Chapter 1

INTRODUCTION

1.1 General Introduction

Aluminum alloys are widely used for production of high strength and light weight components. The high strength, high durability, better formability, weldability, resistance to oxidation and corrosion make these materials versatile and could have many applications, such as; in the area of structural materials, aerospace, automotive and petrochemical industries, etc [1-2]. However, as number of aluminum alloys are heat treatable and among them Al-Si-Mg alloys (such as; work hardening, grain size hardening and precipitations hardening) forming precipitate such as; Mg_2Si, Al_3Mg_2 are most suitable candidates to achieve above properties as well as applications and shows exceptional properties [3-7]. These properties led to the application of Al-Si alloys in the automotive industry, especially for cylinder blocks, cylinder heads, pistons, and valve lifters [8, 9]. An addition of Mg to Al-Si alloys enhances their properties of the system and such a system is designated as A356 aluminum alloy family[10].

Metal-matrix composites (MMCs) have continued to receive considerable attention from researchers due to their excellent physical and mechanical properties [11-13]. Much interest on aluminum composites is significantly growing due to their enhanced material

properties, such as; wear resistance, creep resistance, specific strength and specific modulus compared to pure metal matrix.

Conventional powder metallurgy (PM) is a widely used technique for synthesizing metal matrix composites with uniform distribution of reinforcing agent consequently improving the structural and mechanical properties [14]. This technique involves the mixing of the powders and the reinforcing particles after which compacting and sintering are performed. Reports in literature on PM on aluminum matrix composites have shown superb mechanical properties when compared with those from other alternative manufacturing processes and monolithic aluminum systems.

1.2 Carbon Nanotubes (CNTs) Reinforcement

To enhance the strength of Al-based alloys and their properties, CNTs [15-17] have received considerable attention over the past 20 years as they possess remarkable properties [18]. High CNTs conductivity and high length to radius (diameter) ratio (aspect ratio) makes them exceptional in composites, these properties attracted interest in low weight composites for structural applications. From mechanical property point of view, SWNTs have the highest Young's modulus [19,20] if normalized to their diameters though literature suggested there are limits to the use of SWNTs which gives room for the use of MWNTs which have stronger bonds between host material and the CNTs.

A study by Esawi et al. [21] showed the effect of the morphology and diameter of CNTs in processing Al/CNT composites, they concluded that the smaller the diameter bent and entangled the more difficult to disperse as compared with larger straight and stiff CNTs [22]. Generally, CNTs reveal poor dispersion into the metal matrix which is attributable to the strong agglomeration of CNTs in the powder resulting in weak interface between

CNTs and metal matrix. Studies show promising dispersion of the CNTs in the matrix using ball milling at different milling conditions [23-28] and surface treatment of the CNTs [29-32]. Other studies have shown good dispersion of the CNTs by adopting nonconventional way of synthesizing composites either molecular-level mixing or modify the surface of the CNTs or introducing liquid state process and synthesis CNTs on the matrix materials [33-35].

1.3 Silicon Carbide (SiC) Reinforcement

To further augment the strength of Al-based alloys and improve their thermal stability, it was commonly practiced to reinforce Al-6061 [36], Al-7075 [37] and pure Al [38,39] with SiC particulates. Besides its density being slightly higher than that of aluminum, SiC is primarily used because of its low cost and wide range of available grades. It promotes an increase in the Young's modulus and tensile strength of the composite materials. Another interesting advantage of SiC reinforcement is the possible increase in the wear resistance. The improved mechanical properties of particulate SiC_p/Al are thought to be a result of a transfer of shear load at the matrix/reinforcement interface. Nevertheless, while the yield and ultimate strength of the matrix improve with increasing the concentration of micro-ceramic particles, the ductility of the composites significantly deteriorates at higher concentrations. The use of nano-sized ceramic particles to strengthen the matrix might help in retaining some ductility.

Yong Yang et al.,[40] reported that yield strength of Al-alloy fabricated by an ultrasonic-assisted casting method was improved more than 50% with the addition of 2.0 wt % of nano-sized SiC particles. This result is significantly better than what aluminum alloy with

the same percentage of micro-particle reinforcement can offer, with little change in the elongation. In another study by K. D. Woo et al., [41], SiC reinforced Al–7Si–0.4Mg composite powders were synthesized by ball milling, giving an increase in the sintering rate of the composite powder due to increased diffusion rate. The microstructure of the sintered specimen obtained using the milled composite powder was finer than that of the sintered specimen obtained from simple mixing. A further study by A. Simchi et al., [42] investigated the effect of SiC particles on the laser sintering of Al-7Si-0.3Mg alloy. It was shown that densification rate follows first-order kinetics and the rate constant was found to increase with low SiC fractions.

1.4 Sintering

In sintering, densification and average grain size increases as a result of the thermal energy applied to the powder compact. Generally, between 0.1 and 100 μm is the range of size of powder used for sintering. Sinterability and the sintered microstructure of a powder compact are dependent on two important variables i.e. material and process variables, and the sintering equations are governed by these variables [43]. Sintering atmosphere affects sintering mechanism in addition to impurity/reinforcing content and composition. High gas transportation rates and pore structure, grain structure, impurity content, kinetics and surface structures are major changes caused by sintering atmosphere. Therefore, determination of atmospheres that are most effective for control of impurity is necessary. However, consolidation of powders through isostatic technique is a feasible technique for composite materials which are intricate or costly to fabricate by other methods [44].

Non-conventional sintering techniques such as spark plasma (SPS) and microwave (μW) are novel techniques and the basic difference between them and conventional ones is the heating mechanism, In conventional sintering, heat is generated and transferred to the material through conduction, convection and radiation while in non-conventional sintering, either the material themselves absorb microwave energy and then transform them into heat within their bodies or employs an electrical discharge combined with resistance heating and pressure for sintering (SPS) [45]. Spark plasma sintering has numerous advantages over the conventional ones like very rapid heating and cooling rates, shortened sintering times, better microstructure, higher densification as well as improved mechanical properties. These non-conventional methods have made it possible for the processing of advanced materials.

Conventional sintering techniques (cold isostatic pressing (CIPing) or hot isostatic pressing (HIPing)) are done at room or high temperatures while using liquid and gas in CIPing and HIPing respectively as the medium of transmission of pressure [46]. In CIPing, the powder is converted from a loose aggregate into a partially-dense compact that has enough green strength to permit cautious handling and transfer to the following process operation. HIPing is required when full or considerable consolidation of composite powders are needed and CIPing may be involved at a preliminary processing stage, since HIPing commence with pressurization of the HIP unit while it is still comparatively cold. However, HIPing is characterized as a low heating sintering technique [47]. Chunfeng Deng et al. [48], Jin-zhi Liao et al. [49] and A.M.K. Esawi et al. [50] used the conventional sintering technique to consolidate Al-CNT matrix and reported significant increase in tensile strength and stiffness as well as good dispersion of

the CNTs after ball milling. J. K. Rana et al. [51], Hansang Kwon et al. [52] and Kawasaki, Akira et al. [53] investigated the effects of non-conventional sintering techniques on Al-CNT system and reported increase in hardness, stiffness as well as finer microstructure.

1.5 Aims/Objectives

- To develop an optimum processing route to produce both CNTs and SiC reinforced Al-7Si-0.3Mg and Al-12Si-0.3Mg nanocomposite powders by mechanical alloying/milling technique in which these strengthening agents are uniformly distributed within the composite powder.

- To consolidate/sinter both monolithic alloys and the developed nanocomposite powders using non-conventional sintering method i.e. spark plasma to produce bulk samples- allowing a comparative analyses.

- To gain an understanding of the mechanism/kinetics of these processes by carrying out a thorough characterization of the monolithic alloys and the developed nanocomposites using FESEM/EDS, Mapping, XRD, PSA, Optical microscopy and densimeter.

- To comparatively study the Al-based alloys (Al-7Si-0.3Mg and Al-12Si-0.3Mg) to determine the effect of silicon percentage (the 5% difference) in both alloys with the incorporation of two different reinforcements (Silicon carbide (SiC) and Carbon nanotubes (CNTs).

Chapter 2

LITERATURE REVIEW

2.1 Background and History of Mechanical Alloying

Mechanical alloying is a technique used for the production of homogeneous materials starting from blended elemental powder. The technique was first developed in 1966 by John Benjamin and his colleagues at the Paul D. Merica Research Laboratory of the International Nickel Company (INCO). This technique was a result of nickel based super alloys for gas turbine application. The idea was to combine the high temperature strength of the dispersed oxides with the intermediate temperature strength of the gamma prime precipitates, while taking into account the required corrosion and oxidation resistance [54-56].

This process by Benjamin was referred to as “milling/mixing”. Mr. Ewan C. Mac Queen, a patent attorney for INCO coined the term *mechanical alloying* to describe the process in the first patent application, and this term has now come to stay in the literature.

Mechanical alloying is normally a dry, high-energy ball milling technique used to produce commercially and scientifically important materials [56]. However, it was not widely acknowledged that the milling process was a true alloying process until in the early 1980s, Koch et al. published a landmark paper which, for the first time,

demonstrated that mechanical milling can facilitate true alloying, and the outcome of the alloying can be a metastable material such as an amorphous alloy. In the study, they milled a mixture of Ni and Nb powders, and found that over time the powder became an amorphous Ni–Nb alloy powder. This means that true alloying does occur during milling. This discovery raised the understanding of mechanical milling as a materials processing to a new level. Since publishing Koch et al.'s work, the term, ''Mechanical Alloying'' has been widely accepted and used.

Also in the paper published by C. Suryanarayana [56], he summarized the important milestones in the development of mechanical alloying which is tabulated below

Table 2.1 Shows the Important Milestones in the Development of MA Over the Years [56].

1966	ODS nickel-base alloys development
1981	Amorphization of intermetallics
1982	Disordering of ordered compounds
1983	Amorphization of blended elemental powder mixtures
1987/88	Synthesis of nanocrystalline phases
1989	Occurrence of displacement reactions
1989	Synthesis of quasicrystalline phase

MA is a process targeted for industry from inception and its gaining popularity now after the understanding of the basics and mechanisms involved which resulted in several reviews and conference proceedings. C. Suryanarayana, reviewed the present status of

MA and milling from 1970-1994 in his publication ‘bibliography of MA and milling’. The figure below shows the growth of publication in the field of MA.

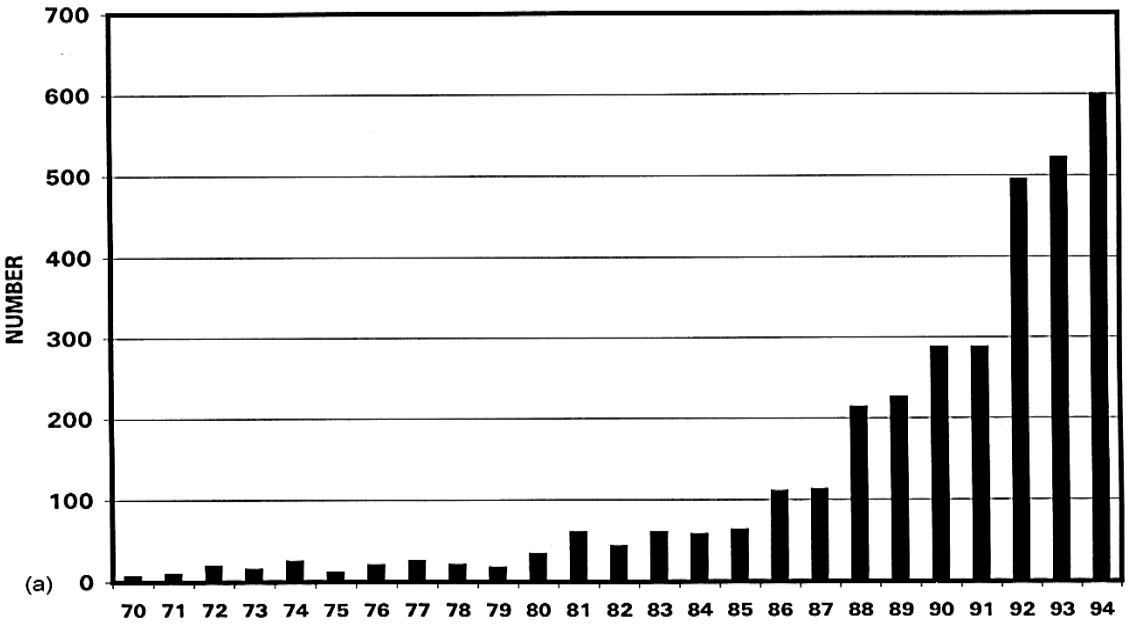

Figure 2.1 Growth of publications in the area of MA during 1970-1994 [56].

2.2 Definitions

2.2.1 Mechanical Alloying (MA)

MA has been defined by C. Suryanarayana [56] as is a solid-state powder processing technique involving repeated welding, fracturing, and rewelding of powder particles in a high-energy ball mill and involves material transfer to obtain a homogeneous alloy. Another definition by S. Scudino et al., [57] is that MA as ball milling of powders with different compositions (mixture of elemental powders as well as of intermetallic compounds), in which material transfer and solid state inter diffusion reaction occurs.

Another by D.L. Zhang [58] defined MA as a process which is customarily used in powder metallurgy and mineral processing used for blending powders or crushing rocks. Again by A Calka and A.P Radlinski [59] defined MA as a complex process of deformation, fragmentation, cold welding, and micro-diffusion, occurring within a thin layer of powder between the two colliding surfaces during impact.

2.2.2 Mechanical Milling (MM)

Suryanarayana, [56] defined MM as milling of uniform (often stoichiometric) composition powders, such as pure metals, intermetallics, or prealloyed powders, where material transfer is not required for homogenization. S. Scudino et al., [57] said MM is ball milling of single composition powders, such as single-phase compounds, where material transfer is not required and further showed that MM has advantage over MA in that since the powders are already alloyed and only a reduction in particle size and/or phase transformations need to be induced mechanically, the time required for processing is generally shorter than that for MA.

2.2.3 Mechanical Disordering (MD)

MD is the destruction of long-range order in intermetallics to produce either a disordered intermetallic or an amorphous phase.

2.2.4 Reaction Milling

It is an MA process accompanied by solid state reaction; in this process the powder is milled without the aid of any process control agent (see later for its function during milling) to produce fine dispersions of oxides and carbides in aluminum.

2.2.5 Cryomilling

It is a process in which the milling operation is carried out at cryogenic (very low) temperatures and/or milling of materials is done in cryogenic media such as liquid nitrogen.

2.2.6 Mechanically Activated Annealing

Is a process that combines short mechanical alloying duration with a low-temperature isothermal annealing. The combination of these two steps has been found to be effective in producing different refractory materials such as silicides.

2.2.7 Double Mechanical Milling (DMA)

In this milling process 2 stages are involved. First, the powder sizes are refined and distributed uniformly as an intimate mixture which is heat treated at elevated temperatures during which intermetallic phases are formed. The second stage involves the refining of the heat treated powder through milling again while reducing the grain size of the matrix.

2.2.8 Mechanically Activated Self-Propagating High-Temperature Synthesis (MASHS)

Is a process based on a combination of mechanical alloying (MA) and self-propagating high-temperature synthesis (SHS).In this process the powder mixture is mechanically alloyed to produce a nanocrystalline structure and then the SHS reaction is initiated by pressing the powder into a pellet and igniting it in a furnace.

2.3 Preparation for Mechanical Alloying

2.3.1 Mechanical Alloying Process

The MA/MM process is a solid state powder process where the powder particles are subjected to high energetic impact by the ball in a vial. As the powder in the vial are impacted continuously by the balls, cold welding between particles and fracturing of the particles takes place during the process. The entire process includes blending of the powder mixture prior to the ball milling, vacuuming and/or filling with protective gasses to prevent oxidation and contamination and the ball milling process itself [60]. The powder milled is then consolidated into a shape and heat treated to obtain the desired microstructure and properties taking into account the raw materials, the mill and the process variables.

2.3.2 Raw Materials

The raw materials used for MA are widely available commercially pure powders that have particle sizes in the range of 1-200 μm. The powder particle size should be smaller than the grinding ball size though it is not critical. This is because the powder particle size decreases exponentially with time and reaches a small value of a few microns only after a few minutes of milling. Pure metals, master alloys, prealloyed powders, and refractory compounds are the board class of the powder. Dispersion strengthened materials usually contain additions of carbides, nitrides, and oxides. Oxides are the most common and these alloys are known as oxide-dispersion strengthened (ODS) materials [56]. Alloy formation has been satisfactorily made by mixing fully brittle materials in

recent years. Also ductile-ductile, ductile-brittle, and brittle-brittle powder mixtures are milled to produce novel alloys. Mixtures of solid powder particles and liquids have also been milled in recent times.

2.3.3 Types of Mills

There are different types of milling equipment used to produce mechanically alloyed powders. These equipment differ in their capacity, efficiency of milling and additional arrangements for cooling, heating, etc. Below are the different types of mills used for MA

- SPEX shaker mills,
- Planetary ball mills, example; the work done by A. Calka and A.P Radhinski [59] where they used planar type mill to illustrate the concept of milling device.
- Attritor mills
- Commercial mills

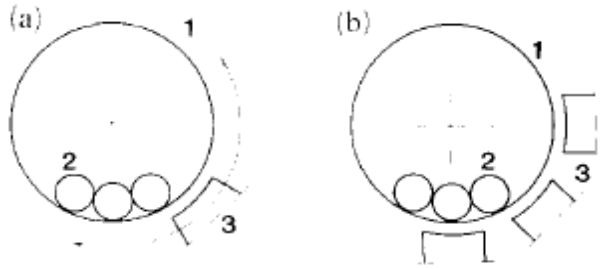

Figure 2.2 Schematic diagram of ball-milling device with controlled ball movement 1: rotating 2: balls 3: magnets [59].

2.3.4 Process Variables

MA is a process that involves a lot of processes and has complexities and for optimization of the desired product and/or microstructure, certain process parameters

must be put into consideration. The final powder is affected by the following important parameters.

- **Type of mill***;* the mills are of different types and differ in their capabilities, speed and ability to control the operation. A suitable mill can be selected depending on the powder type, quantity and final constitution required. Example the SPEX shaker mills are used for alloy screening purposes, planetary ball mills or the attritors are used to produce large quantities of the milled powder etc.
- **Milling container***;* the milling container material is important due to the impact of the grinding medium on the walls of the container. Suryanarayana, [56] stated if the material of the grinding vessel is different from that of the powder, then the powder may be contaminated with the grinding vessel material. On the other hand, if the two materials are the same, then the chemistry may be altered unless proper precautions are taken to compensate for the additional amount of the element incorporated into the powder. Milling containers are also grinding vessels, vial, jar or bowl.
- **Milling speed**; the faster the speed the higher the energy input into the powder and there are certain limitations to the maximum speed that can be employed. An example is in a conventional ball mill, increasing the speed of rotation will increase the ball speed and at above the critical speed, the balls are pinned to the walls of the vial and do not fall down for impact force to be applied, therefore, a maximum speed just below the critical speed is recommended for the balls to fall down. Again, at maximum speed temperature of the vial will be high which can be advantageous when homogenization is desired through diffusion at the same it

can be disadvantageous in the sense that high temperature can contaminate the powder.

- **Milling time***;* this is the most important parameter which is selected to achieve steady state between the fracturing and cold welding of powder. The time also depends on other factors such as ball-to-powder ratio, temperature, type of mill etc. if the powder is milled for time longer than required then contamination increases and unwanted phases form.
- **Type, size, and size distribution of the grinding medium***;* Hardened steel, tool steel, hardened chromium steel, tempered steel, stainless steel, WC-Co, and bearing steel are the most common types of materials used for the grinding medium. The density of the grinding medium should be high enough so that the balls create enough impact force on the powder. The size of the grinding medium also has an impact on the milling efficiency. A large size (and high density) of the grinding medium is useful since the larger weight of the balls will transfer more impact energy to the powder particles and reports have shown the dependence of final powder constitution on size of grinding medium.
- **Ball-to-powder weight ratio (BPR)***;* this is sometimes called charge ratio (CR) and it is an important parameter especially on the time of milling, the higher the ratio the shorter the milling time. We have different values of ratio as low as 1:1 to as high as 250:1 but 10:1 is the most commonly used ratio. Example of the effect of BPR on milling time is the formation of an amorphous phase was achieved in a Ti-33at%Al powder mixture milled in a SPEX mill in 7 h at a BPR of 10:1, in 2 h at a BPR of 50:1 and in 1 h at a BPR of 100:1 [56].

- **Extent of filling the vial;** alloying of powder particles involves impact forces exerted on them, it is necessary that there is enough space for the balls and the powder particles to move around freely in the milling container. Therefore extent of filling of powder and balls is an important factor in alloying of powder particles. Care has to be taken not to overfill the vial; generally about 50% of the vial space is left empty
- **Milling atmosphere**; milling atmosphere has a major effect on contamination of the powder. Therefore, the powders are milled in containers that have been either evacuated or filled with an inert gas such as argon or helium. Nitrogen is only used when nitrides are desired because it has been found that Nitrogen reacts with metal powders and cannot be used to prevent contamination during milling. High-purity argon is the most common ambient to prevent oxidation and/or contamination of the powder.
- **Process control agent (PCA);** A process control agent (PCA) (also referred to as lubricant or surfactant) is added to the powder mixture during milling to reduce the effect of cold welding. For powder particles to be truly alloyed, a balance is maintained between cold welding and fracturing of particles. The PCAs can be solids, liquids, or gases. They are mostly, but not necessarily, organic compounds, which act as surface-active agents. The PCA adsorbs on the surface of the powder particles and minimizes cold welding between powder particles and thereby inhibits agglomeration. A wide range of PCAs has been used in practice at a level of about 1-5 wt% of the total powder charge. The most important of the PCAs include Stearic acid, hexane, methanol, and ethanol. The nature and quantity of

the PCA used and the type of powder milled would determine the final size, shape, and purity of the powder particles. Use of a larger quantity of the PCA normally reduces the particle size by 2-3 orders of magnitude.

- **Temperature of milling;** the temperature of milling is another important parameter in deciding the constitution of the milled powder. Since diffusion processes are involved in the formation of alloy phases irrespective of whether the final product phase is a solid solution, intermetallic, nanostructure, or an amorphous phase, it is expected that the temperature of milling will have a significant effect in any alloy system. Only a few investigations where done in the verifying the effect of temperature of milling. Either dripping liquid nitrogen on the milling container to lower the temperature or electrically heating the milling vial to increase the temperature of milling.

All these process variables are not completely independent. For example, the optimum milling time depends on the type of mill, size of the grinding medium, temperature of milling, ball-to-powder ratio, etc. [56].

2.3.5 Problems of Mechanical Alloying

With all the numerous advantages and simplicity associated with MA techniques, problems are also associated with the technique; these can be discussed under three groups viz.; powder contamination, limited knowledge and limited applications.

- **Powder contamination**

During MA powder contamination is a major concern and a lot of factors contribute to this unwanted phenomenon, some of these are;

- Condition of milling (grinding medium, grinding vessel, time of milling, intensity of milling, etc)
- Atmosphere been milled
- The small size of the powder particles, availability of large surface area, and formation of new surfaces during milling.

These conditions that contribute to the powder contamination level can be eliminated/mitigated using some suggested methods like

- ✓ Use of balls and container of the same material that is being milled
- ✓ Use of high-purity atmosphere
- ✓ Shortest milling times allowed
- ✓ Use of high-purity metals
- ✓ Self-coating of the balls with the milled material [56].

- **Limited science content**

The knowledge base for MA is poor despite the technique is efficient and useful; one is not very clear on how and why the process works. The reason is because of the complex stochastic process and the number of variables involved is too many e.g. ball-to-powder weight ratio; milling atmosphere; purity, size, shape, and hardness of the powder particles; milling time; milling temperature; and type and amount of the PCA. Modeling the process of MA has been done and only limited success was achieved. For example, it has been possible to establish a relation between the experimentally observed phase formation and some of the process variables. But, it has not been possible to predict the

final chemical constitution (type and description of phases) for a given set of milling conditions [56].

- **Limited application**

MA is simple and achievable but has only limited industrial application and the most important is the ODS materials. Potential applications have been suggested, many of them have not been industrial realities. Identification of some niche applications for the MA products is likely to accelerate the rate of growth in this field.

2.3.6 Safety hazards in Mechanical Alloying (MA)

There are hazards associated with MA process; this is due to the fine size of the powders and other factors. These include heat evolution, reaction rates, gas evolution causing pressure build-up in the milling chamber or ancillary equipment, and finally explosions. During milling operations temperature increases caused by the energy added through the mechanical system used to drive the mill, and heat generated by exothermic processes occurring during the milling process and if the critical temperature is exceeded uncontrolled reactions can occur and can lead to explosions. This heat generated can increase the reaction rates of the system. Gases may also be produced during milling due to the decomposition of PCAs or due to the reactions between the components. Some of the gases produced may be flammable and so the potential for fire or explosion exists. Handling of MA powders also has some safety hazards; this is because these powders are very fine in size and have a large surface area. Such powders have an increased tendency toward pyrophoricity [56]. The cleaner and fresh powder surfaces produced during MA accentuate their sensitivity to pyrophoricity. Some precautionary motives are highly

recommended during MA such as; care should be taken during unloading of the powders after MA, the vial should not be immediately opened as these powders are hot.

2.4 Mechanism of Alloying

During milling, powder particles are repeatedly flattened, cold welded, fractured and rewelded. Powder is trapped when balls collide; around 1000 particles with an aggregate weight of about 0.2 mg are trapped during each collision as depicted in the figure below.

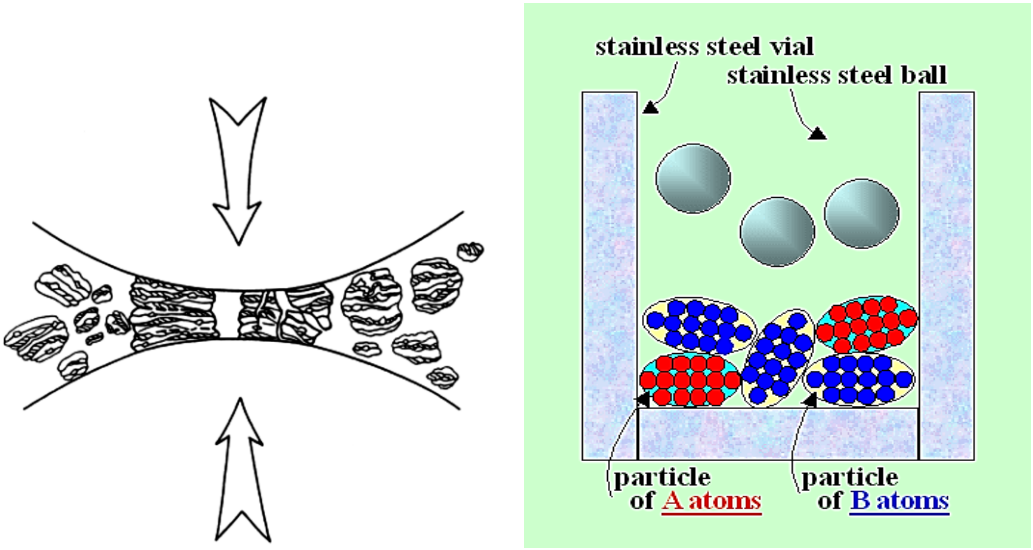

Figure 2.3 Ball-powder-ball collision of powder mixture during mechanical alloying [56].

The impact force plastically deforms the powder particles leading to work hardening and fracture. With continued deformation, the particles get work hardened and fracture by a fatigue failure mechanism and/or by the fragmentation of fragile flakes. Fragments generated by this mechanism may continue to reduce in size in the absence of strong agglomerating forces. Here fracture predominates over cold welding. The structure of the particles is steadily refined and the size of the particles remains the same.

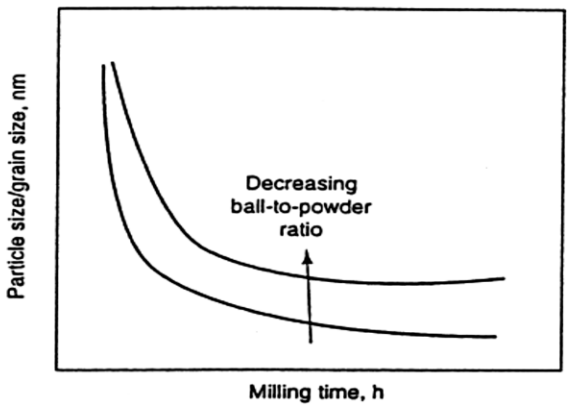

Figure 2.4 Refinement of particle and grain sizes with milling time. Rate of refinement increases with higher milling energy, ball-to-powder weight ratio, lower temperature, etc [56].

Nanostructured materials can be synthesized easily which is why MA has been widely used for nanocrystalline materials production. MA can be conducted in 3 different combinations of metals and alloys namely; Ductile-ductile, ductile-brittle and brittle-brittle.

2.5 Application of Mechanical Alloying

Since the development of MA, it has been used in a wide variety of applications which are highlighted below

- The most important application of MA is the production of ODS alloys which have complex compositions and show higher creep resistance and greater stability than conventional alloys [60]. Typical ODS alloys mainly used are based on nickel, iron and aluminum e.g. MA754, MA957, MA956, MA6000 etc.
- MA is used for the production of Nanostructured materials/composites for example AL-based nanocomposite, typical work done by N. Al-Aqeeli et al., [61] where they development a new Al-Mg-Zr nanocomposite by MA by mixing Al based binary Al-Mg and ternary Al-Mg-Zr powders.

- Super alloys can be produced through MA technique, paper by Benjamin et al. where a super alloy was produced for jet engine blades in which the very high strength of cast nickel-base superalloys at moderate temperatures.
- MA technique can also be used for the production of PVD (physical vapor deposition) which are targets for electronic industry; this is because chemically homogenous products are easily produced by MA than conventional means.
- Another interesting application of MA is the use of its products in MRE (Meal, Ready-to-Eat) in heaters which have been used during desert storm operation by USA in 1996 Heat is produced when Mg and Fe powders which are finely ground by MA are in contact with water.
- MA technique is most appreciated for the highly homogeneous product without any segregation effects.
- Hydrogen storage can be done from Mg-based materials produced by MA technique.

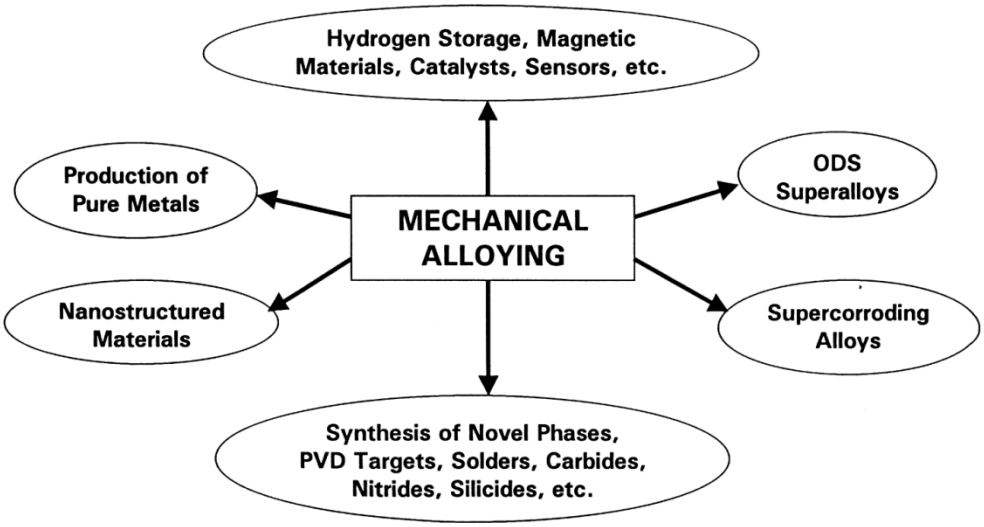

Figure 2.5 Typical current and potential applications of mechanically alloyed products [56].

Conclusively mechanically alloyed materials generally show higher mechanical properties than those fabricated by conventional means. For example in comparing the mechanically alloyed Al-5Fe-4Mn and rapidly solidified Al-5Fe-4Mn alloy, it was found that their tensile properties at room temperature were almost the same, however when heating temperature is above 423K, MA alloy shows a clear advantage in its remarkable temperature resistance at 573K, the material is 90MPa higher than that of the rapid solidified counterpart [60].

Powder contamination is a major concern in milling and formation of amorphous phases were discovered due to the presence of considerable amounts of impurities. Similar radial distribution functions and crystallization temperatures were found during the amorphous phases synthesized by MA and RSP techniques.

2.6 Aluminum and Its Alloys

2.6.1 General Introduction and Properties of Aluminum

Aluminum is one of the most abundant metal and the third most abundant chemical element in the earth's crust, comprising over 8% of its weight. Only oxygen and silicon are more prevalent. Yet, until about two centuries ago aluminum in its metallic form was unknown to man. The reason for this is that aluminum, unlike iron or copper, does not exist as a metal in nature. Because of its chemical activity and its affinity for oxygen, aluminum is always found combined with other elements, mainly as aluminum oxide. As such it is found in nearly all clays and many minerals. Rubies and sapphires are aluminum oxide colored by trace impurities, and corundum, also aluminum oxide, is the second hardest naturally occurring substance on earth—only a diamond is harder. It was

not until 1886 that scientists learned how to economically extract aluminum from aluminum oxide via electrolytic reduction. Yet in the more than 100 years since that time, aluminum has become the second most widely used of the approximately 60 naturally occurring metals, behind only iron [62].

One property of aluminum that everyone is familiar with is its light weight or, technically, its low specific gravity. The specific gravity of aluminum is only 2.7 times that of water and roughly one-third of steel and copper. The following are some other properties of aluminum and its alloys.

- *Formability.* Aluminum can be formed by every process in use today and in more ways than any other metal. Its relatively low melting point, 1220ºF, while restricting high-temperature applications to about 500-600ºF, does make it easy to cast.
- *Mechanical Properties.* Through alloying, naturally soft aluminum can attain strengths twice that of mild steel.
- *Strength-to-Weight Ratio.* Some aluminum alloys are among the highest strength to weight materials in use today, in a class with titanium and superalloy steels. This is why aluminum alloys are the principal structural metal for commercial and military aircraft.
- *Cryogenic Properties.* Unlike most steels, which tend to become brittle at cryogenic temperatures, aluminum alloys actually get tougher at low temperatures and hence enjoy many cryogenic applications.
- *Corrosion Resistance.* Aluminum possesses excellent resistance to corrosion by natural atmospheres and by many foods and chemicals.

- *High Electrical and Thermal Conductivity*. On a volume basis the electrical conductivity of pure aluminum is roughly 60% of the International Annealed Copper Standard, but pound for pound aluminum is a better conductor of heat and electricity than copper and is surpassed only by sodium, which is a difficult metal to use in everyday situations.
- *Reflectivity.* Aluminum can accept surface treatment to become an excellent reflector and it does not dull from normal oxidation.
- *Finishability.* Aluminum can be finished in more ways than any other metal used today [62].

2.6.2 Aluminum Alloys

While commercially pure aluminum (defined as at least 99% aluminum) does find application in electrical conductors, chemical equipment, and sheet metal work, it is a relatively weak material, and its use is restricted to applications where strength is not an important factor. Some strengthening of the pure metal can be achieved through cold working, called strain hardening. However, much greater strengthening is obtained through alloying with other metals. Due to its low strengths, Al is alloyed with other metals namely: magnesium, copper, zinc, manganese and nickel, in order to significantly improve its mechanical properties and the alloys themselves can be further strengthened through strain hardening or heat treating. Other properties, such as castability and machinability, are also improved by alloying. Thus, aluminum alloys are much more widely used than is the pure metal, and in many cases, when aluminum is mentioned, the reference is actually to one of the many commercial alloys of aluminum.

It is most appropriate to categorize Al alloys into two groups viz; casting composition and wrought compositions [63]. For wrought compositions, a four-digit system is used to produce a list of wrought composition of families while casting compositions are described by a three- digit system followed by a decimal value. The decimal 0.0 in all cases pertains to casting alloy limit and decimals 0.1 and 0.2 are ingot compositions. The tables below show the designation system for wrought and cast alloys and their major alloying element.

Table 2.2 Wrought Composition of Aluminum Alloys [63].

Alloy Series	**Description or Major Alloying Element**
1xxx	99.00% minimum aluminum
2xxx	Copper
3xxx	Manganese
4xxx	Silicon
5xxx	Magnesium
6xxx	Magnesium and silicon
7xxx	Zinc
8xxx	Other element
9xxx	Unused series

Table 2.3 Cast Composition of Aluminum Alloys [63].

Alloy series	**Description or Major Alloying Element**
1xx.x	99.00% minimum aluminum
2xx.x	Copper
3xx.x	Silicon plus copper and /or magnesium
4xx.x	Silicon
5xx.x	Magnesium
6xx.x	Unused series
7xx.x	Zinc
8xx.x	Tin
9xx.x	Other element

2.6.3 Al-Mg-Si Alloys

Al-Si system possesses high wear resistance, low thermal-expansion coefficient, good corrosion resistance, and improved mechanical properties at a wide range of temperatures. These properties led to the application of Al-Si alloys in the automotive industry, especially for cylinder blocks, cylinder heads, pistons, and valve lifters [64]. Al-Mg-Si alloys are an important group of alloys that are widely used in both cast and wrought forms. The alloys are age hardenable, and are routinely heat treated to the T6 condition to develop adequate strength [65]. These are successfully produced by MA technique with enhanced properties. The alloys' response to age-hardening is paramount and precipitation control during heat treatment is essential for realization of maximum performance of the alloy.

Another study of static and dynamic ageing of two Al-Mg-Si alloys i.e. Al6061 and Al6069 at 170ºC in which the dynamic ageing was conducted through the procedure of equal channel angular extrusion ECAE and they concluded that dynamic ageing using ECAE technique resulted in an increase in UTS of both alloys when compared to conventional static peak ageing at the same temperature, dislocation- assisted precipitation occur during dynamic ageing and finally the ageing using ECAE is superior to static ageing in both mechanical properties and time to peak strength [15].

2.7 Reinforcements in Mechanically Alloyed Powders

Mechanical alloying as a technique that consists of repeated welding-fracturing-welding of powder particles in a high energy ball mill which are trapped between the colliding balls during milling. This process is influenced by the mechanical behavior of the powder

elements [66]. MA can be used to produce numerous alloys with reinforcements e.g. Al alloys with reinforcements (Al-based MMCs) to primarily better the properties of the alloy than that from other techniques. Metal Matrix composites (MMCs) are classes of materials that seek to combine the high strength and stiffness of a ceramic with the damage tolerance and toughness provided by a metal matrix. Another defined MMCs as an engineered combination of two or more materials in which customized properties are realized by bringing the combined advantages of both the reinforcement and metal matrix into full play.

These MMCs have excellent physical and mechanical properties. Compared with unreinforced matrix, MMC reinforced with ceramics usually exhibit better service temperature, strength, creep and wear resistance as well as thermal stability. Adopting MA technique for the production of MMCs, agglomeration avoidance of the reinforcement particles is necessary and leads to a homogenous distribution of the reinforcement within the matrix [67]. Factors that contribute to the agglomeration are geometries, particle sizes, densities and flow or development of an electrical discharge. Highlight of previous works done to produce MMCs by MA/MM techniques are;

E.M Ruiz et al., [67] produced Al based MMCs where the base material was AA2014 and two different carbides were used as reinforcements i.e. VC and TiC. The powders were mixed together in a high energy horizontal ball mill and the BPR was 20:1 at 700 rpm for 5, 7 and 10 hours. The amount of elemental powders was such that the composition of AA2014 alloy (4.4% Cu, 0.5% Mg, 0.7% Si, Al bal., all wt.%) reinforced with 5%vol carbide powders was obtained and analysis of the powder were done. The effect of the mechanical alloying factors on morphology, particle size, micro hardness, and

microstructure of the final powder was studied. The results showed that composite powders can be acquired in an only step with improved properties by means of mechanical alloying.

J.B Fagagnolo et al., [68] where they investigated the production of Al6061 reinforced with Zirconium diboride by MA followed by cold pressing and hot extrusion and subsequently compared the result with the same composite produced by PM and hot extrusion. They found that about 100% improvements in the composite's UTS and hardness were achieved as compared to composite by PM technique.

Another work where Fagagnolo and his colleagues [69] studied the importance of correct milling time of Al6061 reinforced with silicon nitride particles developed by MM; this study was to ensure that the characteristics of the powder will be such as to enhance the final properties of the composite material.

2.7.1 SiC Reinforced Al Composites

Al-Si alloys are commonly used in automotive industries especially for cylinder blocks, cylinder heads, pistons and valve filter. These alloys are used because of the improved mechanical properties at a wide range of temperature, low thermal expansion coefficient, good corrosion resistance and high wear resistance. These alloys are commonly reinforced with SiC and Al_2O_3, while SiC is the most widely used followed by Al_2O_3 because of its low cost, density slightly higher than that of Al and the wide range of available grades. For example some composites like SiC/Al have shown a significant increase in their tensile strength and elastic modulus as well as wear resistance. The improved mechanical properties of particulate SiCp/Al are as a result of transfer of shear load at the matrix/reinforcement interface.

To highlight some previous work on that, Hyo Lee and co-workers [70] investigated the fabrication process and mechanical properties of SiCp/Al–Si metal matrix composite pistons for automobile air-conditioner compressor. To produce the composites, they used powder metallurgy process with vacuum hot pressing at a temperature of 540–570°C with 30 MPa followed by hydrostatic extrusion at 500°C with an extrusion ratio of 8:1. The compressor pistons were made from the developed composites by one-step forging of extruded bars at 400°C. They reported that the tensile strength and hardness of Al–Si alloys (10-12wt.%) and their composites (reinforced with 5-10wt.%SiC_p) were increased by hydrostatic extrusion and forging, mainly due to a decrease of the grain size in the matrix through plastic deformation.

The field of nanocomposite has currently attracted significant interest as researchers attempt to enhance the composite properties and extend their utility by using nanoscaled reinforcements as a replacement of the more conventional particulate filled composites. While smaller reinforcements have a better reinforcement effect than larger ones. However, while the yield and ultimate strength of the matrix improves with increasing the concentration of micro-ceramic particles the ductility of the composites deteriorates at higher concentrations. Therefore, it is of interest to use nano-sized ceramic particles to strengthen the matrix to produce metal matrix nano-composite (MMNC) while maintaining good ductility.

For example, the yield strength of Al-7Si-0.3Mg alloy fabricated by an ultrasonic-assisted casting method was improved more than 50% with the addition of 2.0wt.% of nano-sized SiC particles which is significantly better than what aluminum alloy with the same percentage of micro-particle reinforcement can offer. Moreover, there was little

change in the elongation and ultimate tensile strength [71]. It is expected that with nanoparticles reinforcement, high ductility, high temperature creep resistance and better fatigue life could be achieved.

In another study, high energy ball milling was used to produce nanocrystalline Al-SiC nanocomposites. It was found that with increasing volume fraction of nanosized SiC, a finer composite powder with more uniform particle size distribution is obtained; and the crystallite size of the aluminum matrix decreased with increasing reinforcement volume content while the lattice strain changed marginally. As compared with micro scaled SiC particles, it appeared that the effect of nanosized-SiC on the milling stages was more pronounced. The results clearly showed that the reinforcement particles influenced the work hardening and fracture of the metal matrix upon milling, which affected the evolution of the structure.

In another investigation, Woo and Zhang, [41] produced SiC nanometer sized particle reinforced Al–7.0%Si–0.4%Mg composite powder by ball milling. They reported that high energy ball milling increased the sintering rate of the composite powder due to increasing diffusion rate. The microstructure of the sintered specimen obtained using the milled composite powder was finer than that of the sintered specimen obtained from the mixed powder. Moreover, the composite fabricated by using the milled composite powder contained nanometer and sub micrometer sized SiC particles was more sound and had higher hardness than the composite produced by sintering the mixed powder.

A.Simchi and D.Godlinski [42] studied the effect of SiC particles on the laser sintering of Al-7Si-0.3Mg alloy. They showed that densification rates follows first-order kinetics and

the rate constant was found to increase low SiC fractions but suddenly decreases at >~5 vol.%. The melt track becomes more steady and a more continuous sintered surface was attained in the presence of ceramic particles. Major reaction occurred between the Al melt and the reinforced particles resulting in the formation of Al_4SiC_4 and silicon particles. Again, the effect of variable volume fraction of SiC_p on the hardness and aging response of 2024 Al-alloy was investigated by Kiourtsidis and co-workers, [71]. They manufactured the alloys by stir-casting in the semi-solid state and reported that the hardness increased as a function of the SiC content.

On the other hand, the effect of clustering in SiC-Al2024 alloy was studied by Hong and co-workers [72]. They produced the alloys by centrifugal atomization and subsequent hot extrusion. They concluded that an optimization of reinforcement content and clusters is crucial in ensuring high strength and reasonable fracture toughness.

The homogenous distribution of reinforcement particles in the matrix is very important where the work by Zhao et al., [36] was performed to study the effect of mechanical alloying (MA) on the distribution of SiC particles in an Al 6061 matrix. They concluded that MA was quite effective in ensuring homogeneous distribution of SiC particles in the alloy matrix. Nevertheless, the integrity of sintering was partially affected by gas contamination and low compressibility of the powder. They suggested a degassing procedure to improve sintering and compressibility. They further stated that MA at 400 rpm rotational speed for 5 hrs homogenous distribution of SiCp could be achieved.

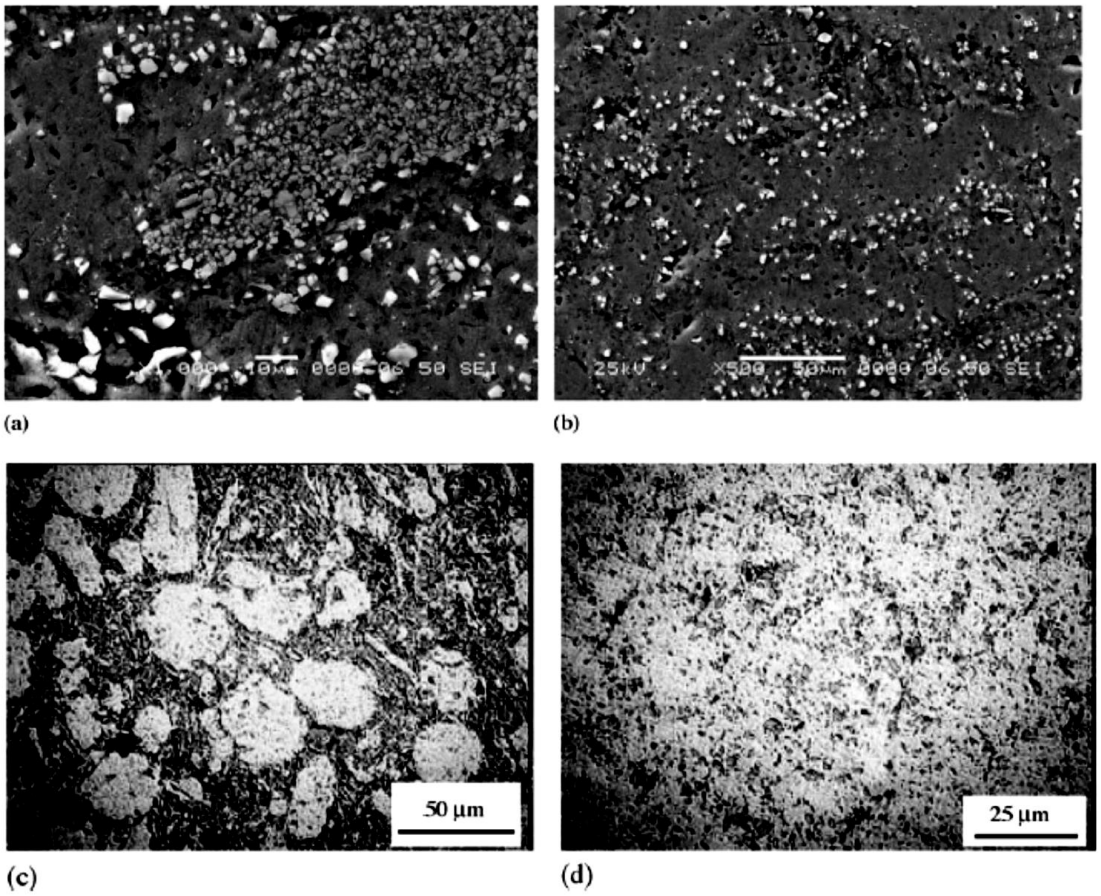

Figure 2.6 The distribution of SiC particles in the matrix during MA for (a) 2h SEM (b) 5h SEM (c) 2h OM 400X (d) 5h OM 1000X [36].

2.7.2 CNTs Reinforced Aluminum Composites

Since the discovery of CNTs about two decades ago, wide research associated to nanotubes in the field of physics, chemistry, material science and engineering etc has found increasingly [73]. Nanotubes have a small physical size of 1nm diameter and are produced by 3 methods viz;

i. *Laser furnace*; not for large scale production

ii. *The arc*; there is a problem of purification which is more costly than the production itself.

iii. *Chemical vapor deposition CVD*; this has the advantage of controlling the purity by careful process control [74].

There are single walled nanotubes (SWNTs) and multi walled nanotubes (MWNTs) which have young moduli ranging from 1-5TPa and an average of 1.8TPa respectively [23,73-75]. These nanotubes have remarkable mechanical, electrical and thermal properties with providing strong, light and high toughness characteristics. Again these CNTs are defect free and possess low dislocation density which makes development of composites reinforced with CNTs feasible. These nanotubes composites have good surface finish with applications in antistatic shielding, on airplane wings and fuselages as well as transparent conductor. Recently, there has been a steadily increasing interest in the development of carbon nanotube (CNT) reinforced composites like CNT/Al composites. The primary motive is to transfer the exceptional mechanical and physical properties of CNTs to bulk engineering materials. Though, work on MMCs CNT reinforced has been scare which is related to the difficulty in attaining a homogeneous dispersion of CNTs within metal matrices. It can be said powder metallurgy is a practical technique used in nanocomposites production with improved properties example aluminum based composite.

More recently, powder metallurgy was used to prepare aluminum based nanocomposites and remarkable improvement and structural stabilities were achieved in these alloys.

Work by Morsi and Esawi, [23] showed that mechanical alloying is a promising technique for dispersing CNTs in aluminum and controlling CNT–Al nanocomposite powder morphology and size.

In another recent study, Lee and co-workers, [31] successfully used conventional powder metallurgy method to fabricate bulk nanocrystalline Al-matrix composite reinforced with CNTs. They reported high improvements in mechanical properties with the incorporation of CNTs. Also, Deng and co-workers, [48] showed the possible fabrication of CNT/2024Al composite by a procedure of mixing 2024Al powders and CNTs, cold isostatic pressing followed by hot extrusion. They showed that CNT is an effective reinforcement for metal matrix to obtain high damping capacities at an elevated temperature without sacrificing the mechanical strength and stiffness of the composite.

R.George et al., [75] mixed CNTs (MWNT and SWNT) and Al powder (200 mesh) and milled at 200rpm for 5mins after dispersing the CNT in ethanol and sonicated for 20mins. They showed that the shorter duration and slower speed ensured that the CNTs were intact and this can be seen from the TEM image of the composite shown below.

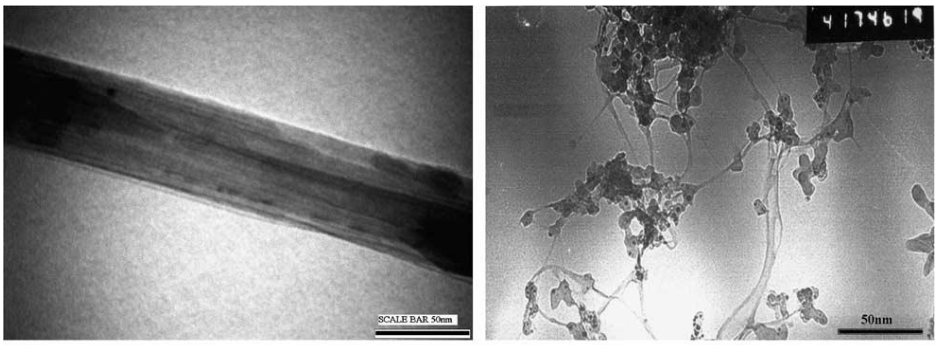

Figure 2.7 TEM images of (a) MWNT (b) SWNT (scale bar 50mm) [75].

R.George and his colleagues further investigated the important strengthening mechanism involved in CNT/Al composites where they used three major mechanisms namely; thermal mismatch, Orowan looping and shear lag model and concluded that shear lag model is the only mechanism associated with young modulus and all three were

associated to increased yield strength and that strengthening of the composite could be due to the synergistic effect of the mechanisms.

2.8 Sintering

Sintering is a technique of consolidating powder compacts by use of thermal energy and dates back to the prehistoric time with the firing of pottery and considered as one of the oldest human technologies which is now extensively used to fabricate bulk ceramic components and parts from powder metallurgy [76].

Densification and average size increases as a result of the thermal energy applied to the powder compact. This phenomenon is called *sintering*.

G.S. Upadhyaya [43] stated that; Hausner defined sintering which reads as follows, 'sintering is the bonding of particles in a mass of powders by molecular or atomic attraction in the solid state, by application of heat, causing strengthening of the powder mass and possibly resulting in densification and recrystallisation by transport of materials'. Kuczynski defined sintering as diffusional creep under action of capillary forces. He further added that deformation and diffusion mechanisms are the two main mechanisms discussed by researchers.

The driving force of sintering is total interfacial energy reduction and energy of a compact is expressed as **σA** where **σ** is specific energy (interface) and **A** is total surface area of the compact.

The reduction of the energy can be expressed as

$$\mathbf{\Delta (\sigma A) = \Delta \sigma A + \sigma \Delta A}$$

$\Delta\ \sigma$ is due to densification and change in interfacial area is due to grain coarsening [76]

Generally, the size of the powder for sintering is in the range of 0.1 to 100 μm. Consolidation of mechanically alloyed powder particles to full density is a complex phenomenon. The particles became very hard and strong due to the small size and also because of the incorporation of a high density of crystal defects. Consequently, the pressures required for compaction are expected to be higher. But, once compacted, the process of sintering is expected to take place quickly due to the small size of the particles, and therefore increased grain boundary area, in the mechanically alloyed powder particles. Occasionally, a combination of more than one technique is expected to be utilized to achieve full densification [77-79]. During sintering, the density and average particle/grain size increases as a result of the thermal energy supplied to the powder compact. The sinterability and the sintered microstructure of a powder compact are dependent on two important variables, viz., material and process variables and the sintering equations are governed by these variables. The atmosphere maintained during sintering affects the sintering mechanism in addition to impurity/reinforcement content and composition. High gas transportation rates and pore structure, grain structure, impurity content, kinetics and surface structures are major changes caused by the sintering atmosphere. Therefore, determination of atmospheres that are most effective for control of impurity is necessary. However, consolidation of powders through isostatic technique is a feasible technique for composite materials which are intricate or costly to fabricate by other methods.

All sintering equations comprises of a number of variables such as particle size, pore volume, surface tension etc. These variables determine the sinterability and the sintered

microstructure of a powder compact and can be categorized into 2 groups i.e. material and process variables as shown in the table below;

Table 2.4 Variables Affecting Sinterability and Microstructure [76].

Material variables	➢ Powder: shape, size and distribution, agglomeration ➢ Chemistry: composition, impurity, non-stoichiometry, homogeneity
Process variables	➢ Temperature, time, pressure, atmosphere, heating, and cooling rate.

These two variables are in one way or the other dependent on each other for example; fully dense Al_2O_3 fabrication, maneuvering of the chemistry system avoids the embellished grain growth, thereby almost complete removal of defects (porosity).

Homogeneity is paramount when more than two powders are compacted, MA/MM and also chemical processes such as sol-gel and co-precipitation processes have been applied to improve homogeneity.

Sintering atmosphere and pressure are much more complicated and important and this complication in real system during sintering can be categorized into 3;

- *Powder;* particle size, distribution and shape, agglomeration chemical composition homogeneity, impurities etc.
- *Compact pressed*; Pore size, distribution, parking density, granulation effect etc.
- *Sintering*; temperature, temperature gradient and cycle, atmosphere, pressure etc.

Sintering atmosphere affects sintering mechanism in addition to impurity content and composition. High gas transportation rates and pore structure, grain structure, impurity

content, kinetics and surface structures are major changes caused by sintering atmosphere. Therefore determination of atmospheres that are most effective for control of impurity is necessary.

Sintering techniques can be done through conventional techniques such as cold isostatic pressing (CIPing), hot isostatic pressing (HIPing) and non-conventional means such as microwave sintering and FAST. Non-conventional techniques are considered as novel processes and have numerous advantages over their counterpart which will be discussed in the following sections.

2.8.1 Spark Plasma Sintering Technique (SPS)

This is a non-conventional technique that was first developed by Inoue et al, 1960 where they developed it on the basis of using the plasma on electric discharge machine for sintering metal and ceramics.

Joanna R. Groza and Antonion [80] defined FAST or SPS as a powder consolidation technique where densification is enhanced by the application of an electrical discharge combined with resistance heating and pressure. In a review paper by Morteza Oghbaei and Omid Mirzaee, [45], they defined FAST as a process that allows densification of powder at a relatively lower temperature with short holding time due to very rapid heating and cooling rates. This technique is also called spark plasma sintering (SPS), plasma activated sintering.

Both microwave and FAST techniques have shown good refinement in microstructure and improved microstructure but microwave sintering seems to be a more appealing substitute for FAST for large specimens because dielectric loss mechanism is use to

deposit energy in the bulk of the material. FAST technique has enhanced the sinterability of a lot of metals and also leads to the development of new advanced materials and improving their properties [81].

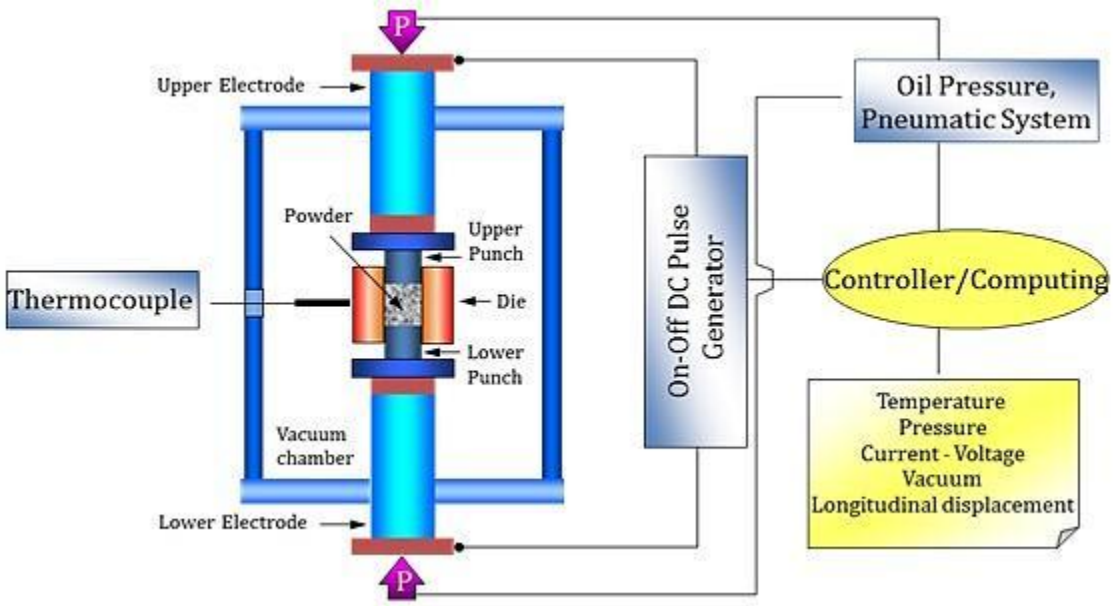

Figure 2.8 Schematic illustration of Spark Plasma Sintering (SPS).

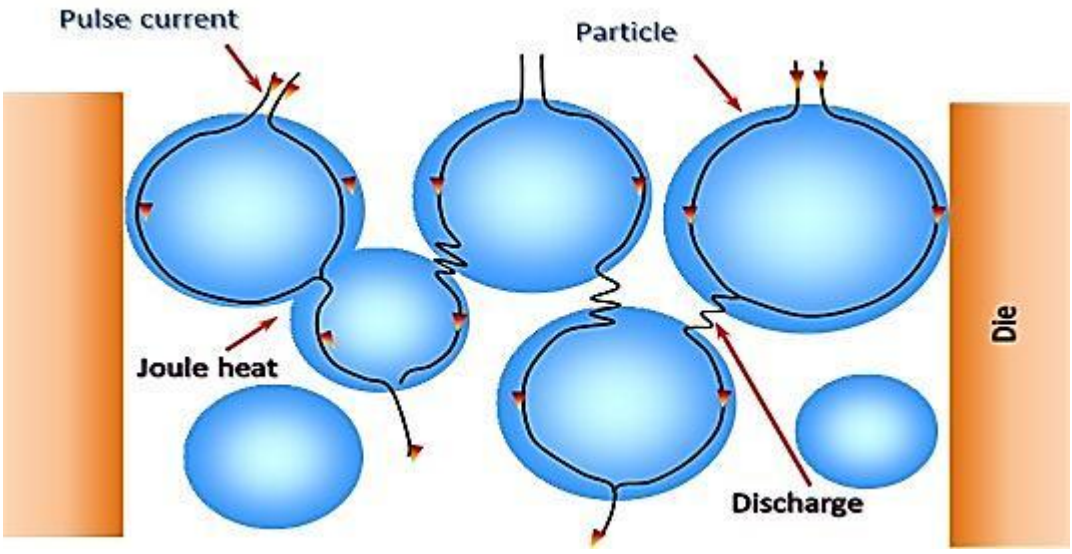

Figure 2.9 Illustrates how pulse current flows through powder particles inside the SPS sintering die.

Figure 2.8 and 2.9 above shows the Schematic illustration of Spark Plasma Sintering and how pulse current flows through powder particles inside the SPS sintering die.

SPS technique has superior advantages over the conventional ones like very rapid heating and cooling rates, shortened sintering times, better microstructure, higher densification as well as improved mechanical properties. The Non-conventional methods have made it possible for the processing of advanced materials. The figure below shows the effect of sintering time with respect to temperature used for conventional and spark plasma sintering techniques, which shows non-conventional sintering techniques like SPS has far more superior than conventional ones like HIP, CIP and furnace sintering.

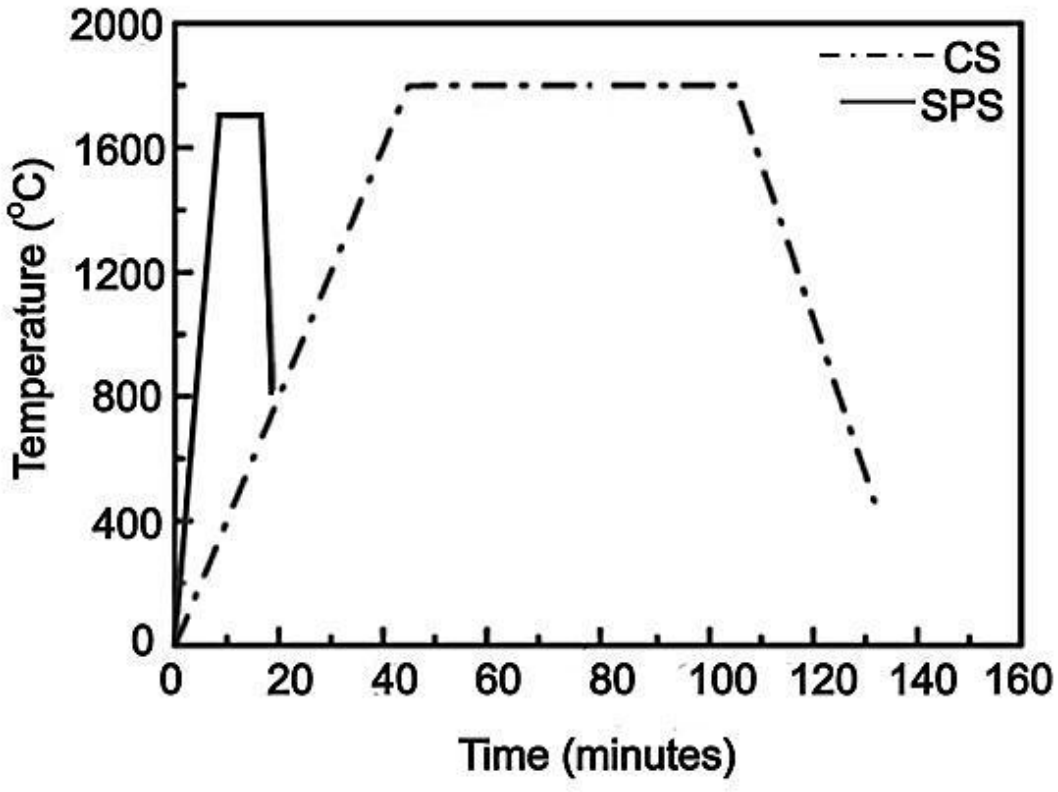

Figure 2.10 Graph showing the temperature Vs sintering time for conventional and spark plasma sintering techniques.

Th. Schubert et al., [82] studied the microstructure and mechanical properties of an Al-Si alloy consolidated by spark plasma sintering, where they stated that high density of bulk material with porosity less than 1% can be prepared by SPS with a temperature of 450°C, holding for 2-10min and a pressure of 170 MPa. Furthermore, the microstructural homogeneity across the diameter of the sintered samples were investigated and compared with in-situ measurements of the temperature distribution within the samples. Residual porosity was localized at the margin close to the wall of the die, corresponding to the lowest measured temperatures. The process parameter effects on the structure and tensile properties of subsequently hot extruded material were studied and compared to material based on hot pressed pre-compacts. The mechanical tensile properties of the SPSed compacts were appreciably lower compared to that of the extruded material due to some residual porosity and the weakness of the joint between the initial atomized alloy powder particles.

Jatinkumar Kumar Ra et al., [51] reported the Microstructure and mechanical properties of nanocrystalline high strength Al–Mg–Si (AA6061) alloy by high energy ball milling and spark plasma sintering where gas atomized microcrystalline powder of AA6061 alloy was ball milled to nanocrystalline powder with grain size of ~30 nm under wet condition at room and then consolidated to fully dense compacts by spark plasma sintering (SPS) at 500°C. After SPS consolidation the grain size was found to be ~85 nm. The resultant SPS compacts exhibited microhardness of 190–200Hv100gf, compressive strength of ~800MPa and strain to fracture of ~15%.

Kwon et al., [52] studied the combined processes of spark plasma sintering and hot extrusion were used to fabricate a multi-walled carbon nanotube (MWCNT) reinforced

aluminum (Al) matrix composite at different sintering temperatures. Raman spectroscopy was used to study the structural defects of carbon nanotubes (CNT) at various sintering temperatures. Al liquid phase in small quantity was generated and it reacted with disordered CNTs, even during the solid-state spark plasma sintering process. They concluded that from microstructural viewpoint and in relation to tensile strength that structurally controlled CNTs could potentially be attractive for metal matrix applications, and could significantly improve the mechanical properties of Al-CNT composites.

H. Kwon et al., [53] studied the combination of hot extrusion and spark plasma sintering for producing carbon nanotube reinforced aluminum matrix composites and concluded that SPS could produce Al–CNT with a relatively high density and degree of orientation for the CNTs after good dispersion of the CNTs within the matrix. In addition, during the SPS, grain growth in the matrix and damage to CNTs did not occur, due to pinning effect by the CNTs and oxides as well as the rapid heating. A small quantity of carbide was generated during the SPS process and thereby affected a strong bonding between the Al matrix and CNTs. Enhancements of density, dispersity, and CNT orientation were noticed due to the subsequent hot extrusion process.

Jin-zhi Liao et al., [83] reinforced Aluminum (Al) matrix composites with 0–2.0 wt.% multi-wall carbon nanotubes (MWCNTs) by thorough mixing using in a roller mill and then sintered using a spark plasma sintering (SPS) machine followed by hot extrusion. Fully dense Al–MWCNT composites were achieved. The characterization of microstructure and mechanical properties of these composites were conducted: there was a significant improvement in the Al–MWCNT composite properties at initial loadings 0.5 wt% of MWCNTs when compared to Al samples without much increase in cost.

Yamanaka Shunsuk et al., [84] fabricated and evaluated the thermal analysis of Carbon Nanotube/Aluminium composite by spark plasma sintering (SPS) method through powder metallurgy employing the slurry mixing process, they successfully dispersed the CNTs using slurry precursors by hetero-aggregation with ethanol which was verified by FESEM. They reported a relative density of over 99% and concluded that as the CNT content increases the thermal conductivity of the composites decreases but these thermal properties are enhanced by extending the holding time during sintering.

Chapter 3

EXPERIMENTAL PROCEDURE

3.1 Materials

The Al-7Si-0.3Mg and Al-12Si-0.3Mg powder alloys from aluminum powder co Ltd, froge lane, minworth, sutton coldfield, West Midlands, B76 1AH were used as matrices and commercial carbon nanotubes (up to 2.0wt.%) and SiC nanoparticles (up to 20wt.%) were used as reinforcements from nanostructured and amorphous materials Inc. Houston, Texas, USA. . The pre-alloyed powders were ball milled with MWCNTs and SiC to produce homogeneous nanopowder. The tables 3.1 and 3.2 below show the characteristics and chemical analysis of each powder respectively.

Table 3.1 Characteristics of Materials of the Study.

Material	**Size**	**Purity (%)**	**Surface density (m^2/g)**
Al-7Si-0.3Mg – alloy 1	~40µm	N/A	N/A
Al-12Si-0.3Mg – alloy 2	~40µm	N/A	N/A
Carbon nanotubes, multi wall (MWCNTs)	20 – 40nm	95	40 – 600
Silicon carbide (Beta) SiCp	20 – 40nm	99	90

Table 3.2 Shows the Chemical Analysis of Starting Powder of Al-7Si-0.3Mg Alloy (Alloy-1) and Al-12Si-0.3Mg Alloy (Alloy-2) As Received.

Composition	**Al**	**Si**	**Mg**	**Fe**	**Mn**	**Cu**	**Zn**	**Pb**	**Co**	**Ni**	**Cr**	**Ti**	**Zr**	**Ga**
Alloy 1	92.06	6.5	0.40	0.35	0.040	0.037	0.015	0.015	0.001	0.011	0.004	0.016	0.001	0.010
Alloy 2	87.49	11.2	0.41	0.64	0.067	0.067	0.023	0.046	0.001	0.014	0.005	0.023	0.002	0.012

3.2 Ball Milling Procedure

3.2.1 Al-Alloy/SiCp Powder Milling

Al-based powder was ball milled with SiC_p to produce a homogeneous mixture. For the milling experiments, the powder was loaded into a stainless steel vial and milled in a planetary mill (Fritsch Pulverisette 5) figure 3.1 under Argon gas (Ar) atmosphere to avoid contamination. Stearic acid (2%.wt) was used as a process control agent (PCA) to avoid excessive cold welding of aluminum powder. Stainless steel balls were used with each ball weighing 4.1g and the ball-to-powder weight ratio (BPR) was set at 10:1. Milling was performed at a speed of 200 rpm for different milling periods of 5, 12 and 20 hours. Alloy composition according to table 3.2 mixed with; 5, 12, and 20wt% of fine SiC nanopowder from table 3.1. The milling experiments were periodically halted after an interval of 3hrs for 30 minutes to avoid temperature build-up in the milling vial. Furthermore, to eliminate any accumulation of unprocessed powders on the internal walls, the vial was opened at regular intervals depending on the milling time and the deposited powders were scraped out from the vial walls.

3.2.2 Al-Alloy/MWCNTS Powder Milling

Al-based powders were ball milled with MWCNTs to produce a homogeneous mixture after sonicating the MWCNTs in ethyl alcohol for 10-15mins in (Cole Parmer 8892, Ultra Sonic Cleaner, CA, figure 3.1 (c)) in a stainless steel vial and milled in a planetary mill (Fritsch Pulverisette 5). Milling was performed at a speed of 200 rpm for different milling periods of 1, 3 and 5 hours. Both alloys 1 and 2 according to table 3.2 composed

of; 0.5, 1, 1.5 and 2wt.% of CNTs. BPR was maintained at 10:1 at the controlled atmosphere. 2wt% stearic acid was also used.

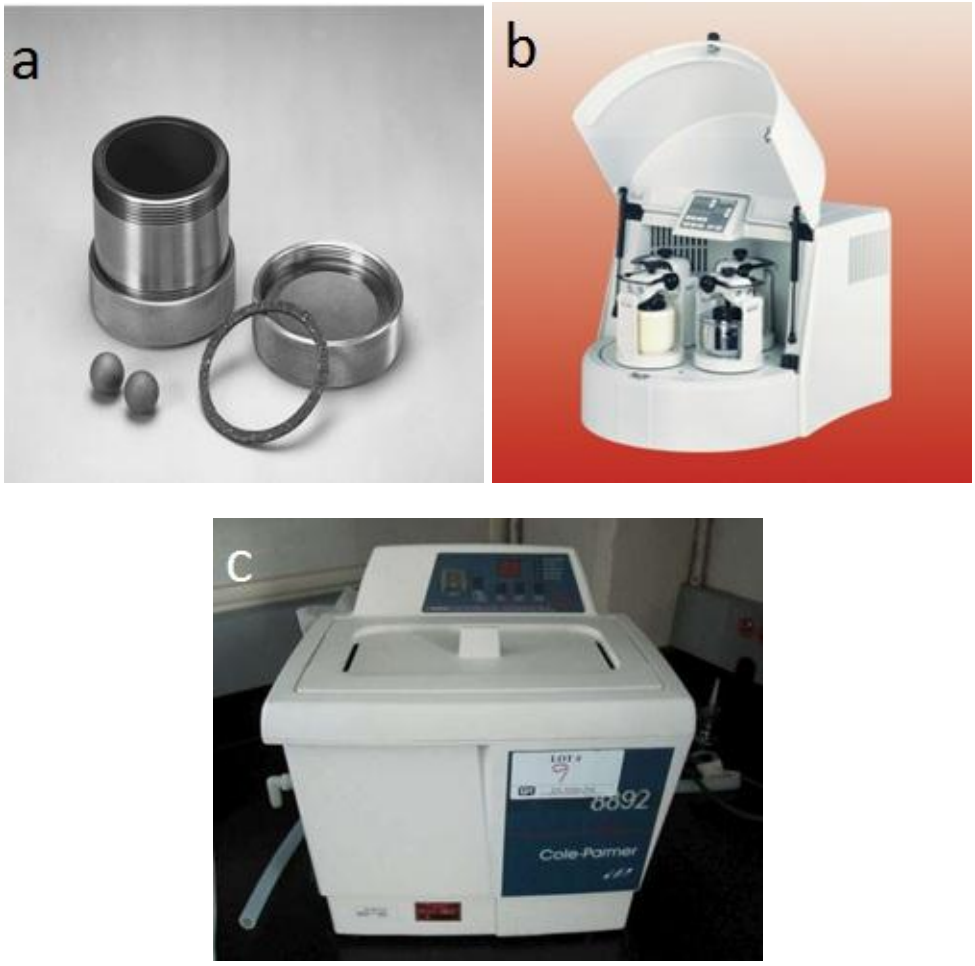

Figure 3.1 Shows (a) Typical vial and ball (b) Ball Milling- Fritsch Pulverisette 5 (c) Cole Parmer-8892- Sonicating machine.

3.3 Powder Characterization using XRD, SEM, EDS, Mapping, PSA.

At successive milling times, a small amount of powder was taken out from the vials to observe any morphological changes. JEOL JSM-6460LV (Japan); scanning electron microscopes (SEM) was used for morphological evaluations. Oxford system for EDS (Energy-dispersive X-ray spectroscopy) along with mapping was utilized for compositional analysis. Bruker D8- X-Ray Diffractometer was employed to study phase evolution, to determine crystallite size and accumulated strain. As received Al powder was annealed and used for broadening correction in estimating the crystallite size and strain accumulated during milling. This annealing was done at 400^{o}C for 1h and allowed to cool in the furnace under controlled atmosphere. Cu-Kα radiation with wavelength 0.1504nm was used and the machine was operating at a voltage of 40kV and a current of 40mA. Scherer relation and Williamson's plot were used to determine crystallite size and strain from the broadening of XRD peaks [85]. Particle size analyzer (PSA) Microtrac, Germany was used to further characterize the monolithic and milled powders.

$$B \cdot \cos(\theta) = \frac{k\lambda}{D} + \eta \cdot \sin(\theta), \quad \text{..... Scherrer Relation}$$

Where ***D***, is the crystallite size, ***k*** is a constant typically 0.8-1.0, ***η*** is the strain, **λ** is the wavelength of Cu-Kα radiation, ***B,*** is the full width half maximum (FWHM).

Thus, from a plot of $B \cdot \cos(\theta)$ vs. $\sin(\theta)$ a straight line with slope η and intercept $\frac{k\lambda}{D}$ are used to calculate the size and strain respectively.

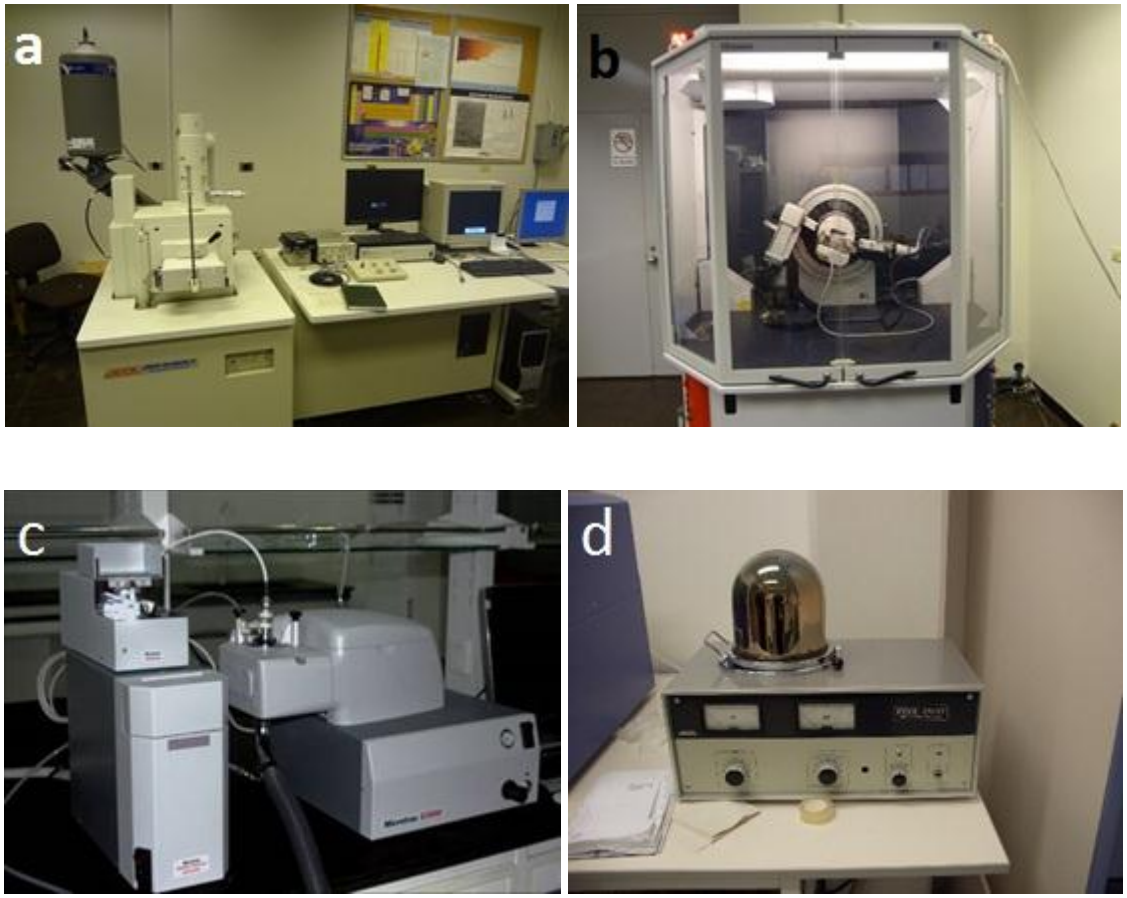

Figure 3.2 Shows (a) JOEL SEM Machine (b) D8 X-Ray Diffractometer (c) Microtrac Particle Size Analyzer Machine and (d) JEOL; Fine Coat Ion Sputter JFC-1100.

3.4 Sintering (Spark Plasma Sintering-SPS) Procedure

As received monolithic and milled powders were sintered in FCT group, Systeme GmBH, Germany at 400°C, 450°C and 500°C, holding time; 20mins and force 11kN (35MPa) applied at a heating rate of 100ºC/min with a die movement of between 6 to 7.5mm. For Al/SiC powder, all the powders were milled for 20hrs containing 5, 12 and 20wt% SiC while Al/MWCNTs, the powders were milled for 3hrs containing 0.5wt% MWCNTs.

Figure 3.3 Shows Spark Plasma Sintering (SPS) Machine.

3.5 Characterization of Sintered Samples

3.5.1 Density Measurement

The density of the sintered samples (monolithic alloys and nanocomposites) was measured using an electronic Densimeter figure 3.4 (MD-300S, Alfa Mirage, SG resolution-0.001g/cm^3, capacity-300g) and the Archimedes principle was followed to quantify the density.

Figure 3.4 Shows Electronic Densimeter (MD-300S, Alfa Mirage, SG resolution-0.001g/cm3, capacity-300g).

3.5.2 Microstructure Analysis

The microstructural features of the processed samples such as distribution of carbon nanotubes or SiC nanoparticles, presence of pores and defects, CNT/matrix and SiC/matrix interfaces were investigated through FESEM Tescan Lyra-3 (Czech Republic); scanning electron microscopes as well as optical microscope (MEIJI-Techno microscope, Japan) also used for further characterization. All microstructural analysis

were done after mounting using Evolution, IPA 40 Remet, Bologna, Italy figure 3.5 (a) with the aid of Buehler Transoptic powder, IL, USA and grinding and polishing using Handimet 2 Roll Grinder Buehler USA and Ecomet 4, Buehler Grinding Machine (variable speed grinder-polisher) USA figures 3.5 (b) and (c) respectively.

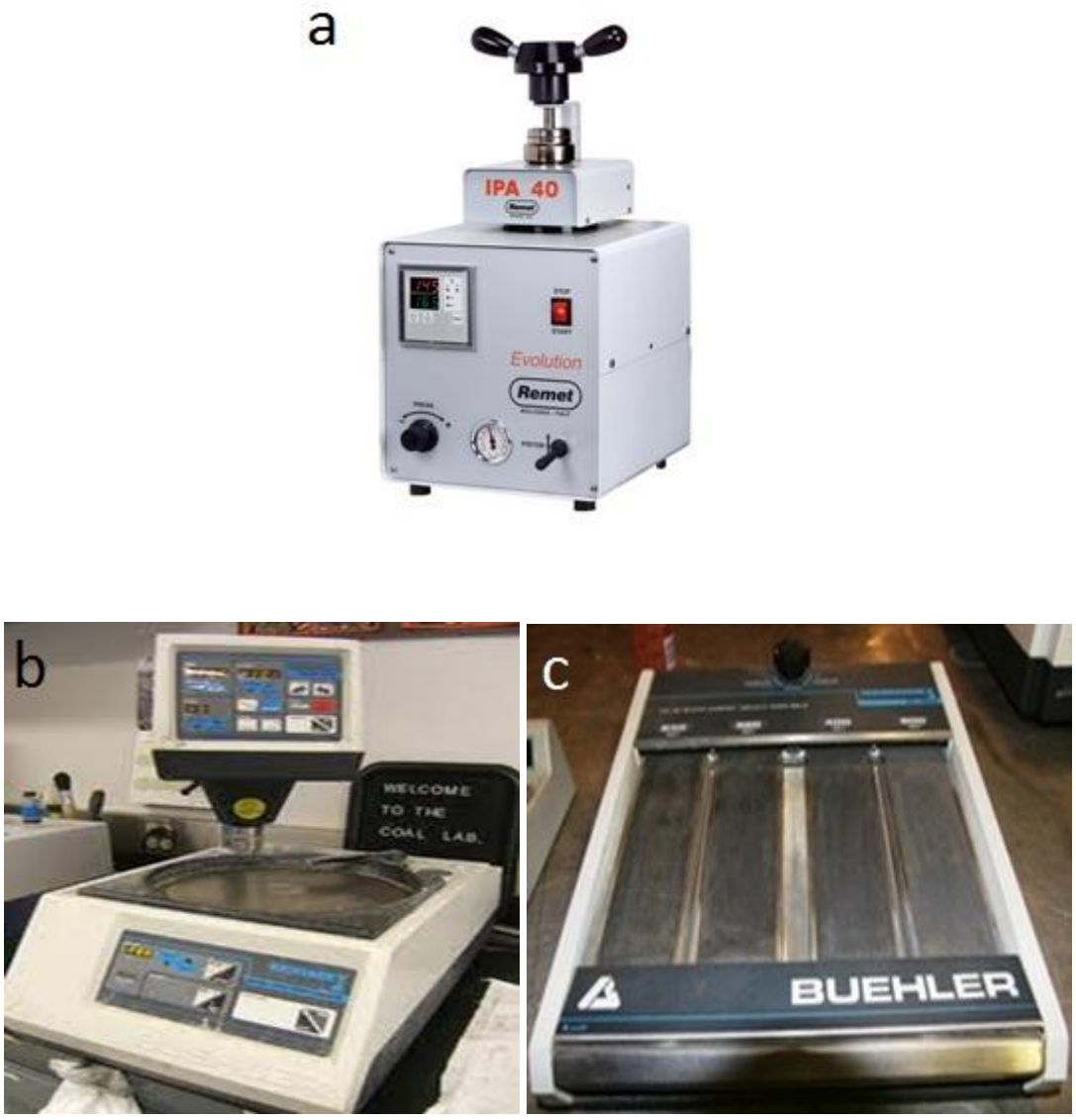

Figure 3.5 Shows (a) Evolution, IPA 40 Remet, Bologna, Italy (b) Ecomet 4, Buehler Grinding Machine (variable speed grinder-polisher) USA (c) Handimet 2 Roll Grinder Buehler USA.

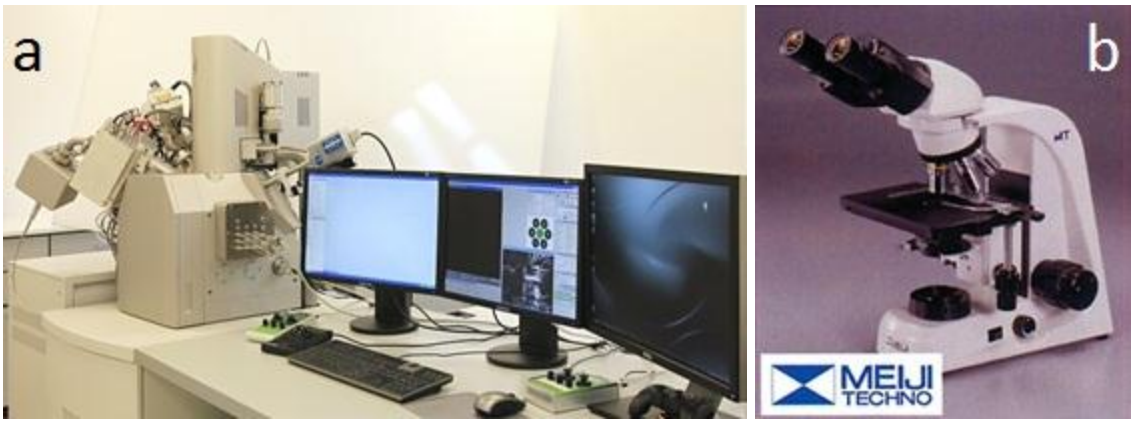

Figure 3.6 Shows (a) FESEM Tescan Lyra-3, Czech Republic (left) (b) MEIJI-Techno Optical Microscope, Japan (right).

3.6 Mechanical Characterization

3.6.1 Hardness Measurement

Micro-Hardness of the monolithic alloys and nanocomposites, prepared through different processing routes was measured using Vickers hardness machine (MMT-3 digital microhardness tester, Buehler, USA) using 100gf taking 10-12 readings.

Figure 3.7 Shows MMT-Series digital microhardness testing machine-USA.

Table 3.3 and 3.4 show the summary of the experimental procedures for the ball milling and spark plasma sintering.

Table 3.3 Summary of Ball Milling Experiment for both Alloys

Alloy	**Reinf.**	**Comp. (wt.%)**	**Milling Time (hr)**	**other conditions**	**Characterization**
Al-7Si-0.3Mg (Alloy 1)	SiCp	5, 12, 20	5, 12, 20	BPR 10:1, speed=200rpm, 2wt.%PCA, 3hr Halt time, Argon atmosphere, Stainless Steel Vials and balls, Sonication.	SEM, EDS, Mapping, XRD, PSA.
Al-12Si-0.3Mg (Alloy 2)	MWCNTs	0.5, 1, 1.5, 2	1, 3, 5		

Table 3.4 Summary of Spark Plasma Sintering Experiment for both Alloys

Alloy	**Reinf.**	**Comp. (wt.%)**	**Milling Time (hr)**	**Sintering Temp. and other conditions**	**Characterization**
Al-7Si-0.3Mg (Alloy 1)	SiCp	5, 12, 20	20	400, 450, 500ºC 20mins holding time, 11KN (35MPa), 100ºC/min	FESEM, XRD, Optical, Densification Microhardness.
Al-12Si-0.3Mg (Alloy 2)	MWCNT	0.5	3		

Chapter 4

RESULTS AND DISCUSSIONS

4.1 Al-Alloy 1 (Al-7Si-0.3Mg) Containing SiC

4.1.1 SEM Micrographs of Milled Powders

Figure 4.1 shows SEM micrographs of the pre-alloyed Al-7Si-0.3Mg alloy 1 in the as-received condition as well as after milling for different periods. 5, 12 and 20wt.% of nano-scaled SiC were milled along with the pre-alloyed Al-based powders to study the effect of adding higher percentages of the grinding medium (reinforcement). The as-received Al-7Si-0.3Mg samples were showing spherical shapes with broad-size distribution shown in figure 4.1(a). At the early stages of milling, the resulting Al matrix was showing a high aspect ratio after deformation with marked irregularity as observed in other locations of the micrograph. As milling progressed the plastic deformation was more pronounced resulting in flak-like particles (figure 4.1b, c and d). Higher deformation was noticed as the concentrations of nano-sized SiC was increased from 5 to 20wt.%, and continuous grinding of the powder has resulted in reduced average powder sizes (figure 4.1bi, ci and di respectively). It can also be seen that at a higher SiC concentration (figure 4.1di-20wt.%SiC) and extended milling times (of 20hrs) more

equiaxed particles were formed which can be attributed to the excessive and repeated grinding. The increased milling time ensures that SiC particles are increasingly embedded into the powder as also confirmed by EDS analysis, a typical EDS is presented for Al-7Si-0.3Mg containing 5wt.%SiC milled for 12hrs in figure 4.2. The employment of ball milling was beneficial in obtaining a homogeneous distribution of SiC particles into the Al-based matrix. This was observed after EDS and mapping analyses as no compositional fluctuation was depicted into the resulting powders.

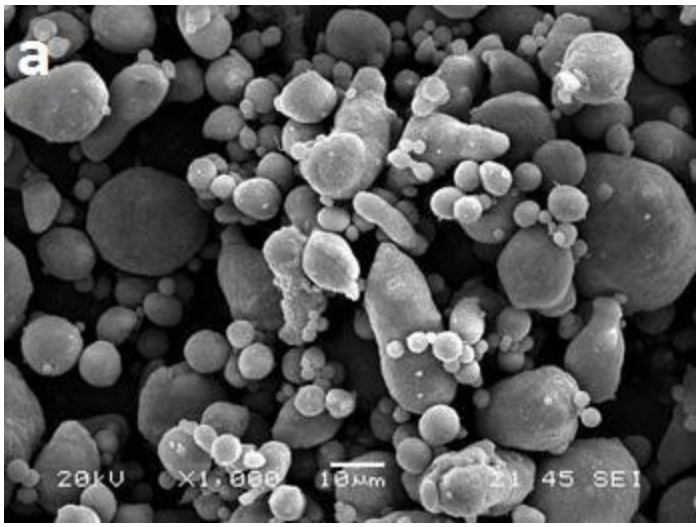
a
20kV X1,000 10µm 21 45 SEI

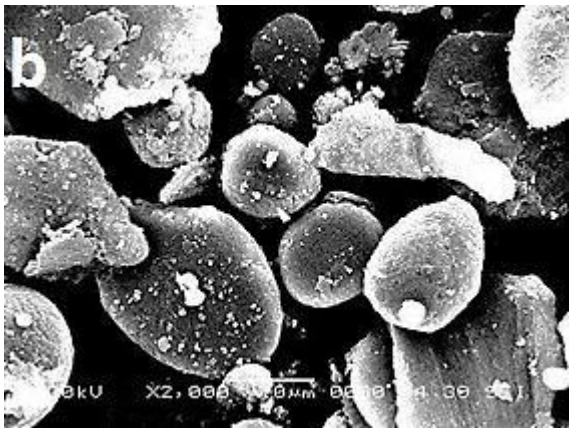
b


bi

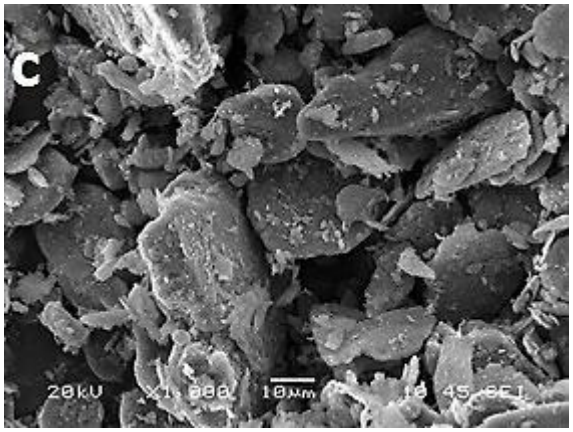
c
20kV X1,000 10µm 10 45 SEI

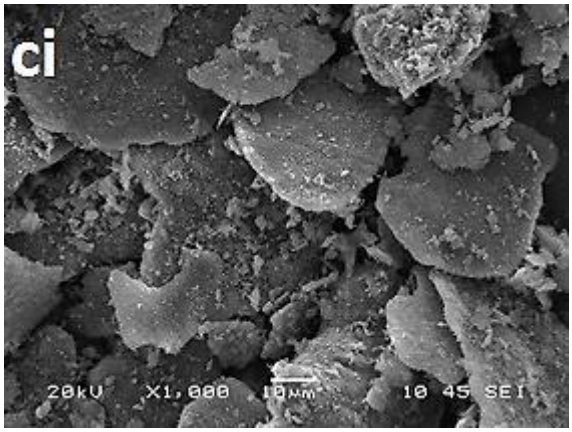
ci
20kV X1,000 10µm 10 45 SEI

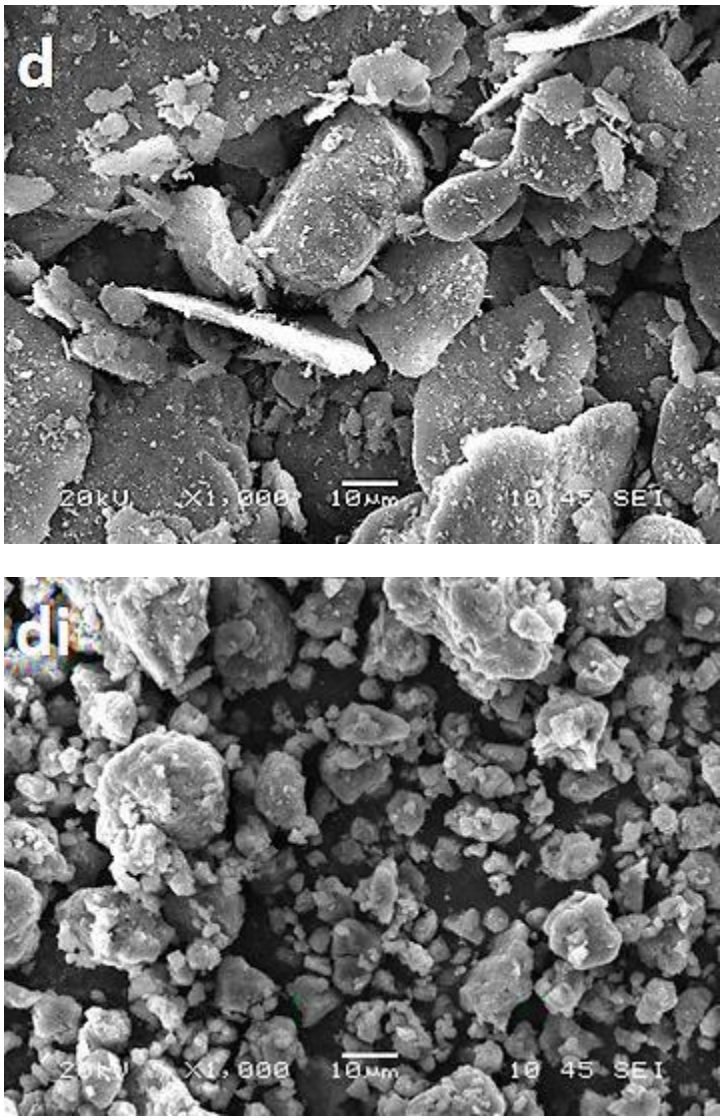

Figure 4.1 SEM micrographs of powders milled at different periods from Al-7Si-03Mg a) as-received, b) 5 hrs, c) 12 hrs, and d) 20 hrs; Left hand side and right hand side (with letter ‘i’) show samples with 5wt.%SiC and 20wt.% SiC, respectively.

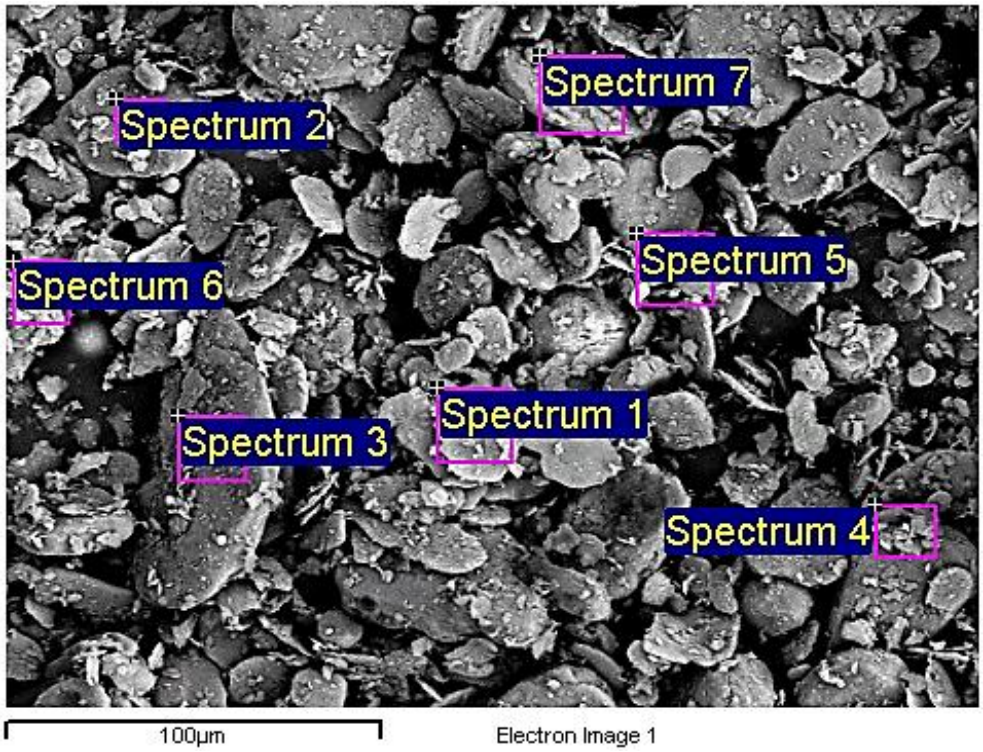

Processing option: All elements analyzed (Normalized in wt.%)

Spectrum	C	Mg	Al	Si	Total
Spectrum 1	4.13	0.49	87.23	8.14	100.00
Spectrum 2	0.00	0.44	91.11	8.46	100.00
Spectrum 3	7.11	0.37	83.01	9.50	100.00
Spectrum 4	4.88	0.00	86.50	8.61	100.00
Spectrum 5	4.10	0.00	87.29	8.60	100.00
Spectrum 6	7.38	0.00	85.41	7.21	100.00
Spectrum 7	4.84	0.00	88.24	6.92	100.00

Figure 4.2 Shows EDS analysis for Al-7Si-0.3Mg containing 5wt.% SiC milled for 12hrs.

4.1.2 X-Ray Diffractograms of Milled Powders

X-ray diffractograms of SiC reinforced Al-7Si-0.3Mg alloy are shown in figure 4.3 for different milling times. Moreover, the graphs show the patterns obtained as the concentration of SiC is increased from 5% to 20wt. %. Due to the nature of mechanical milling process, in which severe plastic deformation occurs into the milled powders, there is continuous reduction in crystallite size and accumulation of lattice plastic strain as milling experiments progressed. This is evident by the continuous broadening of the Al peaks as milling time is increased (figure 4.3). However, by comparing the results obtained for different fractions of SiC (figure 4.1 b-d and bi-di), it can be seen that more refinement into the microstructure is observed and a continuous reduction of crystallite size occurs at higher SiC concentration. This proves the role of the concentration of grinding medium (reinforcement) in refining the structure and achieving reduced crystallite sizes over the same milling periods. It can also be seen that there is a pronounced shift in the Al peaks towards higher angles in the milled powder containing 20wt.% SiC for 12 and 20hrs (figure 4.3). However, this is a clear indication of higher internal strains resulting from the accumulation of higher percentages of cold work.

On the other hand, no intermetallic phases were observed into the resulting powder. The use of solid-state milling techniques doesn't allow the accumulation of necessary temperature for the displacement reaction to take place between Al and C to form Al_4C_3. Furthermore, the peaks indicating the presence of SiC were more pronounced in the X-ray diffractograms at 20wt.% SiC, and this can plausibly be attributed to the detectability limit of XRD machine in which 5wt.% SiC is slightly close to the minimum quantity required for detectability.

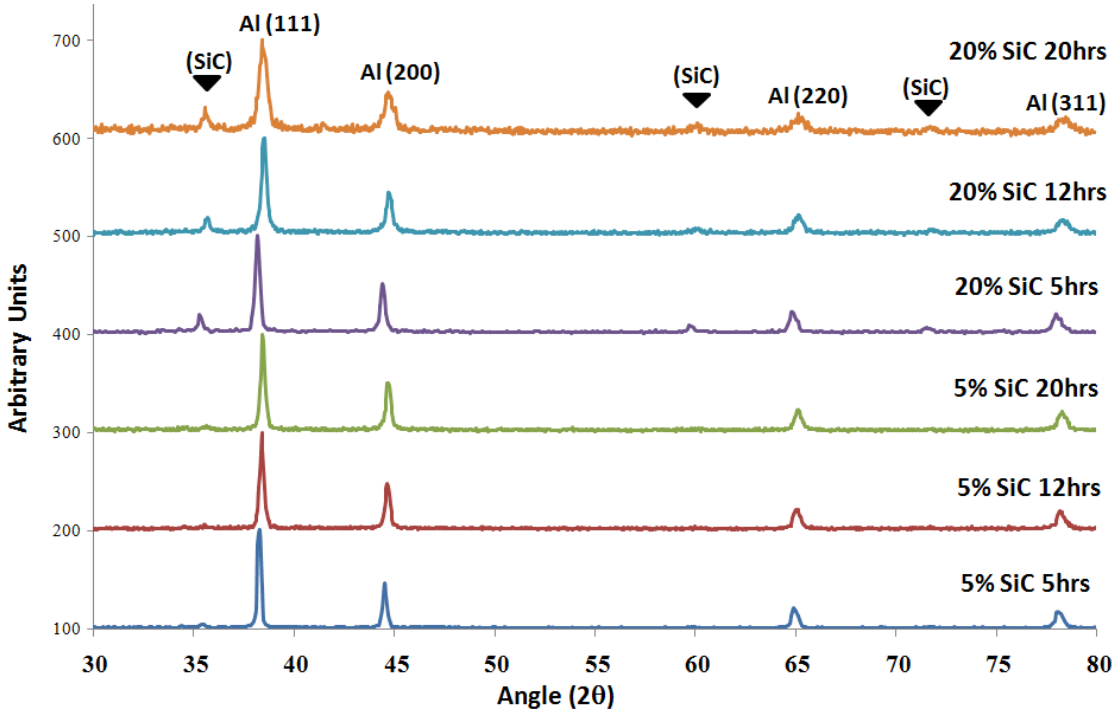

Figure 4.3 X-Ray Diffractograms for the SiC/Al-7Si-0.3Mg (alloy 1) at different milling times and different concentrations of reinforcement.

Additionally, figure 4.4(a) compares the effect of different SiC concentrations and extended milling periods on the resulting crystallite size of the synthesized Al-based alloy. It can be seen from the graph that milling was successful in bringing down the crystallite size of the nanocomposite powder into very fine values (below 100 nm) after 20 hrs of milling. The addition of 20wt.% SiC had an apparent effect on reducing the final crystallite size further, reaching values close to 70-80 nm. This can be related to the presence of more grinding medium, and as time progresses the difference in crystallite size between 5 and 20wt.%SiC is narrowing. This might be attributed to the fact that as milling time increases the possible reduction in crystallite size becomes more difficult as the structure becomes somewhat saturated with the accumulation of defects and dislocation density raises. If milling was increased further, it is expected that the powders will reach a steady-state at different rates depending on the volume fraction of the reinforcement material. The induced internal strain following milling is presented in figure 4.4(b), and it shows that the use of 20wt.%SiC accumulated around double the strain compared to 5wt.% SiC. It has to be mentioned that these results were obtained using indirect measurements from XRD employing the Scherer equation and Williamson-Hall plot and the result can be accurate up to ±5%.

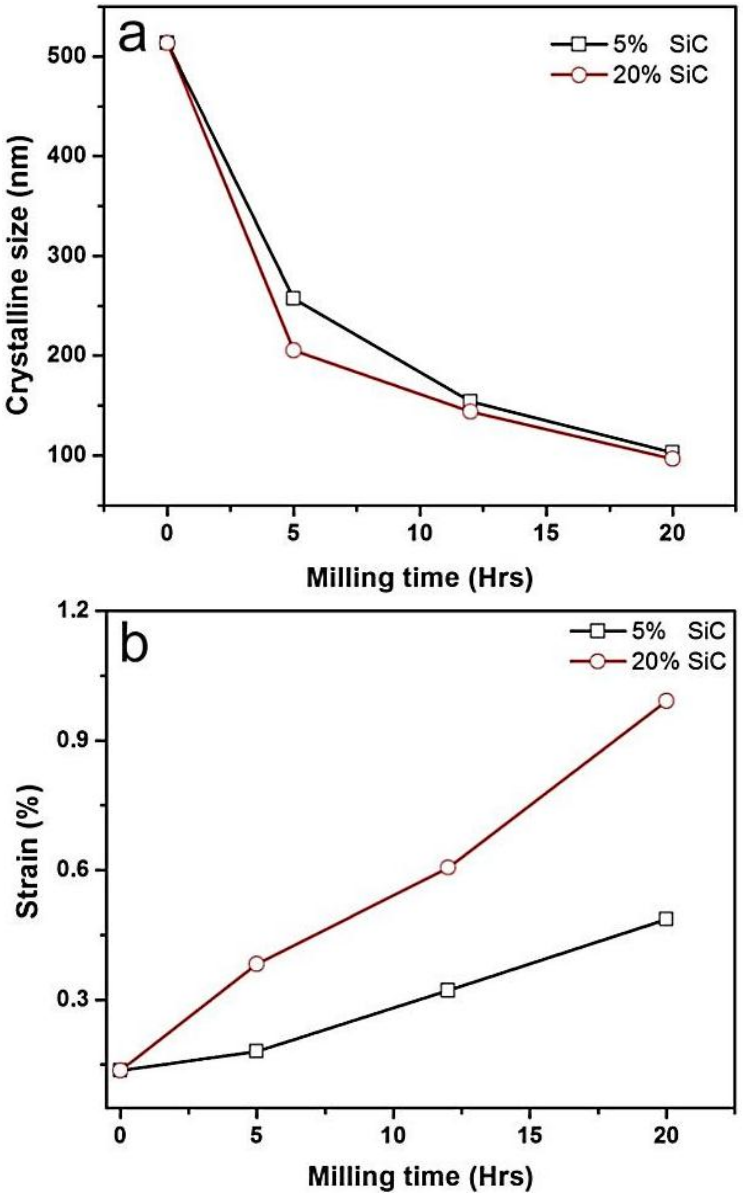

Figure 4.4 Shows (a) the reduction of crystallite size and (b) accumulation of internal strain as milling progresses with increasing SiC content for Al-7Si-0.3Mg alloy.

4.1.3 Optical Micrographs of Spark Plasma Sintered Samples

Characterized powder mixtures with optimized parameters were sintered by spark plasma sintering (SPS) by pouring powder mixture into a 20mm diameter graphite die and pressed with a pressure of 11kN (35MPa) inside the SPS before switching on the heating. After pressing the powder mixture, sintering was carried out at different temperatures of 400, 450 and 500°C. The heating rate was 100°C/min and holding time was 20 mins at the final temperatures and finally the temperature drops to 30°C within 10 min. Figures 4.5 and 4.6 shows the optical micrographs for the sintered as received alloy 1 and Al-alloy reinforced with 20 wt% SiC milled for 20hrs sintered at 400 and 500ºC respectiveliy. In figure 4.5 (a and b), some degree of porosities were observed which also corresponded to the densification data which was sintered at 400°C. However, when sintered at 500°C there was no porosity observed in the optical micrographs (figure 4.6). It is worth mentioning that as-received sample showed spherical shapes and milled samples showed elongated features which show the effect of the milling. A 100% densification was obtained as shown in the table 4.1 below (sample ID-1) in case of as received aluminum sample.

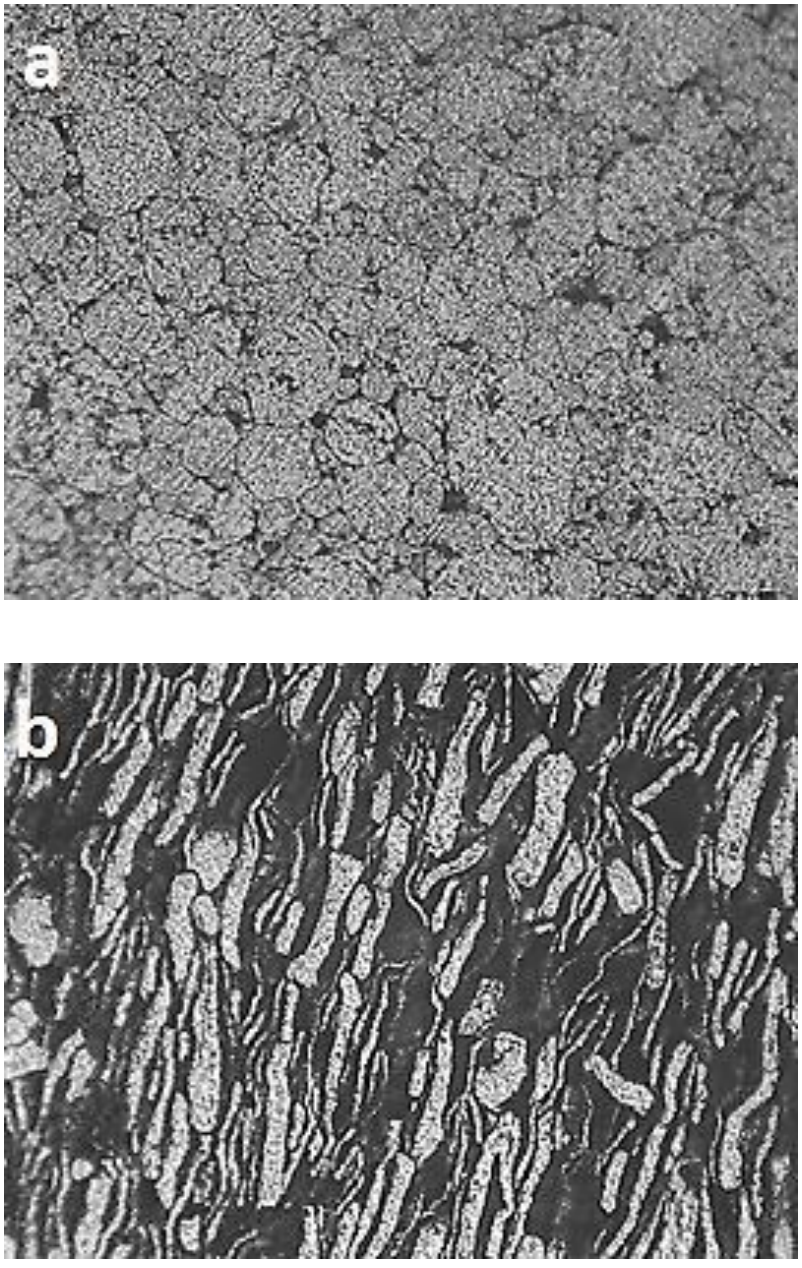

Figure 4.5 Optical micrographs from Al-7Si-0.3Mg containing (a) 0wt.%SiC (b) 20wt.%SiC sintered at 400ºC.

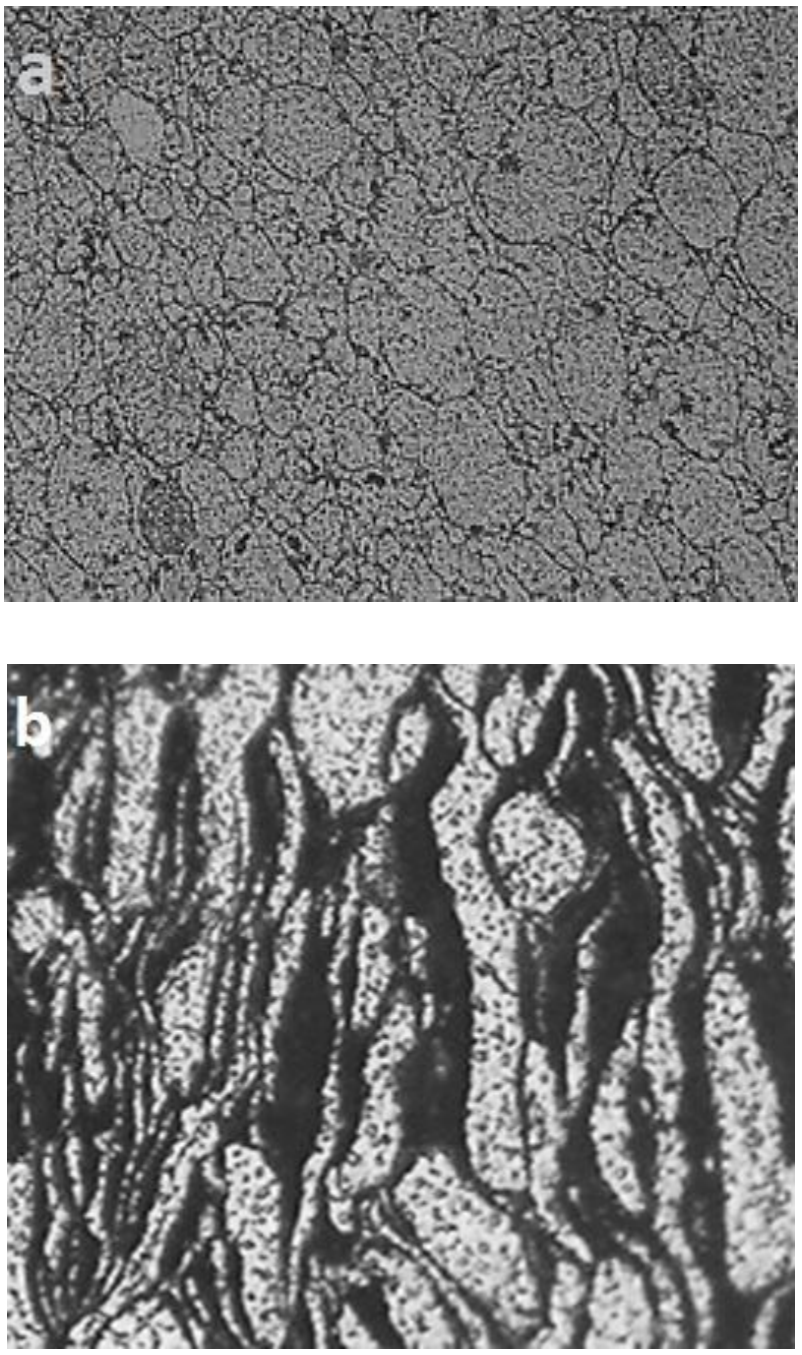

Figure 4.6 Optical micrographs from Al-7Si-0.3Mg containing (a) 0wt.% SiC (b) 20wt.%SiC sintered at 500ºC.

4.1.4 SEM Micrographs of Spark Plasma Sintered Samples

Figure 4.7 and 4.8 are SEM micrographs for the sintered samples at 400 and 500^{o}C for 20mins holding time at 35MPa and heating rate of 100ºC/min, respectively. Similar morphology was observed in SEM micrographs as shown in the optical micrographs in figure 4.5 and 4.6 above. It was observed that at low temperature (400ºC) there was small degree of porosity in the sintered samples compared to samples sintered at 500ºC as well as addition of SiC also affected the sintering and densification of the samples. It is more pronounced in the samples sintered at lower temperature at 400ºC. It was also evident that as SiC increases in the matrix dark grey region increases as it is presumed that regions are partially sintered compared to light grey region (fully sintered regions) as shown in figure 4.7 (a-d) and more apparent in figure 4.8 (a-d) at higher temperature. Similar trends were observed in the optical micrographs that light grey region (sintered region) decreases as SiC increases. This also affects the properties of the composites by mean of decrease in the densification as well as the decrease in the hardness of the composites materials.

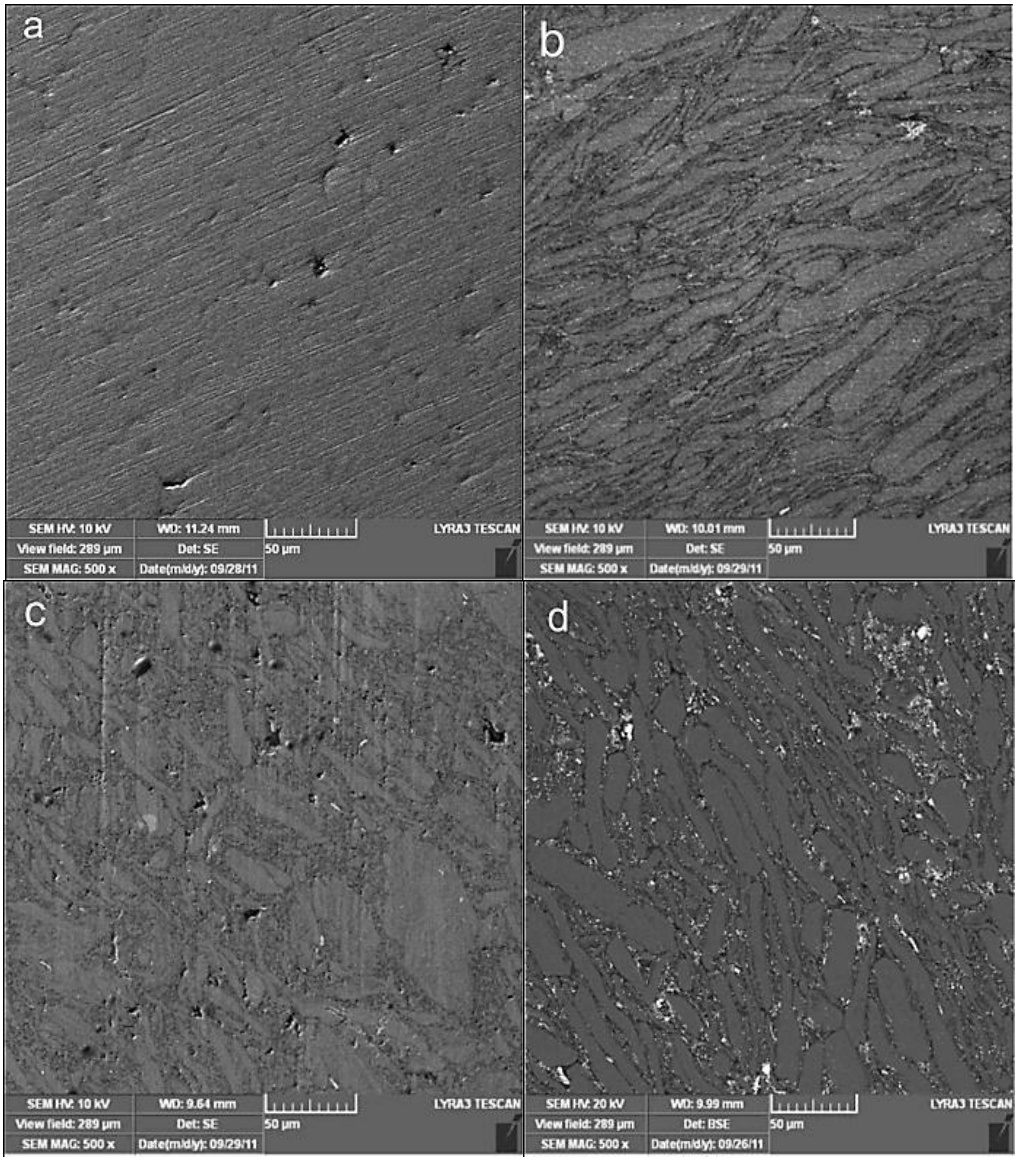

Figure 4.7 FESEM micrographs from Al-7Si-0.3Mg containing a) 0wt.%SiC b) 5wt.% SiC c) 12wt.%SiC d) 20wt.%SiC sintered at 400ºC.

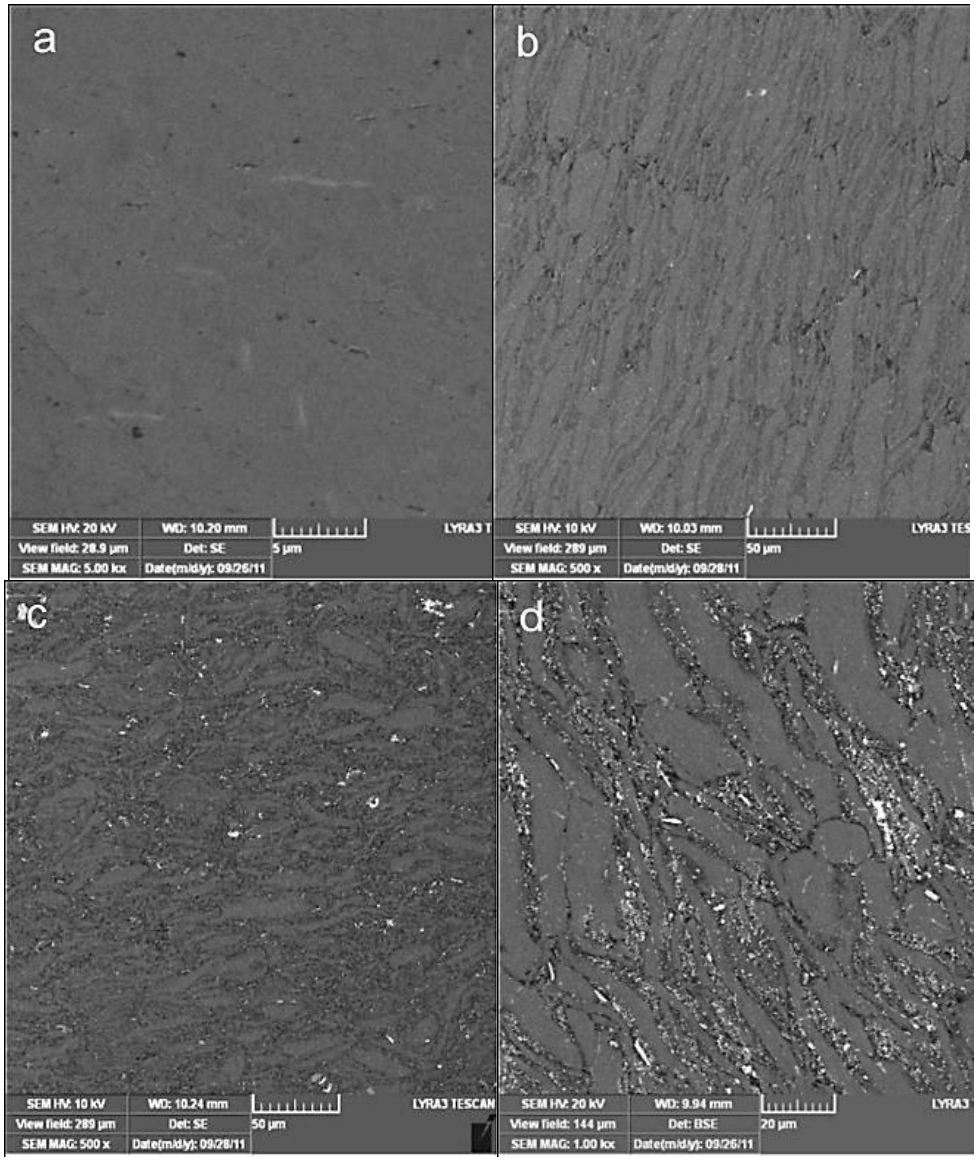

Figure 4.8 FESEM micrographs for Al-7Si-0.3Mg containing a) 0wt.%SiC b) 5wt.%SiC c) 12wt.%SiC d) 20wt.%SiC sintered at 500ºC.

4.1.5 Densification and Hardness of Spark Plasma Sintered Samples

Generally, 500^{o}C sintered samples show higher hardness and densification greater than 98%. As received monolithic alloy sample has the highest densification of 100%. However, it was found that 12wt.% SiC gives maximum values of hardness amongst all the concentration of SiC (Table 4.1 and fig 4.9b). As SiC increases to 20wt.%, both hardness and densification decreased because of partially sintered clusters in the sintered regions. However, it was found that increase of SiC more than 12wt.% may cause decrease in the densification at evaluated temperature (500°C). Therefore, it could be appropriate to increase the sintering temperature at higher concentration of SiC in the matrix or increase of the pressure (from 35MPa to higher values). Below is the table showing the hardness and densification of the SPS samples milled for 20hrs and sintered at three different temperatures and these information are represented in figure 4.9 showing the graphs of densification and hardness vs sintering temperatures for the samples milled for 20hrs.

Table 4.1 Shows the Hardness and Densification of the SPS Sintered Samples Containing 0, 5, 12 and 20wt% SiC at Different Temperatures for Al-7Si-0.3Mg (Alloy 1).

Sample ID		**Densification (%)**			**Vickers Hardness (H_V)**		
		Temperature			**Temperature**		
	SiC wt.%	400°C	450°C	500°C	400°C	450°C	500°C
1	0	94.90	99.30	100.00	41.29	57.29	63.34
2	5	93.60	97.50	98.00	57.84	66.16	70.78
3	12	91.70	95.50	97.50	62.00	70.47	74.82
4	20	89.34	92.80	94.40	48.57	63.33	68.59

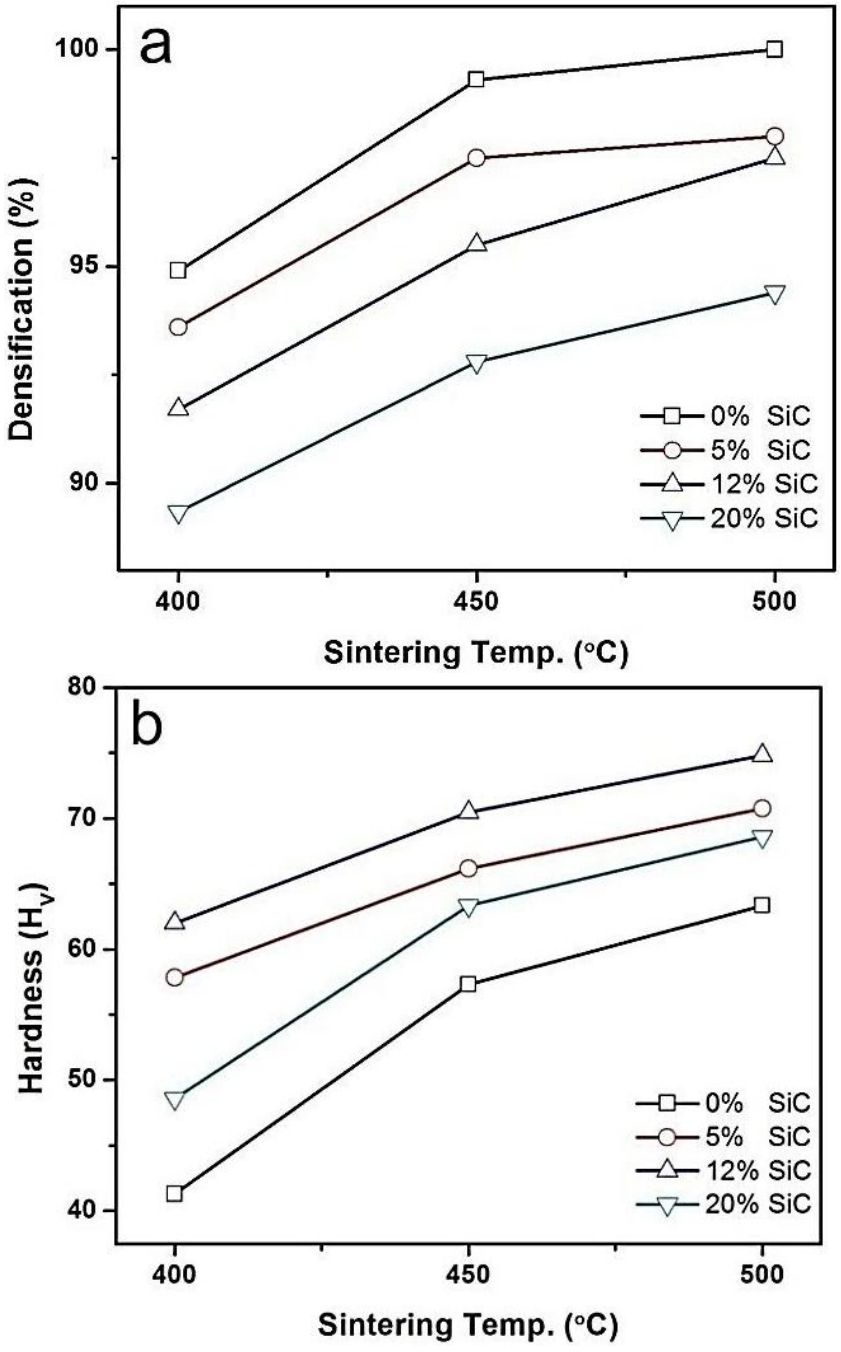

Figure 4.9 Show graphs for (a) densification and (b) hardness against sintering temperature for Al-7Si-0.3Mg with increasing SiC reinforcement.

4.2 Al-Alloy 2 (Al-12Si-0.3Mg) Containing SiC

4.2.1 SEM Micrographs of Milled Powders

Similarly trends were observed in case of the pre-alloyed Al-12Si-0.3Mg containing 5, 12 and 20wt.%SiC milled for 5, 12 and 20hrs as observed in pre-alloyed Al-7Si-0.3Mg. This is evident in the figure 4.10 as well as the EDS analysis shown in figure 4.11; more Si particles were confirmed as a result of the higher percentage of Si in the pre-alloyed Al-12Si-0.3Mg. Higher deformation was noticed as the concentrations of nano-sized SiC (average particles size 30 nm) was increased from 5 to 20wt.%, and continuous grinding of the powder resulted in reduced average powder sizes. It can also be seen that at a higher SiC concentration (of 20%SiC) and extended milling times (of 20hrs) more equiaxed particles were formed which can be attributed to the excessive and repeated grinding as observed from alloy 1. The increased milling time ensures that SiC particles are increasingly embedded into the matrix of the nanocomposite powder.

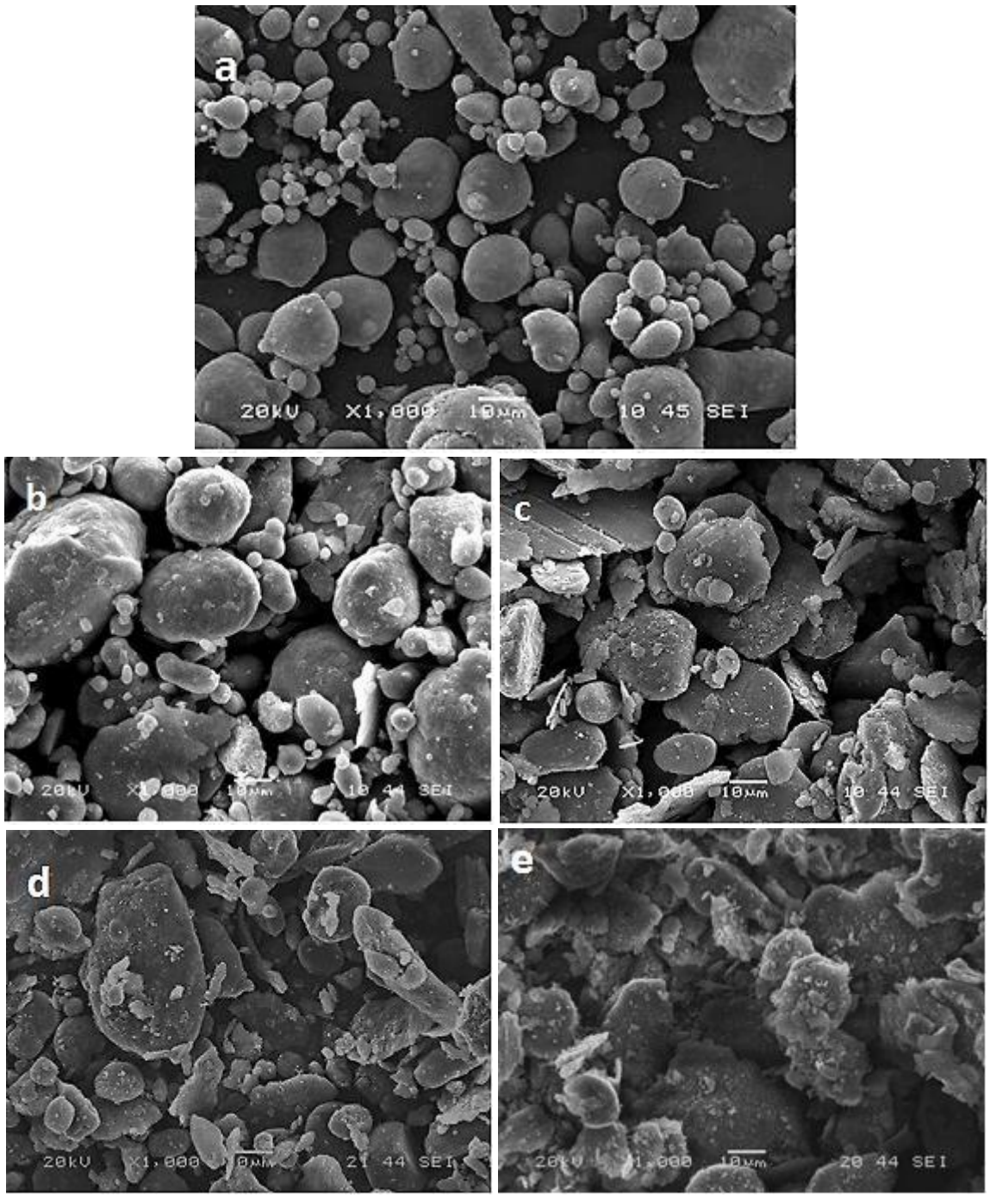
a
20kV X1,000 10µm 10 45 SEI
b
20kV X1,000 10µm 10 44 SEI
c
20kV X1,000 10µm 10 44 SEI
d
20kV X1,000 10µm 21 44 SEI
e
20kV X1,000 10µm 20 44 SEI

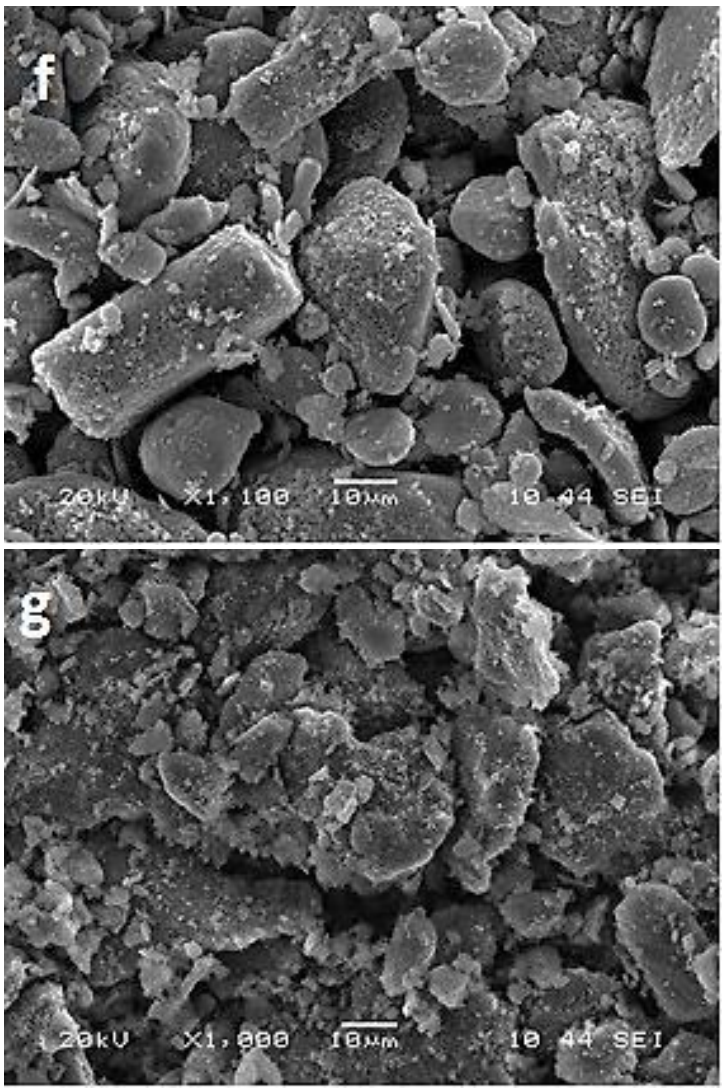

Figure 4.10 SEM micrographs of milled powders for Al-12Si-0.3Mg a) as received monolithic alloy, b-c) containing 5wt.% SiC milled for 5 and 20 hrs respectively, d-e) containing 12wt.% SiC milled for 5 and 20 hrs respectively and f-g) containing 20wt.% SiC milled for 5 and 20hrs respectively.

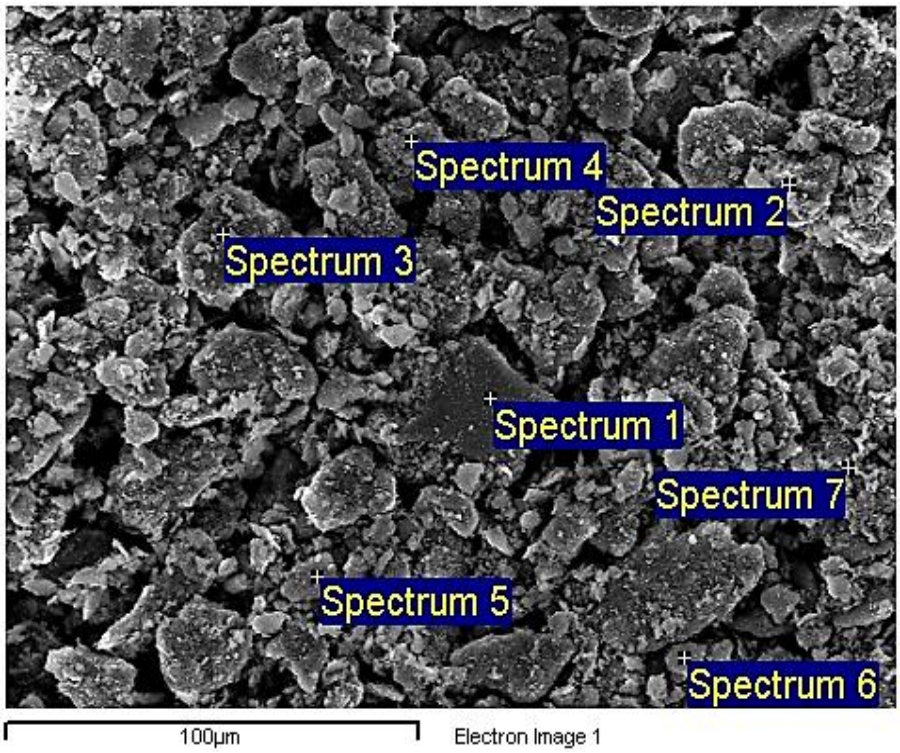

Processing option: All elements analyzed (Normalised in wt.%)

Spectrum	C	Mg	Al	Si	Total
Spectrum 1	3.11	0.00	75.62	21.26	100.00
Spectrum 2	3.51	0.00	50.16	46.33	100.00
Spectrum 3	3.68	0.00	63.54	32.77	100.00
Spectrum 4	4.29	0.00	59.77	35.93	100.00
Spectrum 5	1.81	0.00	74.35	23.84	100.00
Spectrum 6	2.36	0.00	72.29	25.35	100.00
Spectrum 7	4.92	0.00	60.09	34.99	100.00

Figure 4.11 Shows EDS Analysis for Al-12Si-0.3Mg containing 20wt.% SiC milled for 20hrs.

4.2.2 X-Ray Diffractograms of Milled Powders

Figures 4.12 and 4.13 below show XRD pattern and graphs of crystallite size and lattice strain against milling time for alloy 2 containing different percentages of SiC respectively. Similar trends were observed in terms of XRD peak broadening and the reduction in crystallite size and increase in the internal lattice strain as the reinforcement is increased.

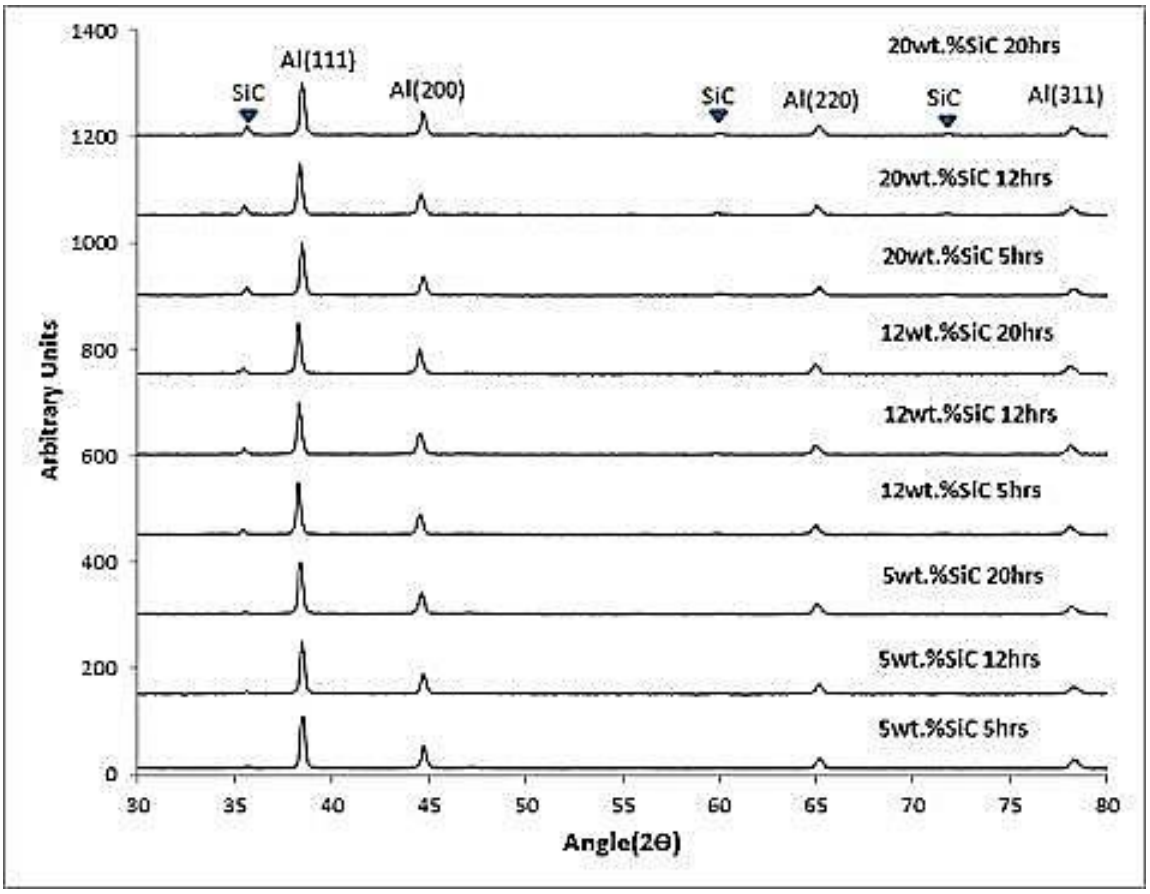

Figure 4.12 X-Ray Diffractograms for the SiC/Al-12Si-0.3Mg (alloy 2) at different milling times and different concentrations of reinforcement.

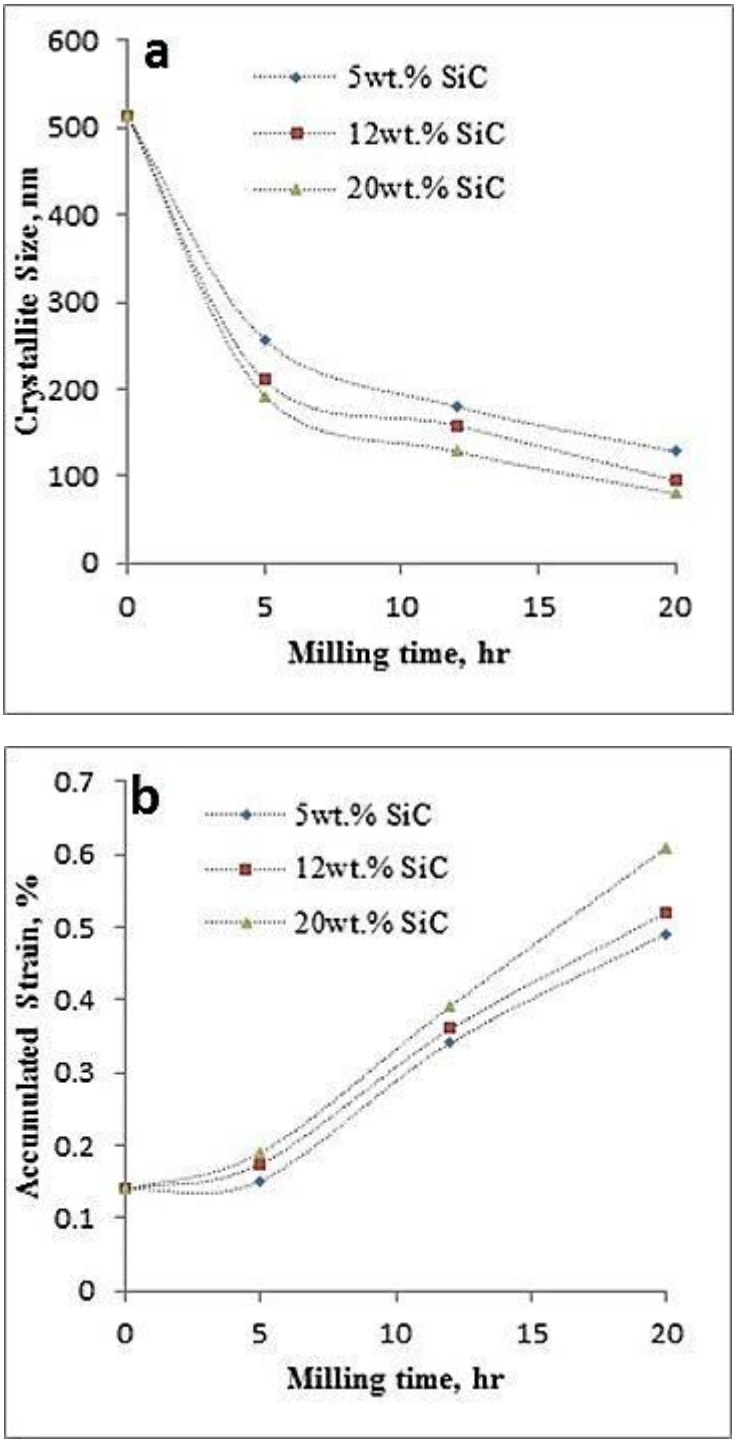

Figure 4.13 Shows (a) the reduction of crystallite size and (b) accumulation of internal strain as milling progresses with increasing SiC content for Al-12Si-0.3Mg alloy.

Particles size distribution curves and effect of the milling time on the size reduction is indicated in figure 4.14 where graph (a and b) shows that as the milling time increase from 5, 12 and 20 hours and frequency of the distribution changes and curves of the graph slightly shift towards smaller size scale. It was found that average particle size of as received monolithic alloy was ~ 38 μm which is quite similar as average size provided by the company. Milling was done for 5, 12 and 20hrs and average particles sizes were 11, 9 and 6μm respectively. Frequency of the particles distribution decreases as the milling progresses at the higher edge of particles size regime and frequency of particles distribution increases at lower edge regime. However, same drift was observed in the powders containing SiC. Similar trend was observed during SEM imaging and analysis. As the milling time increases, the particle size starts to decreases in similar fashion.

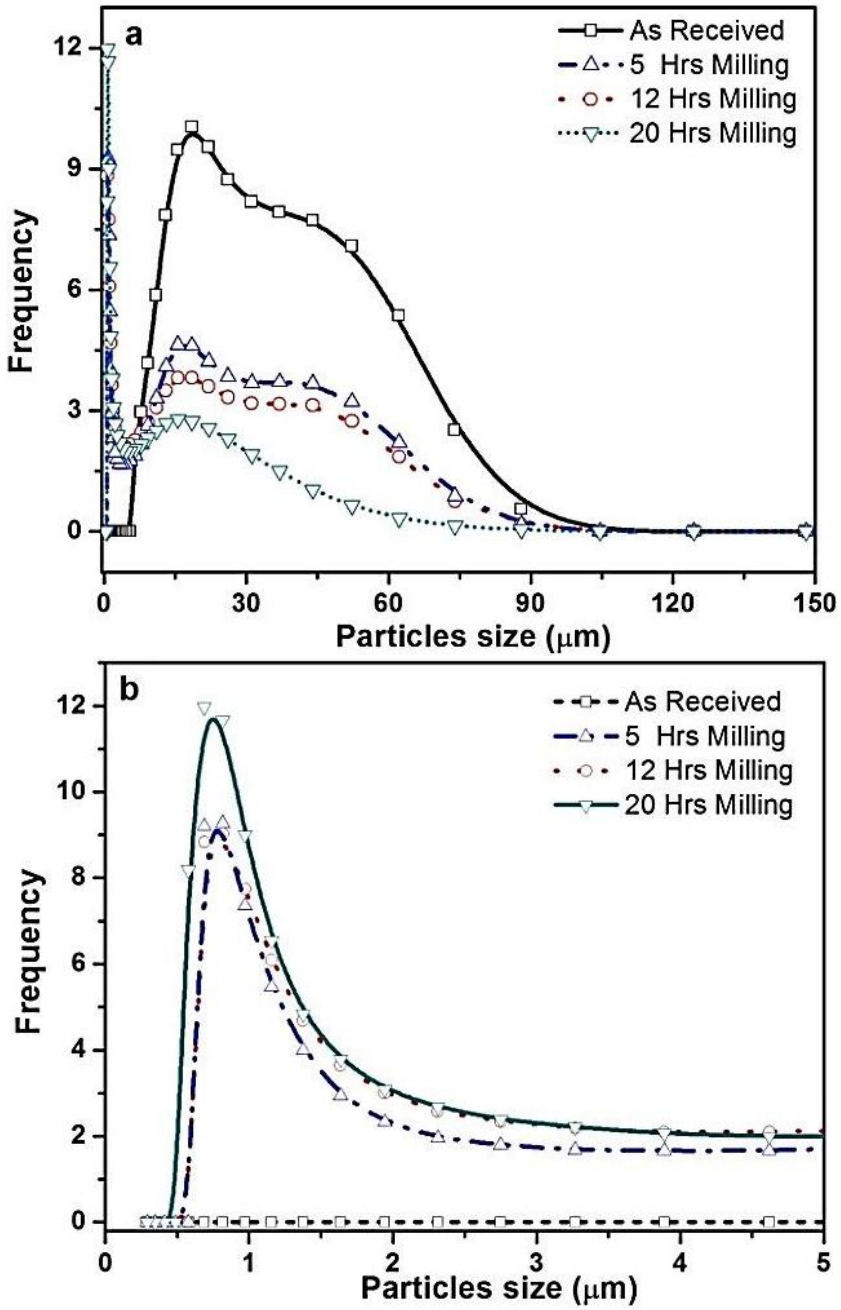

Figure 4.14 Shows (a) particles size distribution of aluminum alloy powder (b) curves at lower edge size distribution from graph (a) with increasing milling time.

4.2.3 Optical Micrographs of Spark Plasma Sintered Samples

The same parameters were employed in sintering the pre-alloyed Al-12Si-0.3Mg as in the pre-alloyed Al-7Si-0.3Mg containing SiC. It was evident by optical (light) micrographs and SP sintered samples shows unique morphologies as shown in the figure 4.15 (a and b); sintering at 400°C shows some porosity, which seen in the black regions in the figure 4.15 (b). However, the addition of SiC into the aluminum matrix shows pits and partially sintered regions were dominating in the microstructure. This may reveal lack of sintering temperature as well as low pressure parameters. Figure 4.15 (c and d) reveals microstructure of samples sintered at 500°C in the figure 4.15 (c) , resulting in much better microstructure as well improved densification than samples sintered at 400°C and 450°C. However, in the figure 4.15 (d) again little porosity was observed in the microstructure as well as partially sintered regions which make the composite weak. These observations were found in the samples containing above 12wt.% SiC in the aluminum alloy matrix.

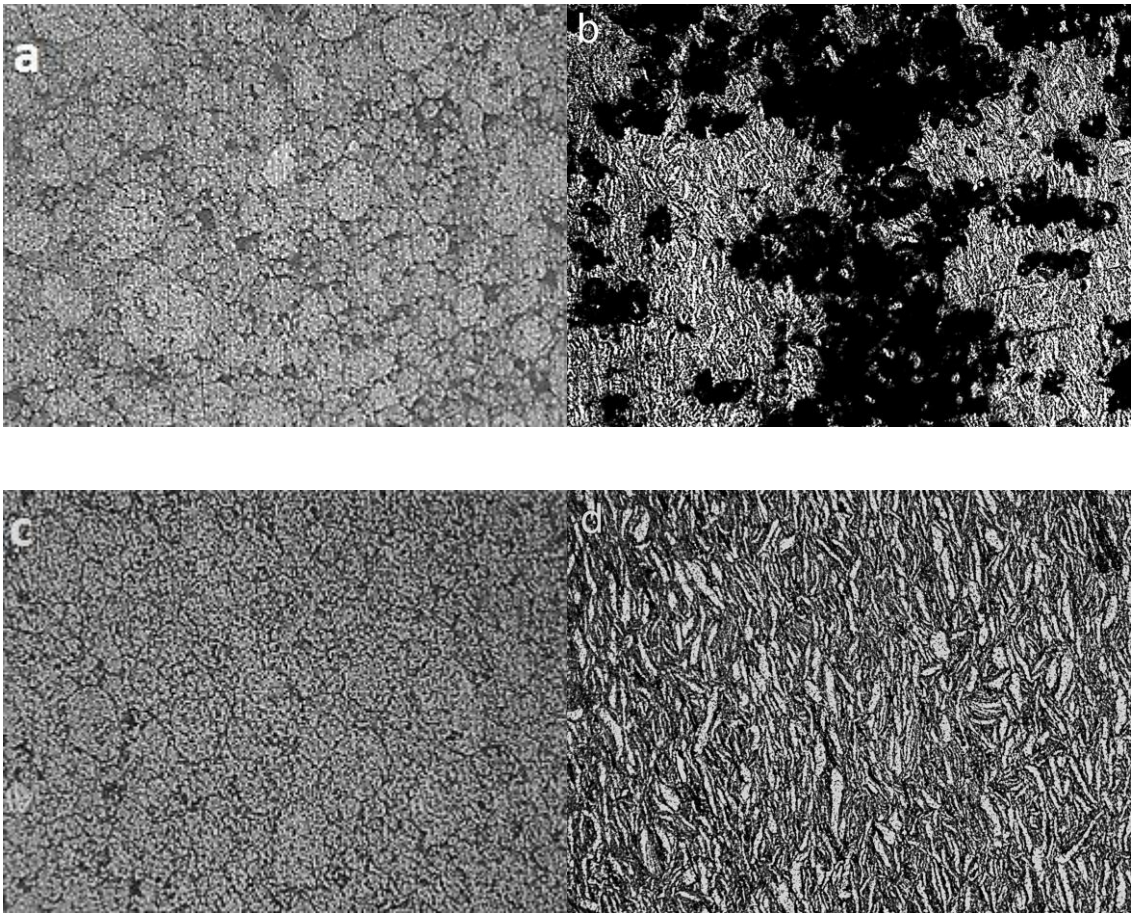

Figure 4.15 Optical micrographs from Al-12Si-0.3Mg containing (a) 0wt.%SiC sintered at 400ºC (b) 20wt.%SiC sintered at 400ºC (c) 0wt.%SiC sintered at 500ºC (d) 20wt.%SiC sintered at 500ºC. Magnified at 200X.

4.2.4 SEM Micrographs of Spark Plasma Sintered Samples

The same trends were also observed as that of alloy 1, where the porosities were more in the samples sintered at 400ºC as compared to those sintered at 500ºC. This is also evident from table 4.2 showing the densification and hardness, where samples sintered at 500ºC showed better densification of more than 98% and higher hardness.

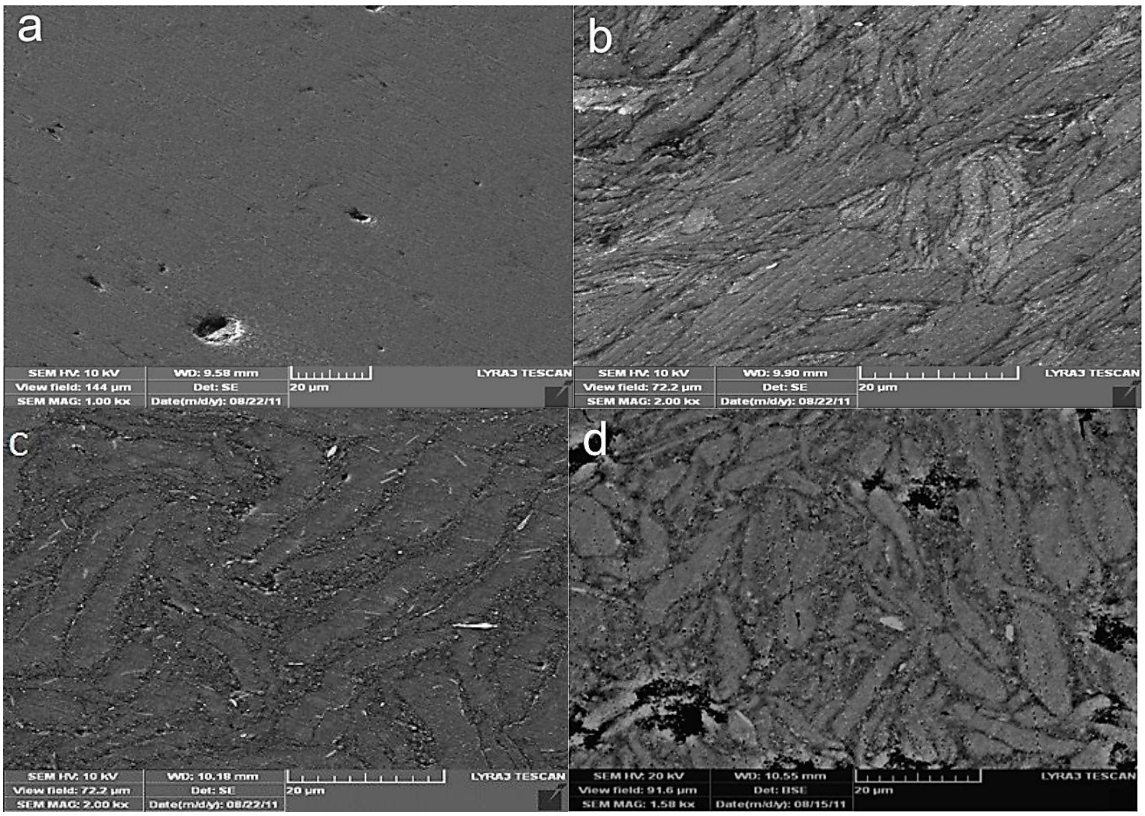

Figure 4.16 FESEM micrographs from Al-12Si-0.3Mg containing a) 0wt.%SiC b) 5wt.% SiC c) 12wt.%SiC d) 20wt.%SiC sintered at 400ºC.

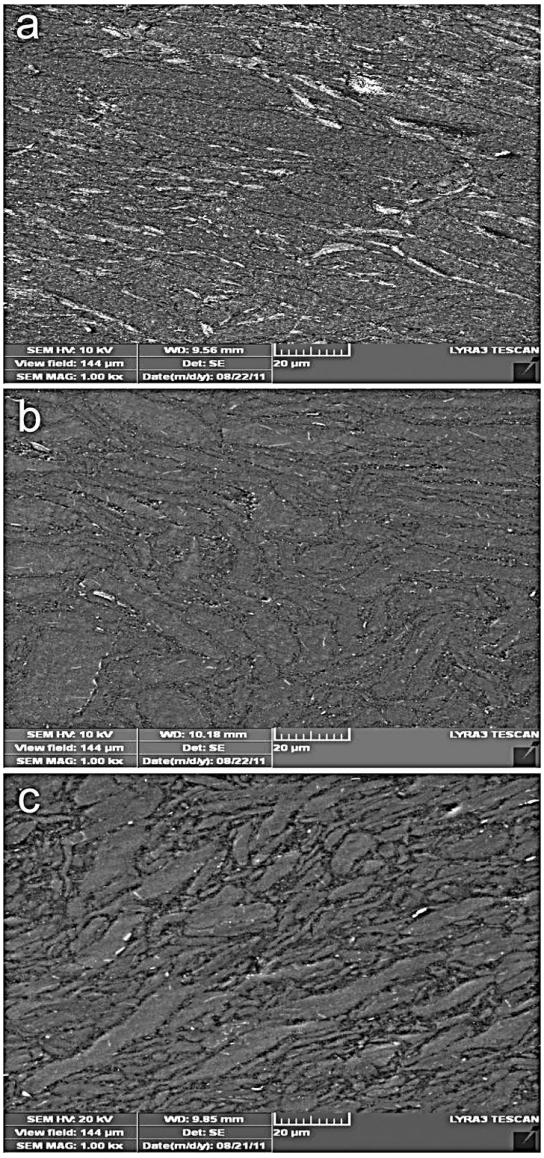

Figure 4.17 FESEM micrographs from Al-12Si-0.3Mg containing a) 5wt.% SiC sintered at 450ºC b) 12wt.%SiC c) 20wt.%SiC sintered at 500ºC.

4.2.5 Densification and Hardness of Spark Plasma Sintered Samples

Mechanical properties are greatly affected by the sintering temperatures and applied load during pressure sintering. Table 4.2 show hardness value and densification at different sintering temperatures. It was observed that sample ID (1) as received monolithic aluminum alloy without SiC, as sintering temperature increases both hardness and percentage densification increases simultaneously. At sintering temperature of 500°C, the Vickers' hardness is 63.13 and corresponding densification of 100%. Similar trend was observed with the addition of SiC but at evaluated temperatures (400, 450 and 500°C), the values were as high as 98.6, 97.8 and 95.8 containing 5, 12 and 20wt%SiC respectively. Figure 4.18 shows the hardness and densification against sintering temperatures and obviously, an increase in the sintering temperatures changes both hardness and densification and found a linear increase in both graphs whereas; curves show different concentration of the SiC present in the aluminum metallic matrix.

From the result, it was estimated that in case of 20wt.% SiC into Al- alloy matrix, the hardness and densification are not showing the proportionality trend because of higher fraction of SiC in the Al-matrix which leaves weak sintering at these sintering temperatures and similarly, densification by slowing down the sintering kinetics at particular temperatures (400, 450 and 500°C). However, quiet good trend up to 12wt.% SiC with relation to hardness and density were observed. It also shows that as the sintering temperature is increasing the densification of the composite also increases.

Table 4.2 Shows the Hardness and Densification of the SPS Sintered Samples Containing 0, 5, 12 and 20wt% SiC at Different Temperatures for Al-12Si-0.3Mg (Alloy 2).

Sample ID	**SiC wt.%**	**Densification (%)**			**Vickers Hardness (H_V)**		
		Temperature			**Temperature**		
		400°C	450°C	500°C	400°C	450°C	500°C
1	0	93.90	98.10	100.00	46.70	63.13	67.91
2	5	93.20	97.80	98.60	61.00	75.00	82.00
3	12	92.80	97.40	97.80	65.00	80.00	85.00
4	20	88.70	93.40	95.80	50.00	65.00	70.01

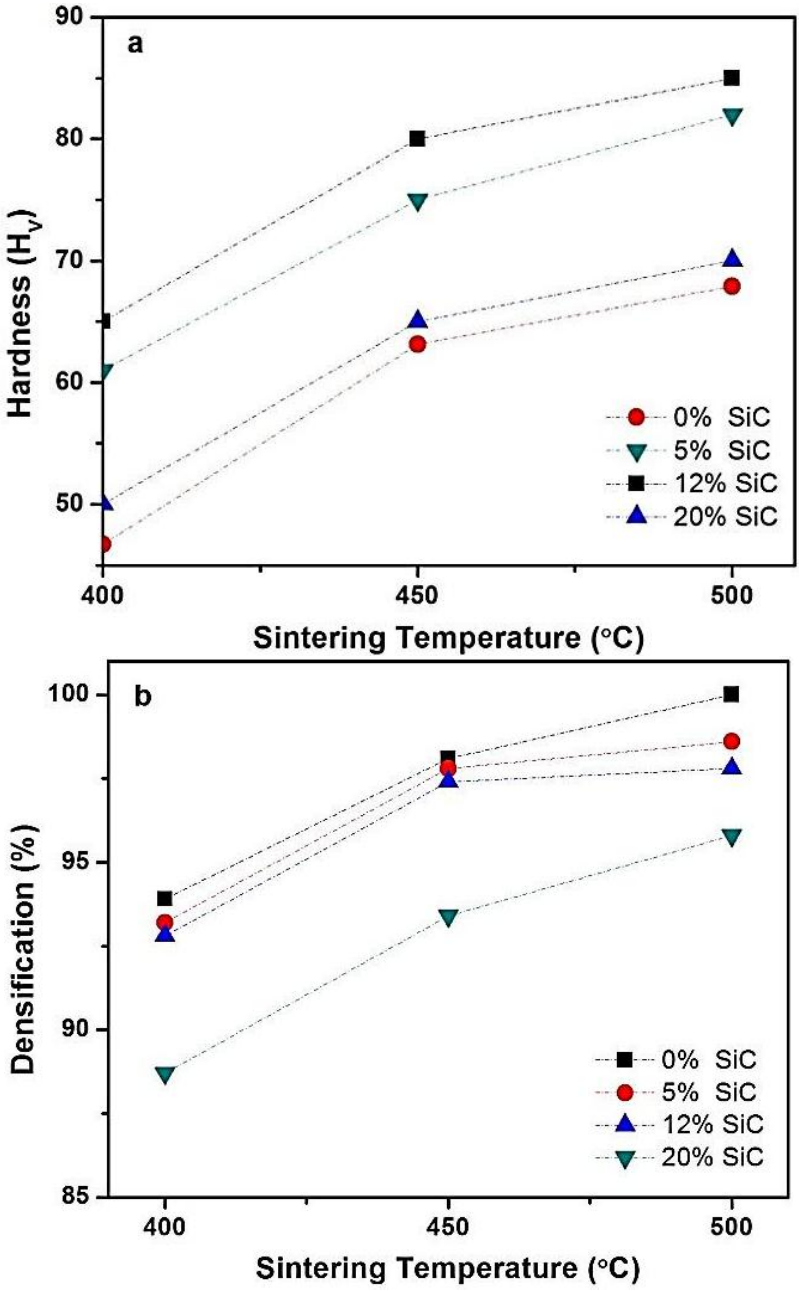

Figure 4.18 Show graphs for (a) densification and (b) hardness against sintering temperature for Al-12Si-0.3Mg with increasing SiC reinforcement.

4.3 Al-Alloy 1 (Al-7Si-0.3Mg) and 2 (Al-12Si-0.3Mg) Containing MWCNTs

4.3.1 SEM Micrographs of Milled Powders

Mixture of aluminum alloy-CNTs (both alloy 1 & 2 according to table 3.2 containing 0.5-2.0wt.% CNTs) composite powders were prepared by 1, 3, and 5hrs of ball milling. Figure 4.19 presents secondary electron SEM micrographs, showing the effect on the morphology of Al-CNT powder for samples milled during 1, 3 and 5hrs.

Figure 4.19 (a and e) shows the morphology of the as received aluminum powders (alloy 1 and 2 respectively) and figure 4.19 (b and f) shows the powder mixture containing 0.5wt% CNTs milled for 1hr for alloys 1 and 2 respectively, where segregation of CNTs were observed with agglomerations. Figure 4.19 (c and g) shows little different morphology than as received powder and shows transformation from spherical to more flattened particles because of 3hrs of ball milling and forming flake-like particles with CNTs more or less disappeared. At the later stage of ball milling, powder forms more flake-like surface of the particles. However, after 5hrs of milling, CNTs were observed on the surface of the flake-like particles (Figure 4.19 d and h). This can be suggested at this stage that the embedded CNTs in between the welded particles during 3hrs of ball milling appeared on the more flattened surface. SEM analysis revealed the presence of CNTs within the aluminum matrix. It can be seen that the CNTs appear intact after being subjected to the MA process. For the 0.5wt % CNT into the mixture, CNT clustering was observed after 1hr of milling, as shown in Figure 4.19 (b and f). This disappeared after 3 hours when the CNTs became dispersed on the cold welded surface of the particles. With the re-welding of the aluminum particles after 3hrs under the impact of the balls,

individual CNTs were observed on the surface of aluminum particles (Figure 4.19 d and h). However, this may be evident of presence of CNTs embedded in the aluminum matrix. Figure 4.20 shows SEM micrographs for both alloys containing 2.0wt.% CNT milled for 1, 3 and 5hrs, similar trends were observed as to the figure 4.19 above. Comparatively, figure 4.20 shows more CNT agglomerations which is attributed to the more CNT content, this is evident from the figure 4.20 a and b showing the morphology as well as wide spread CNT agglomeration. Generally, short milling times show CNTs agglomeration but long milling times mix and disperse the CNTs into the aluminum matrix comparative better at the expense of cold welding of aluminum. It can be suggested that long milling times can be attributed to decrease in the issue of agglomeration. Figure 4.21 shows a typical EDS analysis for Al-12Si-0.3Mg containing 0.5wt.% SiC milled for 3hrs where fluctuation of carbon content was observed which is attributed to the CNT agglomeration despite the low CNT weight percent.

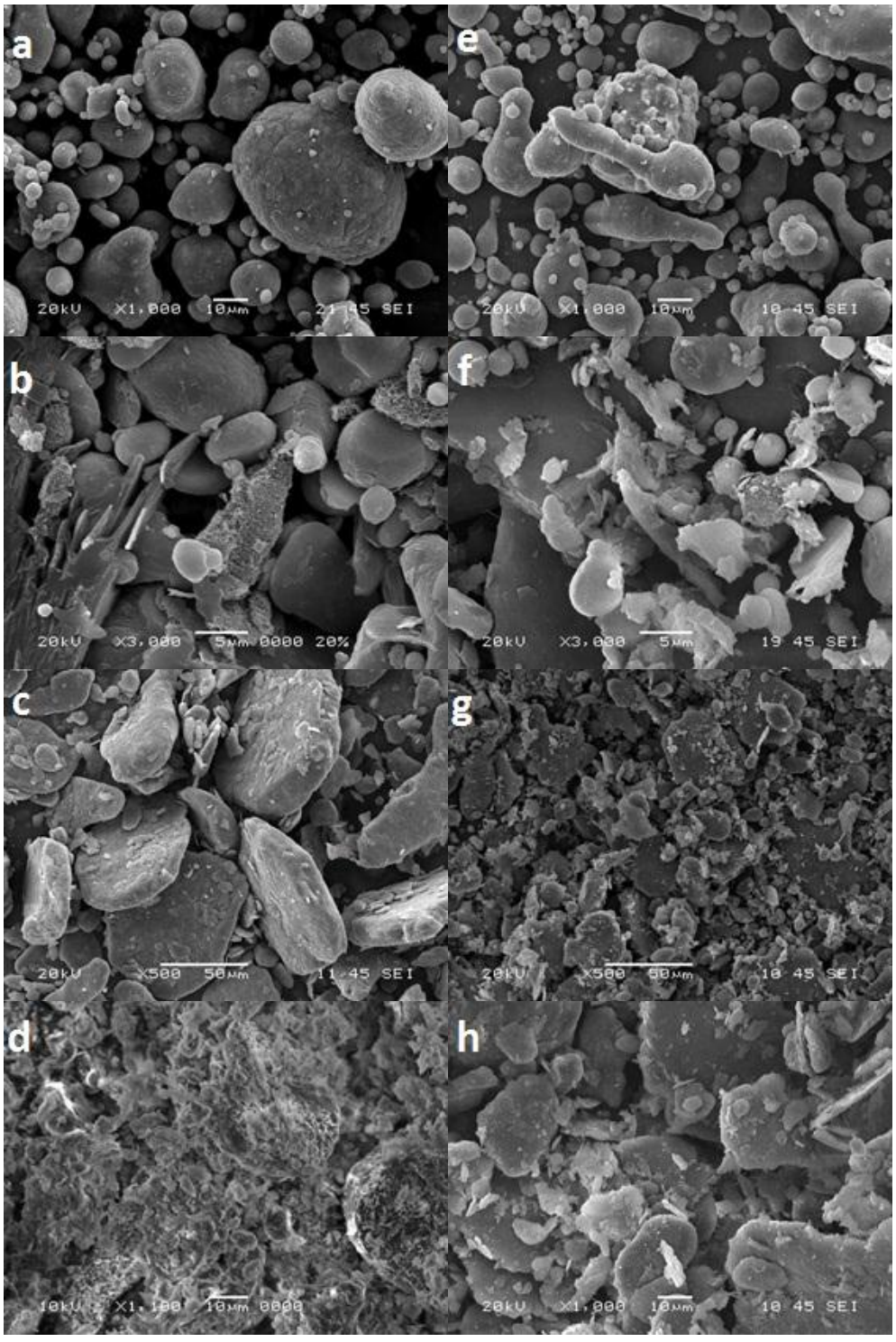

Figure 4.19 SEM micrographs from; (a) as received alloy-1 (Al-7Si-0.3Mg), (b, c, d) alloy-1 containing 0.5wt% CNTs milled for 1, 3 and 5 hours respectively (e) as received alloy-2 (Al-12Si-0.3Mg) and (f, g, h) alloy-2 containing 0.5wt% CNTs milled for 1, 3 and 5 hours respectively.

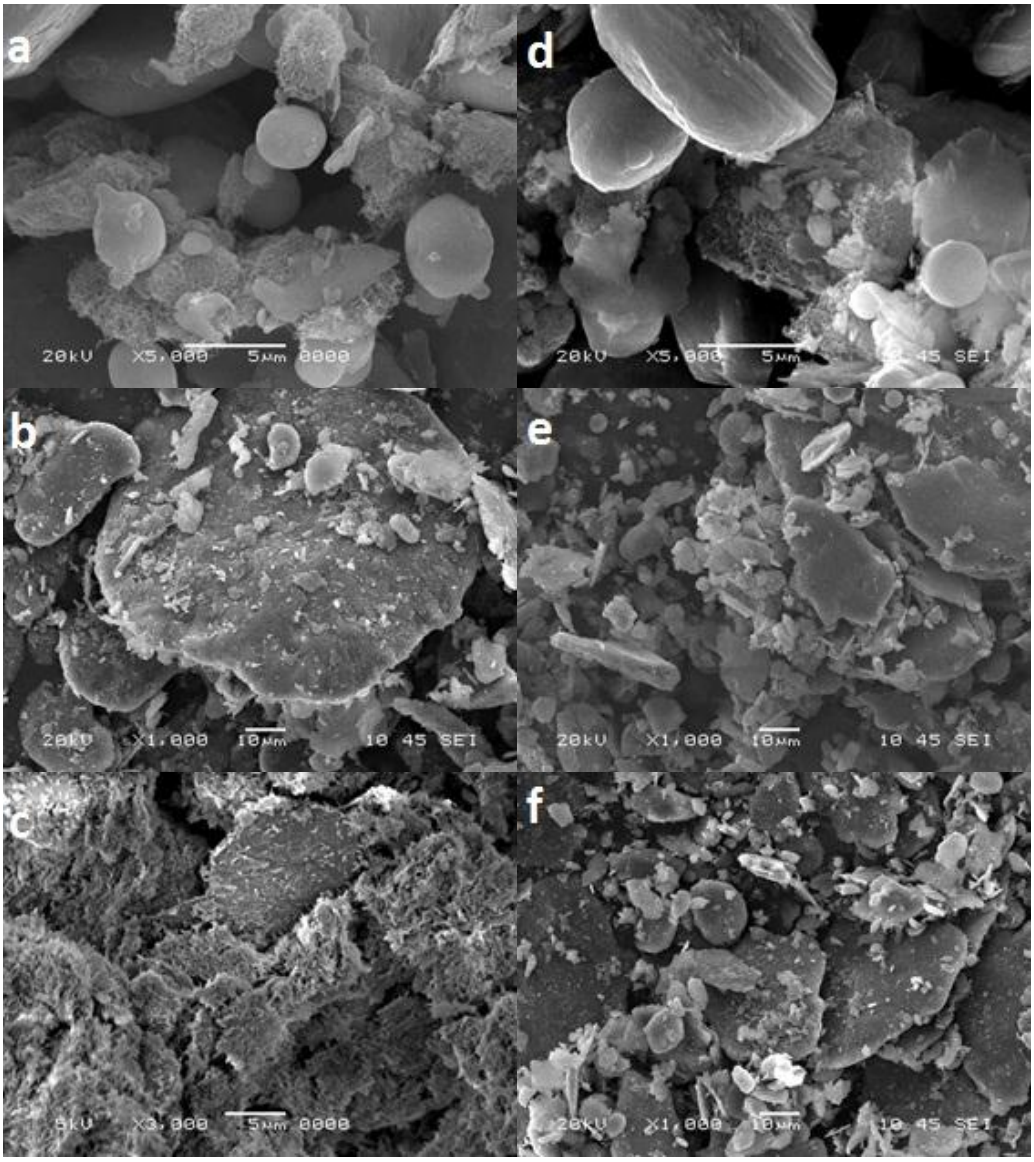

Figure 4.20 SEM micrographs from; (a, b, c) alloy-1 containing 2.0wt% CNTs milled for 1, 3 and 5 hours respectively and (d, e, f) alloy-2 containing 2.0wt% CNTs milled for 1, 3 and 5 hours respectively.

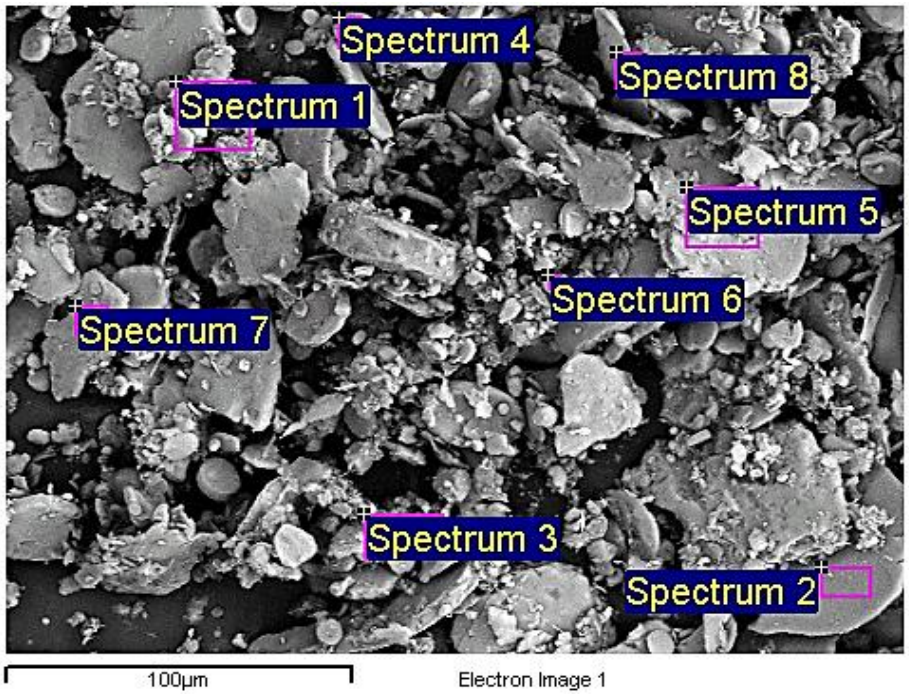

Processing option: All elements analyzed (Normalised in wt.%)

Spectrum	C	Mg	Al	Si	Total
Spectrum 1	6.74	0.78	80.19	12.29	100.00
Spectrum 2	1.56	0.47	82.93	15.04	100.00
Spectrum 3	7.77	0.00	78.39	13.83	100.00
Spectrum 4	3.52	0.40	80.26	15.81	100.00
Spectrum 5	5.69	0.42	81.98	11.90	100.00
Spectrum 6	2.92	0.52	83.34	13.22	100.00
Spectrum 7	2.35	0.45	81.74	15.45	100.00
Spectrum 8	4.14	0.51	81.24	14.12	100.00

Figure 4.21 shows EDS Analysis for Al-12Si-0.3Mg containing 0.5wt.% CNT milled for 3hrs.

4.3.2 X-Ray Diffractograms of Milled Al-MWCNTs Powder

Figure 4.22 shows the XRD spectrums of the alloy (1 and 2) as received and milled powders at different milling times (1, 3 and 5hrs). It was observed in the both alloys that as the milling time increases diffraction peaks starts to decrease in the intensity and peak broadening was observed. It was more pronounced after 5hrs of milling. It was found that the position of the diffraction lines was shifted slightly different angles for longer milling times by comparing with as received sample and similar trends were observed in the both alloy systems. Additionally, the deformation taking place during milling accumulated lattice strain and reduced crystallite size (i.e., after 5 hours of milling the crystallite size was reduced from 513 nm in the reference sample (as received alloy 1) to 192 nm). Table 4.3 and Table 4.4 shows the crystallite size and lattice stain calculated from alloy 1 and 2 containing 0.5 and 2.0wt.% CNT respectively employing the Scherer equation and Williamson-Hall plot.

From figures 4.23 and 4.24, the addition of CNT refined the structure and increased the percentage of strain. Increase in strain was observed at higher percentage of CNTs as well as reduced crystallite size. It was also observed from the XRD and calculated data in tables 4.3 and 4.4 which very much coincided with the data collected from the particle size analyzer. Figure 4.25 shows particles size distribution and it can be seen that low-edge of the curve shows low frequency but particles size of ~200nm. Figures 4.20 and 4.21 SEM micrographs also reveal some traces of particles in the similar range as found by XRD.

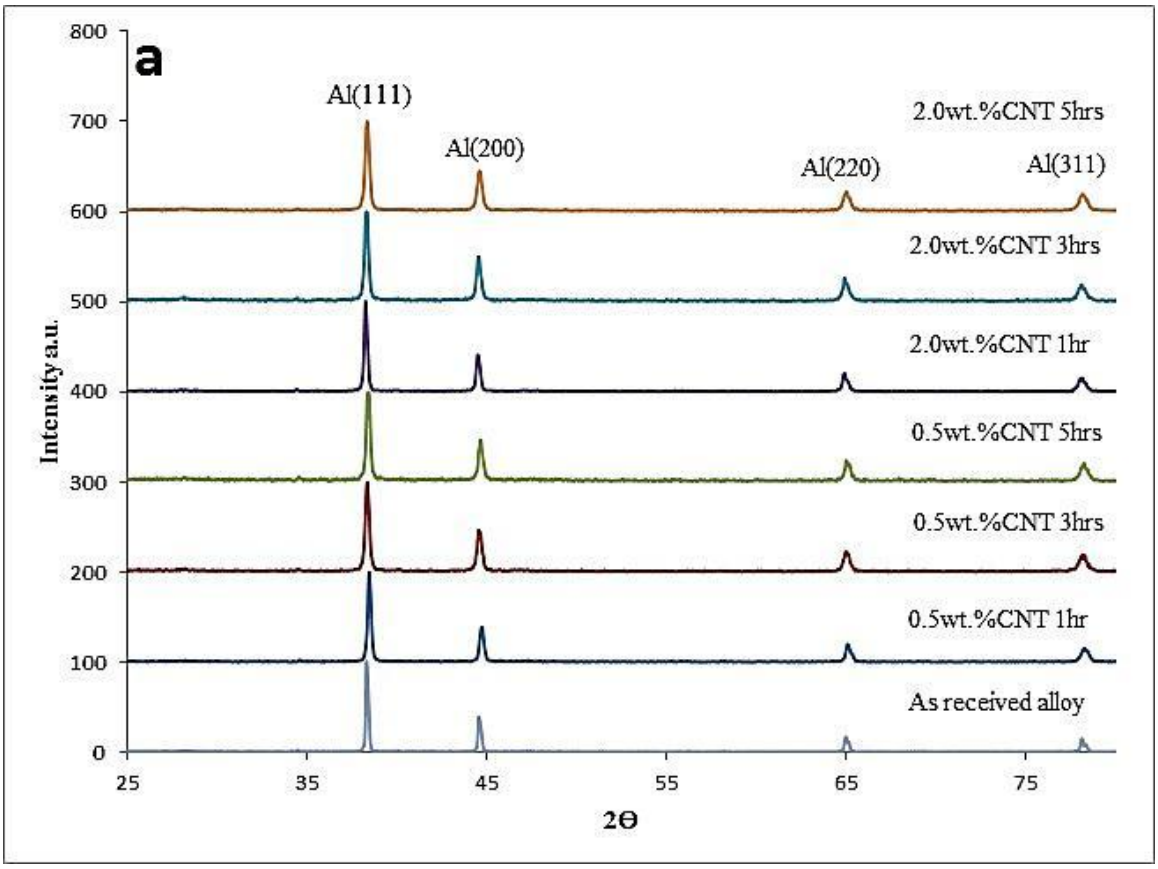
a
Al(111)
Al(200)
Al(220)
Al(311)
2.0wt.%CNT 5hrs
2.0wt.%CNT 3hrs
2.0wt.%CNT 1hr
0.5wt.%CNT 5hrs
0.5wt.%CNT 3hrs
0.5wt.%CNT 1hr
As received alloy
Intensity a.u.
2Θ
800
700
600
500
400
300
200
100
0
25
35
45
55
65
75

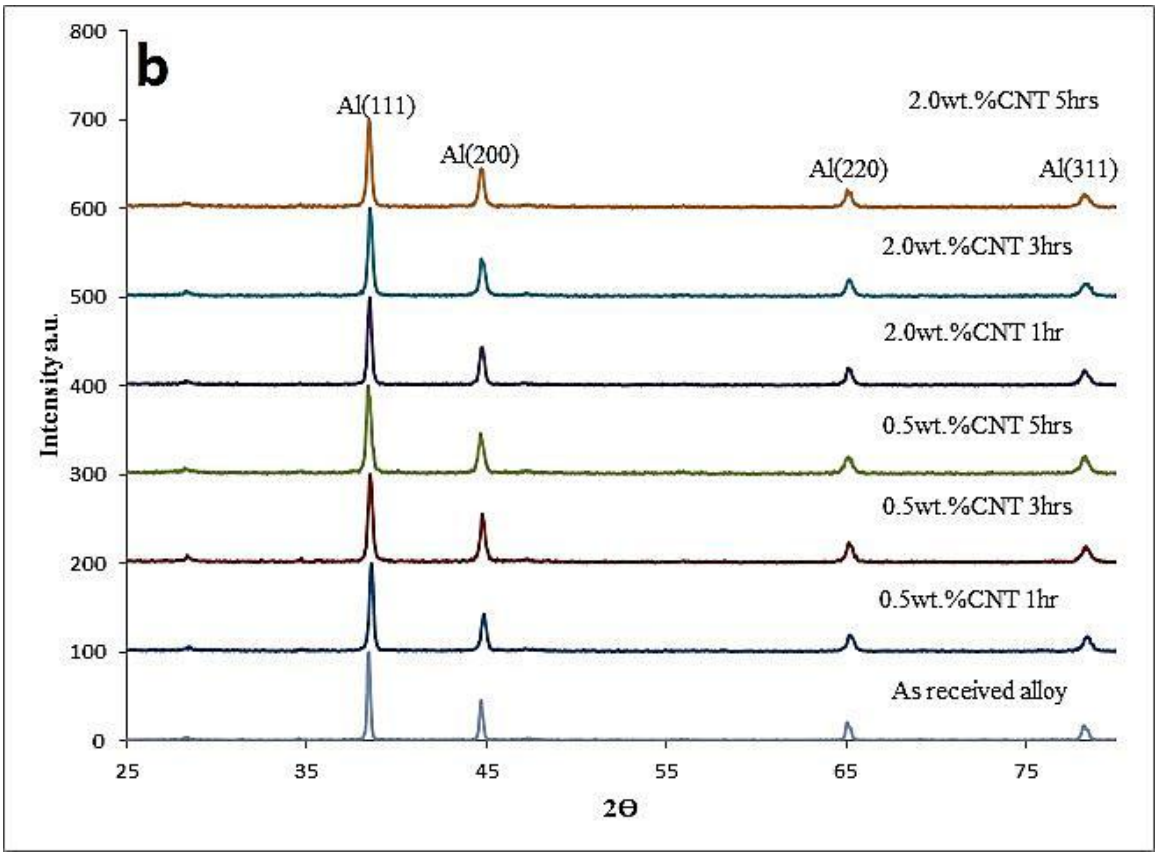

Figure 4.22 XRD spectrums of the alloy 1(a) and 2 (b) of as received powder sample and different ball milling periods.

Table 4.3 Shows the Crystallite Size and Lattice Stain Calculated from Al-7Si-0.3Mg (Alloy 1).

	Al 1 + 0.5wt.% CNT		**Al 1 + 2.0wt.% CNT**	
Milling time (hr)	**Crystallite size (nm)**	**Strain (%)**	**Crystallite size (nm)**	**Strain (%)**
0	513.52	0.14	513.52	0.14
1	385.12	0.26	375.00	0.29
3	280.11	0.42	256.78	0.50
5	192.58	0.60	154.06	0.70

Table 4.4 Shows the Crystallite Size and Lattice Stain Calculated from Al-12Si-0.3Mg (Alloy 2).

	Al 2 + 0.5 wt.% CNT		**Al 2 + 2.0 wt.% CNT**	
Milling time (hr)	**Crystallite size (nm)**	**Strain (%)**	**Crystallite size (nm)**	**Strain (%)**
0	513	0.14	513	0.14
1	308	0.30	300	0.33
3	230	0.42	225	0.47
5	150	0.65	120	0.70

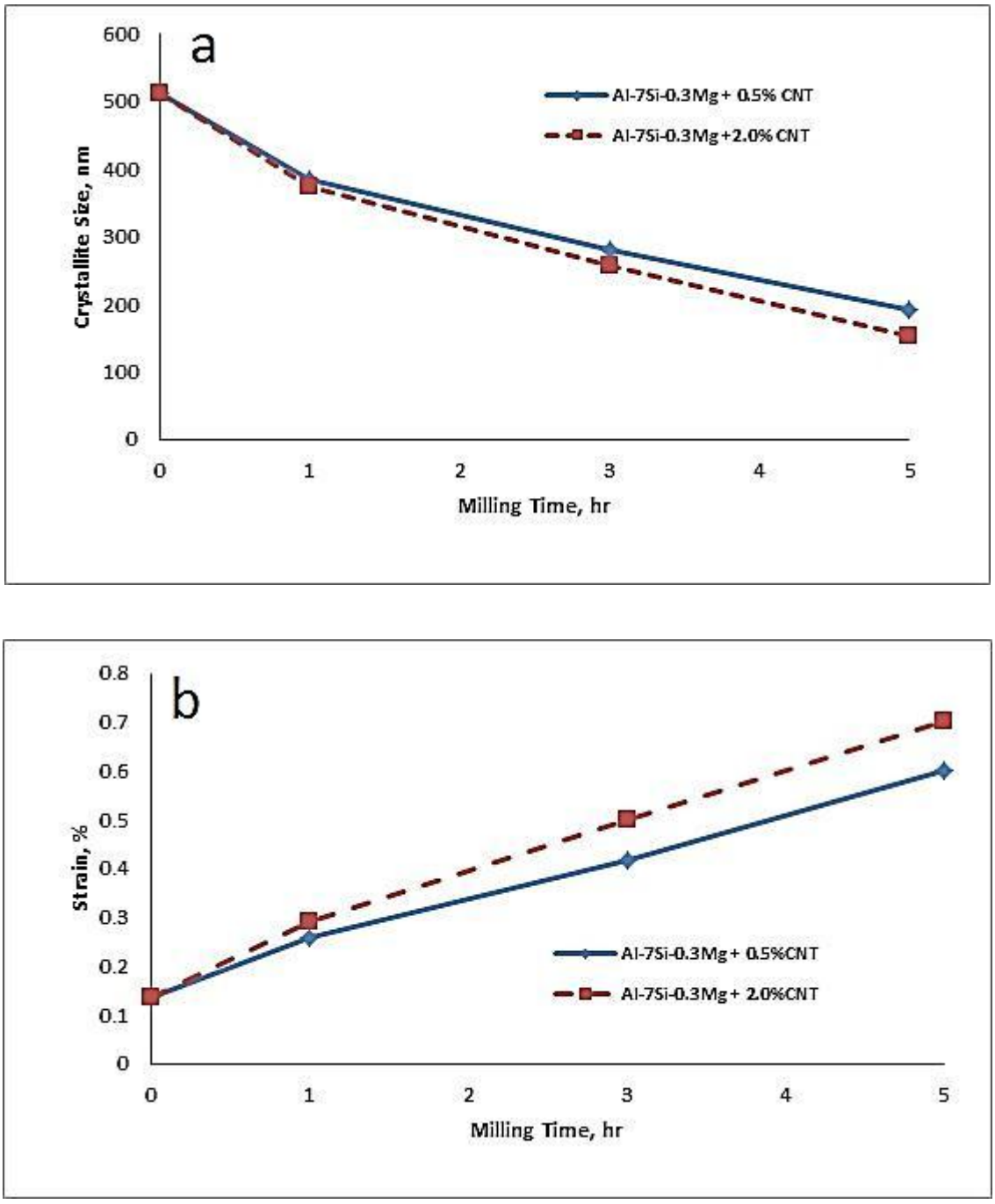

Figure 4.23 Graph showing estimation curve for crystallite size (a) and (b) accumulation of internal strain as milling progresses for Al-7Si-0.3Mg (alloy 1) containing 0.5 and 2.0wt% CNT milled for 3hrs.

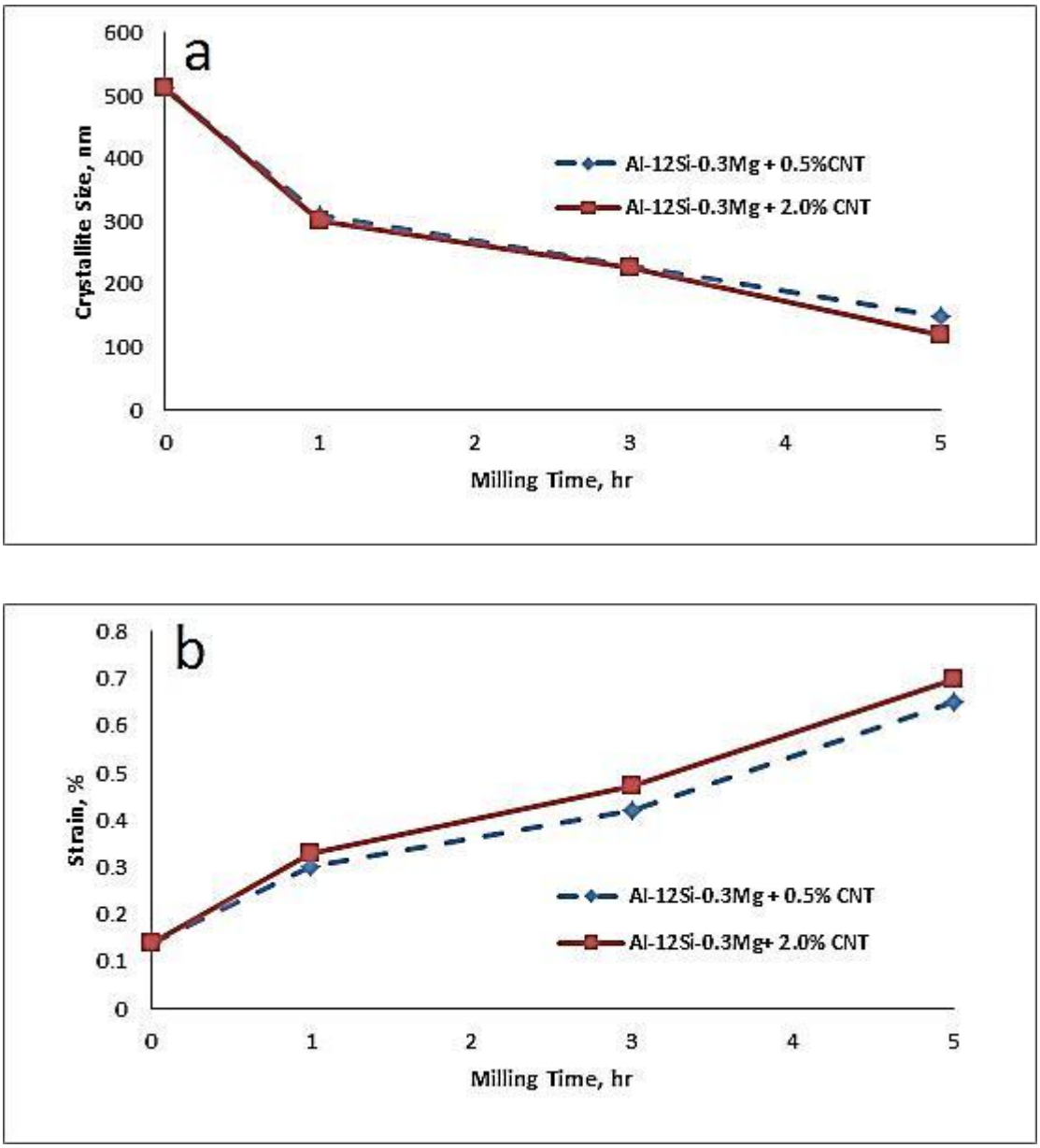

Figure 4.24 Graph showing estimation curve for crystallite size (a) and (b) accumulation of internal strain as milling progresses for Al-12Si-0.3Mg (alloy 2) containing 0.5 and 2.0wt% CNT milled for 3hrs.

The particles distribution and effect of the milling time on the size reduction is indicated in figure 4.25. Graphs below shows that as the milling time increased from 1, 3 and to 5 hours so the frequency of the distribution changed with the curves of the graph slightly shifted towards smaller size scale. It was found that average particle of alloy 1, was 33.72 μm from as received powder, and 19.99, 10.45 and 7.78μm from 1, 3 and 5hrs milling time respectively. Relatively same drift was observed in the alloy 2, where average size of the as received powder was 24μm and 18.44, 7.19, and 5.32μm from 1, 3 and 5hrs milling time respectively. Analysis also shows in both alloys (Table 3.2; alloys 1 & 2) that particles sizes were as small as 250nm. Similar trend was observed during SEM imaging and analysis. As the milling time increases, the particle size decreases. However, short milling times show CNTs agglomeration but long milling times mix and disperse the CNTs into the aluminum matrix. This is suggested that long milling times can be attributed to decrease in the issue of agglomeration.

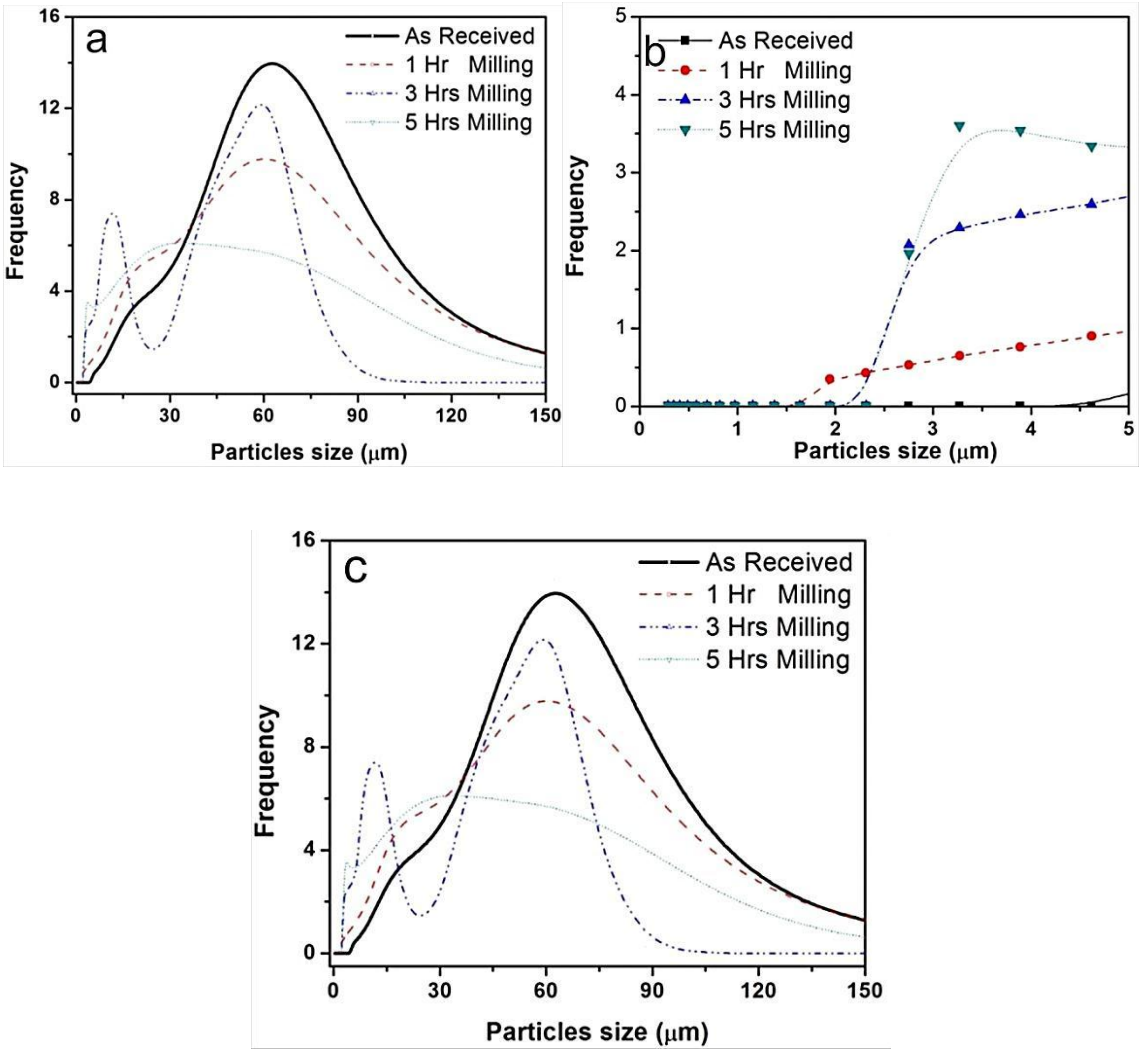

Figure 4.25 Shows (a) particles size distribution of Al-7Si-0.3Mg (alloy 1) (b) lower edge size distribution of graph (a) and (c) particles size distribution of Al-12Si-0.3Mg (alloy 2) with increasing milling time.

4.3.3 Optical Micrographs of Spark Plasma Sintered Samples

Figures 4.26 and 4.27 below shows the optical micrographs from as received and Al-alloy containing 0.5wt% CNT milled for 3hrs sintered at 500°C temperature for alloys 1 and 2 respectively and micrographs were captured at the magnification of 200X. It is evident that from the SP sintered samples at 500ºC that no porosities were observed which suggests that SPS sintering of such alloys at 500ºC is very much suitable and higher mechanical properties can be achieved. Samples sintered at a lower temperature such as 400ºC and 450ºC showed some porosities and reduced hardness and densification values as discussed in the coming sections. It was also observed that as- received sample showed spherical shapes whereas the reinforced sample showed elongated samples which can be attributed to the effect of the milling.

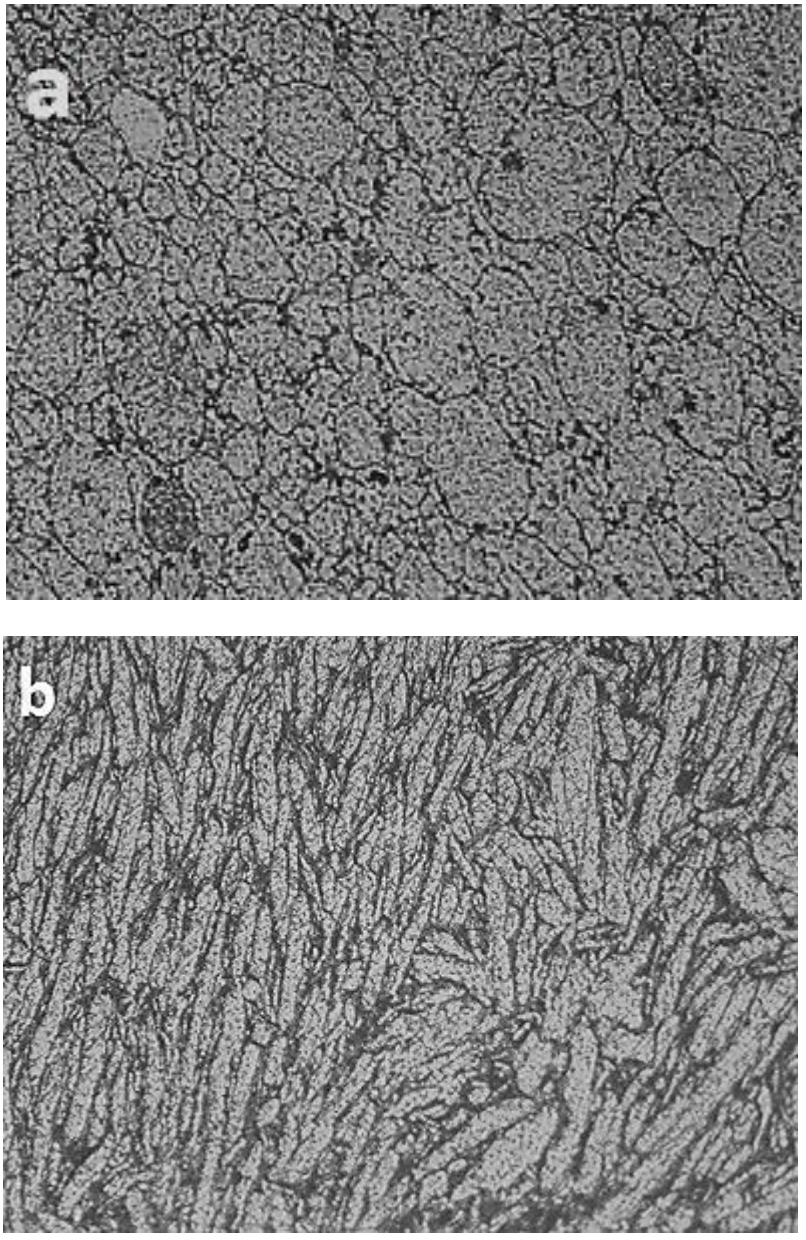

Figure 4.26 Shows optical micrographs from Al-7Si-0.3Mg containing (a) 0wt.%CNT (as-received alloy) (b) 0.5wt.%CNT sintered at 500ºC.

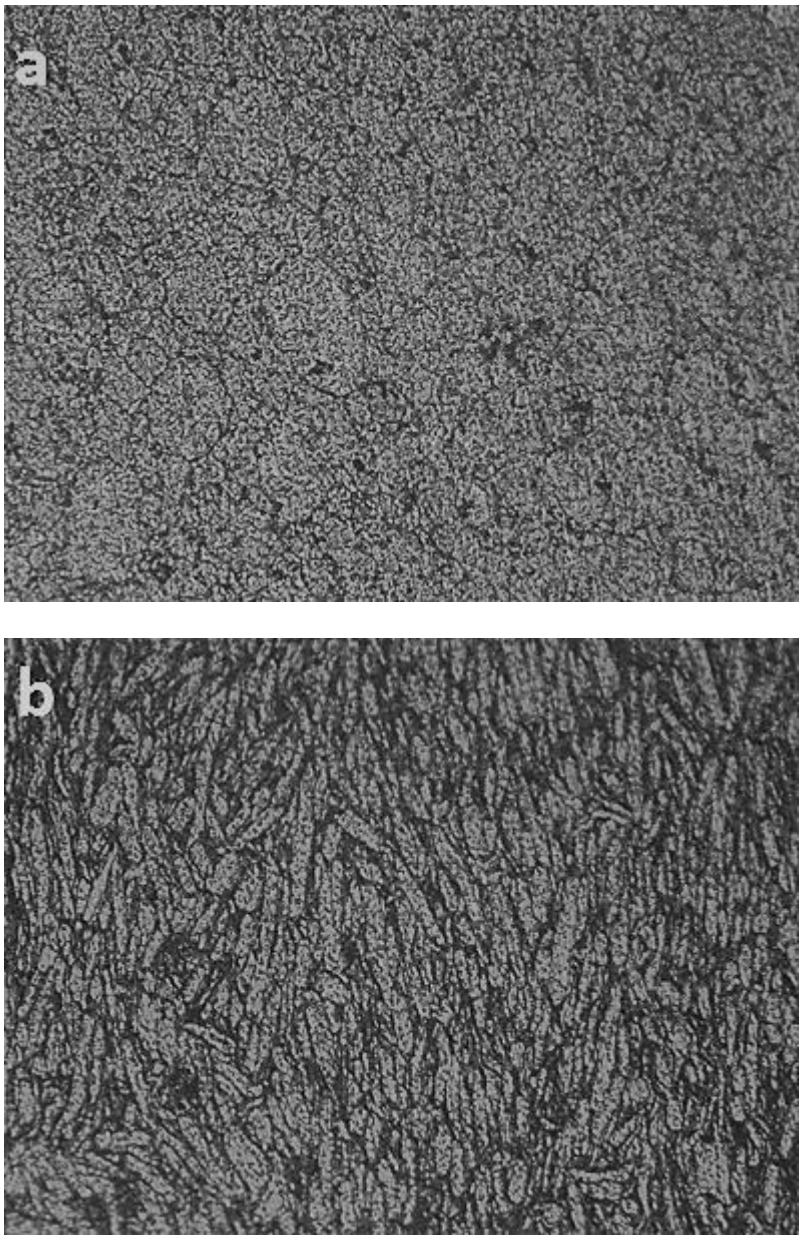

Figure 4.27 Shows optical micrographs from Al-12Si-0.3Mg containing (a) 0wt.%CNT (as-received alloy) (b) 0.5wt.%CNT sintered at 500ºC.

4.3.4 SEM Micrographs of Spark Plasma Sintered Samples

Figures 4.28 and 4.29 shows the SEM micrograph from as received and Al-alloy containing 0.5wt% CNT milled for 3hrs sintered at 400ºC and 500°C temperatures for alloys 1 and 2 respectively, as the temperature is increased the porosity decreased while hardness increased, approximately 5% porosity were observed in samples sintered at 400ºC while 100% densifications were observed for 500ºC sintered samples. This is also evident from the light (optical) images above.

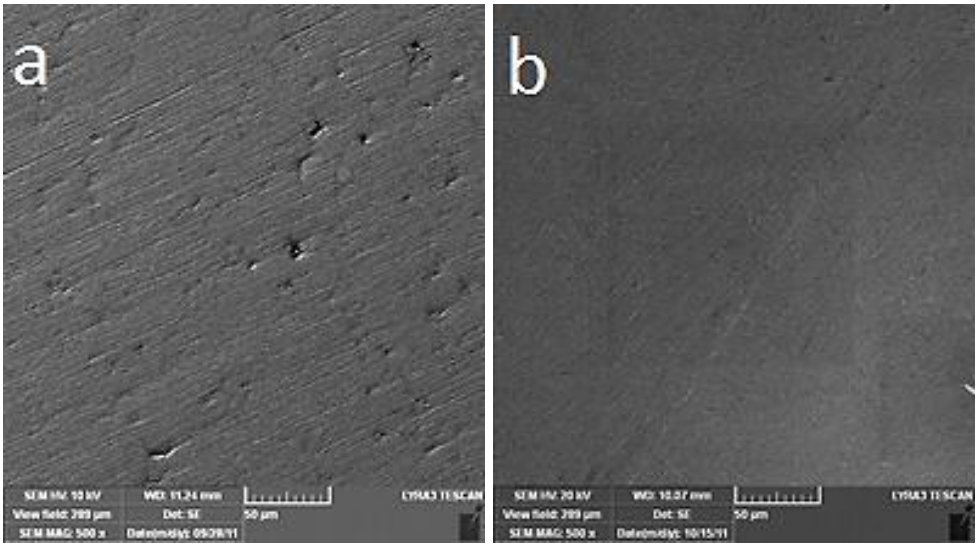

Figure 4.28 Shows FESEM micrographs from Al-7Si-0.3Mg (a) 0wt.%CNT (as-received alloy) (b) 0.5wt.%CNT sintered at 500ºC.

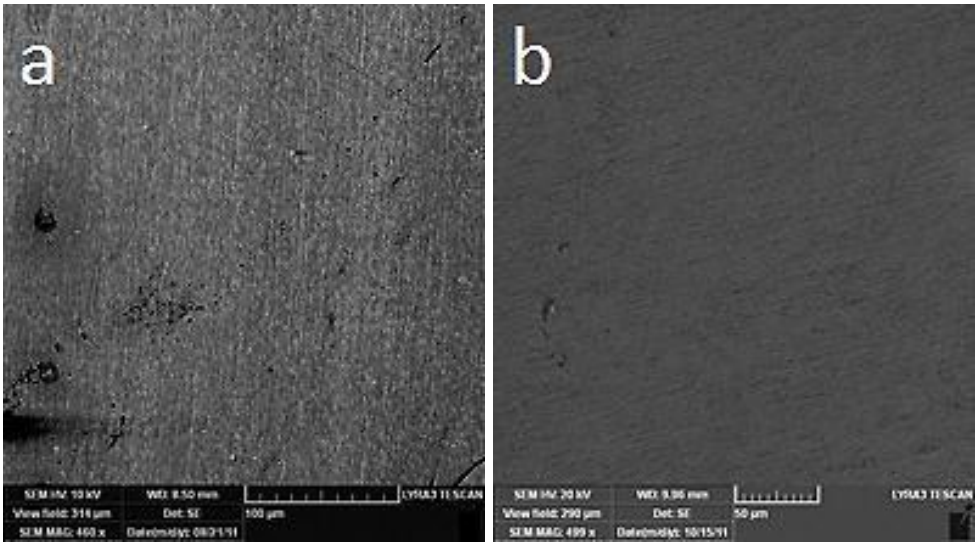

Figure 4.29 Shows FESEM micrographs from Al-12Si-0.3Mg (a) 0wt.%CNT (as-received alloy) (b) 0.5wt.%CNT sintered at 500ºC.

4.3.5 Densification and Hardness of Spark Plasma Sintered Samples

The table below shows the hardness and densification of the SPS sintered samples containing 0 and 0.5wt% MWCNTs at different temperatures using a pressure of 35MPa, 20mins holding time and a heating rate of 100ºC/min for both alloys 1 & 2. These samples were milled for 3hrs after sonication in alcohol for good dispersion of the CNTs into the matrix. From table 4.5, it was observed for both alloys that the hardness and densification increases as the sintering temperature increases with sintering temperature of 500ºC being the most suitable with 100% densification and highest hardness. The use of MWCNTs as reinforced has further increased the properties of the sintered samples recording higher hardness and densification than the monolithic as received Al-alloys. Alloy 2 showed a higher value of hardness which is attributed to the increased percentage of Si in the alloy. The graphs below show how the hardness and densifications increased with temperature and CNTs inclusions. These trends were substantiated using optical and FESEM micrographs.

Table 4.5 Shows the Hardness and Densification of the SP Sintered Samples Containing 0-0.5wt% MWCNTs at Different Temperatures both Al- alloys 1 & 2.

Sample ID		**Densification (%)**			**Vickers Hardness (H_V)**		
		Temperature			**Temperature**		
	CNT wt.%	400°C	450°C	500°C	400°C	450°C	500°C
Alloy 1	0	94.90	99.30	100.00	41.29	57.29	63.34
	0.5	96.10	99.50	100.00	59.50	61.00	68.00
Alloy 2	0	93.90	98.10	100.00	46.70	63.13	67.91
	0.5	95.60	99.60	100.00	59.00	73.00	82.00

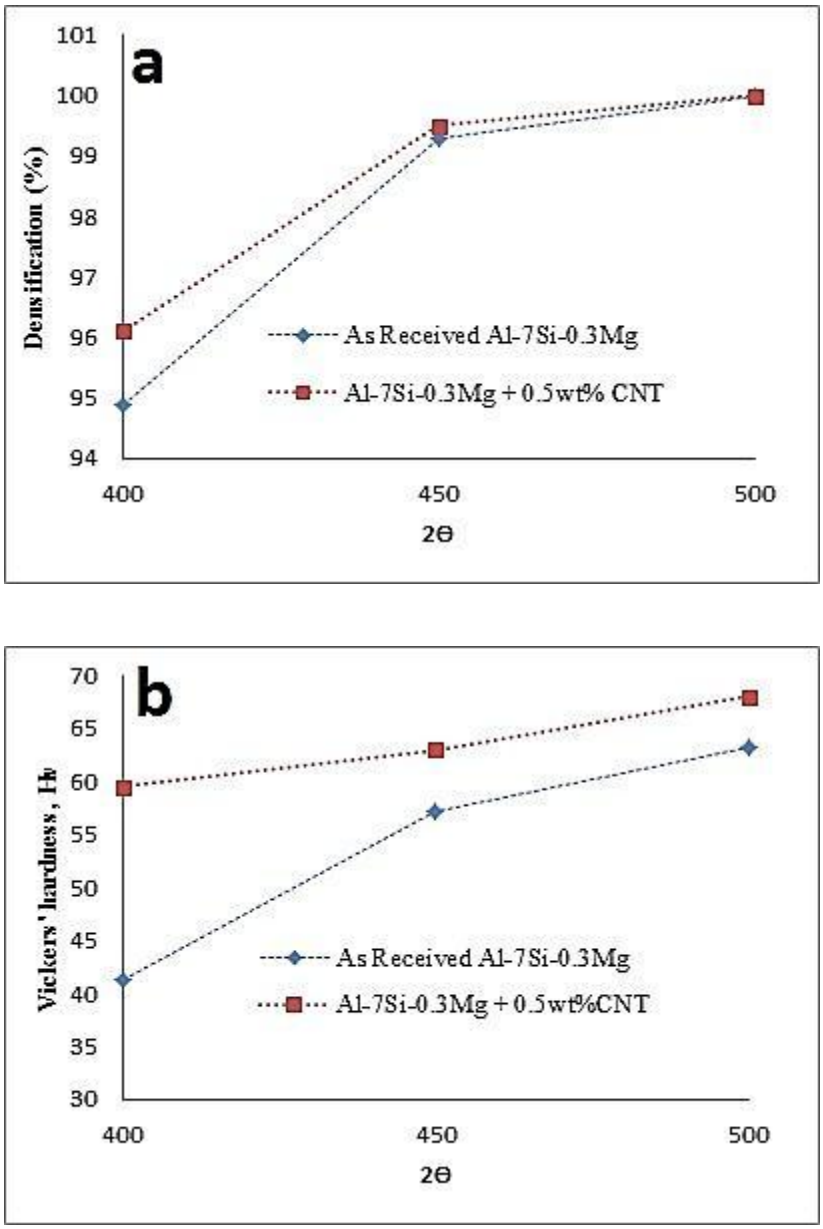

Figure 4.30 Show graphs of (a) densification and (b) hardness against sintering temperature for Al-7Si-0.3Mg (alloy 1) as a function of CNTs.

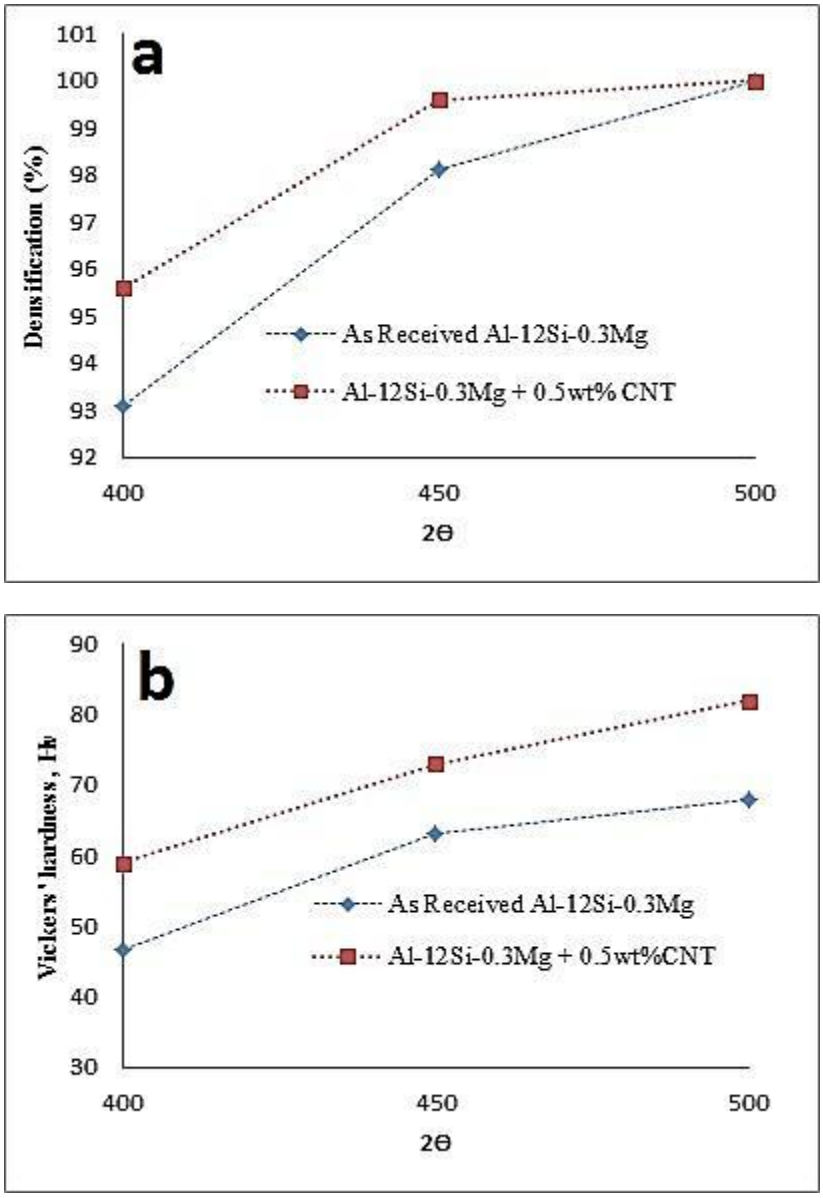

Figure 4.31 Show graphs of (a) densification and (b) hardness against sintering temperature for Al-12Si-0.3Mg (alloy 2) as a function of CNTs.

Chapter 5

GENERAL DISCUSSIONS

Pre-alloyed powders in micron size (Al-7Si-0.3Mg and Al-12Si-0.3Mg) were synthesized using mechanical alloying/milling technique reinforcing both with nano sized silicon carbide particulates (SiCp) and multiwall carbon nanotubes (MWCNTs) at different weight percentages and milled for different periods. Both alloys were milled for 1, 3 and 5hrs using 0.5, 1, 1.5 and 2.0wt.% MWCNTs additionally, they were also milled for 5, 12 and 20hrs using 5, 12 and 20wt.% SiCp maintaining ball-to-powder ratio of 10:1 in all the experiments under controlled Ar atmosphere with a 2wt% stearic acid to avoid excess cold welding. For Al/CNTs milling, sonication for 15mins was done to disperse the CNTs before wet milling. Characterization techniques such as XRD, SEM, EDS, Mapping were employed to characterize the milled powder where the crystallite sizes, accumulated strains as well as morphology and distribution of reinforcements were investigated. Furthermore, spark plasma sintering (SPS), which is a novel technique, was used to sinter both alloys using the as-received and reinforced powders at sintering temperatures of 400, 450 and 500ºC, with 20mins holding time and a pressure of 35MPa with a heating rate of 100ºC/min and cooling to 30ºC within 10mins. Further characterization of sintered samples was done using optical and field emission microscopies after which mechanical characterizations were also evaluated;

microhardness and densification using microhardness machine and densimeter respectively. It is worth mentioning that in all milling, characterization, sintering and Vickers' hardness evaluations, all parameters were kept constant to provide an avenue for comparison between both as-received and reinforced alloys. Below are some of the observations/comparisons from the work.

5.1 Powder Characterization

5.1.1 SEM Micrographs

Figures 4.1 and 4.10 shows the SEM images for Al-7Si-0.3Mg and Al-12Si-0.3Mg containing SiCp respectively where both as-received samples were showing spherical shapes with broad-sized distribution. At the early stages of milling, the resulting Al matrix was showing a higher aspect ratio after deformation with marked irregularity. As milling progressed the plastic deformation was more pronounced resulting in flake-like particles. It can also be seen for both alloys, that at a higher SiC concentration (of 20%SiC) and extended milling times (of 20hrs) more equiaxed particles were formed which can be attributed to the excessive and repeated grinding. The increased milling time ensures that SiC particles are increasingly embedded into the matrix of the nanocomposite. During EDS and mapping analyses, no compositional fluctuation was depicted into the resulting powders. EDS and mapping analysis of Al-12Si-0.3Mg showed more percentages of Si than the other alloy which is naturally attributed to the addition 5% Si in the Al-12Si-0.3Mg. In comparison with published articles, N. Zhao et al., [36] reported the effect of mechanical alloying of 8vol.% SiC distribution and the properties of 6061 aluminum composite. They concluded that a relatively homogeneous

distribution of SiC could be obtained via MA technique after 5h. Similar work from K.D Woo and D.L Zhang [41] showed the same trend with increasing milling time during the fabrication of Al-7Si-0.4Mg with SiC nanocomposites. Similar observation was observed by Kamrani et al., [38] where they studied the morphological changes and microstructural evolution occurred during mechanical alloying of aluminum and micro size SiC and also investigated the influence of particle size as milling time progressed. They found that with increasing volume fraction of n-SiC, a finer composite powder with more uniform particle size distribution was obtained. The morphology of the particles also became more equiaxed at shorter milling times. In another paper by Z. Hesabi et al., [86] they studied the effect of nanoscaled reinforcement particles on the structural evolution of aluminum powder during mechanical milling, aluminum powder of 49μm and SiC of 50nm were milled and they reported that irregular shaped particle with high aspect ratio was observed at the early stages of milling and as they milling progressed the morphology of the particles changed from the irregular to an equiaxed shape. From their SEM study, they suggested that severe plastic deformation occurred which resulted in flakelike grains and this has been noticed as the milling progressed. They concluded that with increasing the milling time results in microwelding and fracture of the work hardened particles which leads to the distribution of nanoclusters throughout the matrix. J.K Rana et al.,[51] showed similar trends. K.S. Foo et al., [87] also investigated the interface characterization of SiCp/Al6061 alloy composite and they showed from EDX and electron energy loss spectroscopy (EELS) that intermetallic compounds such as Mg_2Si and $FeSiAl_5$ were found at the SiC/Al6061 interface.

Figure 4.19 and 4.20 shows the SEM images for both alloys containing MWCNTs where the same trend was observed for the change of spherical as received powders to the flake like shapes after the milling progressed. In both alloys at higher percentage of CNTs i.e 2wt%, clustering of CNTs was observed after 1hr of milling which further disappeared after 3 and 5hrs of milling and the CNTs were significantly dispersed into the Al-Matrix though some agglomerations were also observed. Comparatively, no differences were observed in both alloys on to the distribution of the CNTs. Similar studies on the dispersion and strengthening effect of MWCNT/ Al-matrix were made by L. Wang et al., [8], R. B Srinivasa and A. Agrawal [9], A.M.K Morsi et al., [18, 21, 23, 29], H. Kwon et al., [52, 53], R. George et al., [75], D. Poirier et al., [90] and some of their conclusions were;

- Ball milling technique is an efficient technique in dispersing CNTs in Al matrix.
- The use of the curly small-diameter multi-walled carbon nanotubes (MWCNTs) in the MA prevented the agglomeration of composite powders, which is attributed to the beneficial role of the MWCNTs as grinding aids.
- After 30mins of milling, Al Particles were flattened with agglomeration of CNTs but as the milling progressed to 2h, Al particle shape were sheet-like and more equiaxed after 5hrs of milling with significant dispersion of the CNTs at high magnification.
- Despite the high aspect ratio of the CNTs, dispersing CNTs greater than 2.0wt% is difficult which affect the mechanical properties of the composite. This trend is similar to what we observed in our work.

- Sizes of CNTs and Al powders would allow fine-grinding of composite particles with uniformly distributed CNT reinforcements
- No other phases were observed after the ball milling for different periods.

5.1.2 X-Ray Diffractograms

Figures 4.3 and 4.12 shows the X-Ray Diffractograms for both Al-7Si-0.3Mg and Al-12Si-0.3Mg reinforced with SiC at different milling times and different weight concentrations of grinding medium (reinforcement), following the MA/MM process in which severe plastic deformation occurs into the powders; continuous reduction in crystallite size and increased accumulate internal strains were observed in both Al alloys with SiC, this trend is proportional to the milling time as calculated using the Scherer equation and Williamsons-Hall plot of the first three aluminum peaks. In both alloys, broadening of the peaks was observed with increasing SiC (5, 12 and 20wt.%) concentration and increasing milling time from 5, 12 to 20hrs. Crystallite size reduction and accumulated strains were observed more for Al-12Si-0.3Mg containing SiC which may be attributed to the increased Si concentration compared to the Al-7Si-0.Mg; this is evident in figures 4.4 and 4.13. Similar XRD observations were observed by S. Kamrani et al., [38], Y. Saberi et al., [39] and Z. Hesabi et al., [86] where they employed the Scherer equation and Williamson-Hall plot to quantify crystallite size as the milling progressed. They reported that the crystallite size of the aluminum matrix decreases with increasing reinforcement content while the lattice strain changes marginally which they attributed to the increased plastic deformation during milling. Z. Hesabi et al., [86] also used a particle analyzer and similar results were observed. J.K Rana et al.,[51] also used

the single peak approximation method to quantify the crystallite size and lattice strain and they reported a similar trend.

Figure 4.22 shows the X-Ray Diffractograms for both Al-7Si-0.3Mg and Al-12Si-0.3Mg reinforced with MWCNTs, similar trends were observed in terms of reduction in crystallite size and increased accumulate internal strains as the time and MWCNTs percentage increases. Reports from [38, 39, 52, 53, 75, 86, 90] showed that as the milling progressed, there was crystallite size reduction and increase lattice strains which we found in our present work by employing the Scherer equation and Williamson-Hall plot.

5.2 Sintering Behavior

From the light optical and SEM micrographs for samples containing SiC for both alloys, little porosities were observed at 400ºC temperature compared to higher temperatures of 450 to 500ºC; a densification of over 98% was observed which suggests that 500ºC temperature was suitable for both alloys in addition to a pressure of 35MPa. At the micrograph level, no differences were noticed between the two alloys.

Furthermore, both the as-received and (0 and 0.5 wt.%) CNT reinforced alloys showed an increase in densification as the temperature was increased and a 100% densification was obtained for both alloys at 500ºC, suggesting the suitability of sintering at such temperature as shown in table 4.5. This is evident from the light optical and SEM micrographs of 4.26, 4.27, 4.28 and 4.29 respectively.

Comparatively, using the 0.5wt.% gave more densification values than the SiC-reinforced samples. This may be attributed to the lower content of CNT than the SiC content used for both alloys.

5.3 Mechanical Behavior (Hardness)

The mechanical behaviors are greatly affected by the reinforcement content, milling periods and sintering parameters as well. Tables 4.1, 4.2 and 4.5 showed the properties of the sintered samples for different temperatures and weight percent reinforcements, it can be seen that as the temperature is increased, so the densification and Vickers's hardness values increased. For SiC reinforced alloys, the hardness increased significantly with SiC content up to 12wt.% after which a little decrease was observed at 20wt.% SiC which might be attributed to the lack of good sintering. For CNTs reinforced alloys, the same trends were observed.

Comparatively, alloy containing higher percent of Si in its alloying elements showed better hardness values for both types of reinforcements. The tables 5.1 and 5.2 below summarize the increase in hardness value as a function of SiC and CNT incorporation respectively as compared to the monolithic alloys at the sintered temperatures.

J.K Rana et al.,[51], K.S.Foo et al., [87],T. Schubert et al., [88], M Sherif [89], fabricated Al/SiC using mechanical alloying/milling and spark plasma sintering techniques. Below are some of the findings which were similar to the present work;

- High densifications were observed at high temperatures of 450ºC and above with less than 1% porosity.
- As received samples showed cellular structures and homogenous distribution of SiC was observed in reinforced samples via SEM and optical micrographs.
- X-ray diffraction analysis showed no forming of reactive product Al_4C_3 during the sintering process.

- Minimal grain growth was observed.
- Hardness, density and elastic moduli increases with increase in SiC content up to 15wt.% and sintering temperature. ,

From the literature, SPS technique was also employed to consolidate Al-CNT matrix and the following observations were reported.

- Densifications greater than 98% were achieved as compared to 100% from our present work at high sintering temperature.
- Increase in Vickers hardness as a result of CNT incorporation though strengthening is highest for CNT content less than 2 vol.% [9]. This is in accordance with an abrupt increase at 0.5wt.% CNT from our work and the difficulty of compacting at 2.0wt.%CNT.
- The formation of carbide (Al_4C_3) was observed as a result of reaction between the Al and amorphous carbon or the region of the graphite sheet on the CNTs [50, 52, 90].

NB: It is worth mentioning that our pre-alloyed powder Al-12Si-0.3Mg is not found in the literature as generally ‘aluminum alloy’ term is used frequently in the reviewed articles.

Table 5.1 shows increase in hardness value relative to as received monolithic alloys 1 & 2 corresponding to the sintering temperature with increase in SiC content.

		Sintering Temperature ºC		
		400	450	500
Alloy	wt.%SiC	% increase	% increase	% increase
Al-7Si-0.3Mg	5	40.0	15.5	11.7
	12	50.2	23.0	18.1
	20	16.3	10.5	8.3
Al-12Si-0.3Mg	5	30.1	18.8	20.7
	12	39.2	26.7	25.2
	20	7.1	3.0	3.1

Table 5.2 shows increase in hardness value relative to as received monolithic alloys 1 & 2 corresponding to the sintering temperature CNT incorporation.

		Sintering Temperature ºC		
		400	450	500
Alloy	wt.%MWCNT	% increase	% increase	% increase
Al-7Si-0.3Mg	0.5	44.1	6.5	7.4
Al-12Si-0.3Mg	0.5	26.3	15.6	20.8

5.4 Recommended Material

From the results and discussions, both alloys showed improved characteristics over the as received monolithic alloys as a result of addition of MWCNTs and SiC and it can be deduced that the alloy with 5% more of Si has shown further superior mechanical behaviors than the Al-7Si-0.3Mg under the same milling and sintering conditions used, this is true for both CNT and SiC reinforced systems.

For the same application, Al-12Si-0.3Mg alloy should be considered for usage with the following optimized conditions.

- Addition of 12wt.% SiC with 20hrs ball milling.
- Addition of 0.5wt.% MWCNTs with 3hrs of ball milling after sonication in ethyl alcohol.
- 500^{o}C sintering temperature with 20mins holding time and a pressure of 35MPa.

Chapter 6

CONCLUSIONS AND RECOMMENDATIONS

6.1 Conclusions

Pre-alloyed Al matrix composites reinforced with nanosized SiC and MWCNTs were synthesized using ball milling technique and sintered using non-conventional method i.e spark plasma sintering (SPS) at 400, 450 and 500ºC sintering temperature, 20mins holding time and applied pressure of 35MPa. The effect of variable milling time and secondary phases' concentration on the resulting phase evolution and morphology were elucidated as well as the effect of sintering parameters on the microstructure, densification and hardness. The following specific conclusions can be drawn:

- A good distribution of SiC reinforcement in both the pre-alloyed powders was obtained by employing ball milling technique and from the EDS analyses no compositional fluctuations were observed. This trend was similar for both alloys.
- MWCNTs can be reasonably dispersed into the metal matrix after sonication in ethyl alcohol or methanol, but, agglomeration of the CNTs is almost unavoidable with a similar trend for both alloys.
- As milling progressed with increased wt.% reinforcement, there was a continuous reduction in crystallite size and accumulation of lattice plastic strain. After 20hrs

milling time, the crystallite size of Al-alloy reached a value around 70-80 nm for Al-7Si-0.3Mg (alloy-1) containing 20wt.%SiC and this addition induced more than double the amount of internal strain of about 1% into the alloy matrix. A related trend was observed for SiC reinforced Al-12Si-0.3Mg (alloy-2).

- Increasing content of MWCNTs from 0.5 to 2.0wt.% into both prealloyed powder and increasing the milling time, resulted in similar reduction in crystallite size and accumulation of internal strain; at 0hr for Al-7Si-0.3Mg with 2.0wt.%CNT, the size and strain were 513nm and 0.14% respectively and at 5hrs of ball milling the values were 154nm and 0.7% respectively. A parallel behavior was observed for the other alloy.
- 100% densification and fine microstructures were obtained using spark plasma sintering technique at temperature of 500ºC for both alloys. As received samples showed 100% densification for both alloys and above 98% for the reinforced samples at 500ºC.
- High hardness values were obtained with increase in the amount of reinforcement; i.e from 0, 5 to 12wt.%SiC and up to 0.5wt%CNT sintered at 500ºC. A Vickers' hardness value from 68 to 82 and to 85 was measured with alloy 2 containing 0, 5 and 12wt.% SiC respectively at and a value of 68 to 80 with the incorporation of 0.5wt.% CNT. A related trend was also observed for alloy-1 containing similar wt.% of reinforcements.

6.2 Recommendations

Based on the wide scope of such experiments from applications points of view the following recommendations are paramount in any future work using these techniques.

- More efficient techniques should be investigated for a better dispersion CNTs into MMCs where agglomeration is still an issue.
- Compressive and tensile properties should be investigated to further characterize the composites' mechanical behavior.
- Tribological property investigation would be useful as these composites are for structural applications were tribological behaviors are paramount.
- Computer simulations would be also useful to predict the morphology and properties of the milled and sintered sample respectively.

REFERENCES

[1] J. M. Torralba, C. E. da Costa, F. Velasco, 'PM aluminum matrix composites: an overview'. Journal of Materials Processing Technology, Volume 133, Issues 1-2, 1 February 2003, Pages 203-206.

[2] T. Moons, P. Ratchev, P. De Smet, B. Verlinden, P. Van Houtte, 'A comparative study of two Al---Mg---Si alloys for automotive applications'. Scripta Materialia, Volume 35, Issue 8, 15 October 1996, Pages 939-945.

[3] J. Xiao-song, H. Guo-qiu, L. Bing, F. Song-jie, Z. Min-hao, "Microstructure-based analysis of fatigue behaviour of Al-Si-Mg alloy." Transactions of Nonferrous Metals. Soc. China. Volume 21, 2011 pages 443-448.

[4] K. Fukui, M. Takeda, and T. Endo, "Morphology and thermal stability of metastable precipitates formed in an Al–Mg–Si ternary alloy aged at 403K to 483K." Materials Letters Volume 59, 2005 pages 1444-1448.

[5] K. Matsuda, S. Ikeno, T. Satob, Y. Uetani, "New quaternary grain boundary precipitate in Al–Mg–Si alloy containing silver." Scripta Materialia. Volume 55, 2006, pages 127-129.

[6] K.E Knipling, R.A. Karnesky, C.P. Lee, D.C. Dunand, D.N. Seidman, "Precipitation evolution in Al–0.1Sc, Al–0.1Zr and Al–0.1Sc–0.1Zr (at.%) alloys during isochronal aging." Acta Materialia. Volume 58, 2010, pages 5184-5195.

[7] K. Banizd, "Dislocation Structures caused by Plastic Deformations in an Aged AI-Mg-Si Alloy." Journal of Materials Science and Engineering. Volume 41, 1979, pages 17-24.

[8] L. Wang, H. Choi, J.M. Myoung, W. Lee, ‘Mechanical alloying of multi-walled carbon nanotubes and aluminium powders for the preparation of carbon/metal composites’. Carbon, Volume 47, Issue 15, December 2009, Pages 3427-3433.

[9] R.B Srinivasa, A. Agarwal, "An analysis of the factors affecting strengthening in carbon nanotube reinforced aluminum composites." Carbon. Volume 49, 2011, pages 533-544.

[10] N. Al-Aqeeli, G. Mendoza-Suarez, C. Suryanarayana, R.A.L. Drew, ‘Development of new Al-based nanocomposites by mechanical alloying’. Materials Science and Engineering: A, Volume 480, Issues 1-2, 15 May 2008, Pages 392-396.

[11] T.W. Clyne, P.J. Withers, ‘An Introduction to Metal Matrix Composites’, Cambridge University Press, Cambridge, UK, 1995.

[12] N. Chawla, K.K. Chawla, ‘Metal Matrix Composites’, Springer, 2005.

[13] K.U. Kainer, ‘Metal Matrix Composites: Custom-made Materials for Automotive and Aerospace Engineering’, Wiley-VCH, 2006.

[14] J. B. Fogagnolo, F. Velasco, M. H. Robert, J. M. Torralba, ‘Effect of mechanical alloying on the morphology, microstructure and properties of aluminium matrix composite powders’. Materials Science and Engineering A, Volume 342, Issues 1-2, 15 February 2003, Pages 131-143.

[15] S. Iijima, "Helical microtubules of graphitic carbon " Nature. Volume 354, 1991, pages 56-58.

[16] S. Iijima, T. Ichihashi, "Single-shell carbon nanotubes of 1-nm diameter" Journal of Nature. Volume 363, 1993, pages 603-605.

[17] V.N Popov, "Carbon nanotubes: properties and application " Journal of Materials Science and Engineering: R 434(3), 2004, pages 61-102.

[18] A.M.K. Esawi, K. Morsi, A. Sayed, M. Taher, S. Lanka, 'Effect of carbon nanotube (CNT) content on the mechanical properties of CNT-reinforced aluminium composites'. Composites Science and Technology, Volume 70, Issue 16, 31 December 2010, Pages 2237-2241.

[19] C.F Deng, D.Z. Wang, X.X. Zhang, A.B. Li, "Processing and properties of carbon nanotubes reinforced aluminum composites." Journal of Materials Science and Engineering: A. colume 444(1-2), 2007 pages 138-145.

[20] P.J.F Harris, "Carbon nanotube composites" International Materials Reviews, volume 49(1), 2004 pages 31-43.

[21] A.M.K. Esawi, K. Morsi, A. Sayed, M. Taher, S. Lanka, 'The influence of carbon nanotube (CNT) morphology and diameter on the processing and properties of CNT-reinforced aluminium composites'. Composites Part A: Applied Science and Manufacturing, Volume 42, Issue 3, March 2011, Pages 234-243.

[22] E.T Thostensona, Z. Renb, T.-W. Choua, "Advances in the science and technology of carbon nanotubes and their composites: a review " Composites Science and Technology. Volume 61, 2001, pages 1899-1912.

[23] A. Esawi, K. Morsi, 'Dispersion of carbon nanotubes (CNTs) in aluminum powder'. Composites Part A: Applied Science and Manufacturing, Volume 38, Issue 2, February 2007, Pages 646-650.

[24] R. Pérez-Bustamante, F. Pérez-Bustamante, I. Estrada-Guel, C.R. Santillán-Rodríguez, J.A. Matutes-Aquino, J.M. Herrera-Ramírez, M. Miki-Yoshida, R.

Martínez-Sánchez, "Characterization of Al2024-CNTs composites produced by mechanical alloying " Powder Technology. Online available, 2011.

[25] He, C., N. Zhao, C. Shi, X. Du, J. Li, H. Li, Q. Cui, "An Approach to Obtaining Homogeneously Dispersed Carbon Nanotubes in Al Powders for Preparing Reinforced Al-Matrix Composites " Journal of Advanced Materials. Volume 19, 2007 pages 1128-1132.

[26] M.S.S Saravanan, K. Sivaprasad, S.P.K. Babu, "Dispersion and Thermal Analysis of Carbon Nanotube Reinforced AA 4032 Alloy Produced by High Energy Ball Milling", Society for Experimental Mechanics. Volume 35(3), 2011, pages 1-5.

[27] H. Ahamed, V. Senthilkumar, "Role of nano-size reinforcement and milling on the synthesis of nano-crystalline aluminium alloy composites by mechanical alloying", Journal of Alloys and Compounds. Volume 505, 2010, pages 772-782.

[28] J. Liao, M.-J. Tan, "Mixing of carbon nanotubes (CNTs) and aluminum powder for powder metallurgy use." Journal of Powder Technology. Volume 208, 2011, pages 42-48.

[29] A.M.K Esawi, K. Morsi, A. Sayed, A.A. Gawad, P. Borah, "Fabrication and properties of dispersed carbon nanotube–aluminum composites." Journal of Materials Science and Engineering: A. volume 508(1-2), 2009, pages 167-173.

[30] S.R Bakshi, V. Singh, S. Seal, A. Agarwal, "Aluminum composite reinforced with multiwalled carbon nanotubes from plasma spraying of spray dried powders." Journal of Surface and Coatings Technology. volume 203(10-11), 2009, pages 1544-1554.

[31] Y.J Jeong, S.I. Cha, K.T. Kim, K.H. Lee, C.B. Mo, S.H. Hong, "Synergistic Strengthening Effect of Ultrafine-Grained Metals Reinforced with Carbon Nanotubes." Small. Volume 3(5), 2007, pages 840-844.

[32] H. Choi, J. Shin, and B. Min, "Reinforcing effects of carbon nanotubes in structural aluminum matrix nanocomposites." Journal of Materials Research., volume 24(8), 2009, pages 2610-2616.

[33] S.I Cha, K.T. Kim, S.N. Arshad, C.B. Mo, K.H. Lee, S.H. Hong, "Field-Emission Behavior of a Carbon-Nanotube-Implanted Co Nanocomposite Fabricated from Pearl-Necklace-Structured Carbon Nanotube/Co Powders." Journal of Advanced Materials, volume 18, 2006, pages 533-558.

[34] S.I Cha, K.T. Kim, S.N. Arshad, C.B. Mo, S.H. Hong, "Extraordinary strengthening effect of carbon nanotubes in metal-matrix nanocomposites processed by molecular-level mixing." Journal of Advanced Materials, volume 17, 2005, pages 1377-1381.

[35] B. Abbasipour, B. Niroumand, And S.M.M. Vaghefi, "Compocasting of A356-CNT composite", Transactions of Nonferrous Metals. Soc., volume 20, 2010, pages 1561-1566.

[36] N. Zhao, P. Nash, X. Yang, 'The effect of mechanical alloying on SiC distribution and the properties of 6061 aluminum composite'. Journal of Materials Processing Technology, Volume 170, Issue 3, 30 December 2005, Pages 586-592.

[37] J. Paras, D. Kapoor, C. Haines, S. Bartolucci, T. Zahrah, U.S. Army ARDEC, Matsys Inc., 'Effect of Powder Processing on Aluminum Carbon Nanotube

Composite Consolidation'. Nanotube Reinforced Metal Matrix Composites II: Processing of Nanotube Reinforced MMCs I. Houston, Texas, 2010.

[38] S. Kamrani, A. Simchi, R. Riedel, S. S. Reihani,'Effect of reinforcement volume fraction on mechanical alloying of Al–SiC nanocomposite powders'. Powder Metallurgy, Volume 50, Number 3, September 2007, pp. 276-282(7).

[39] Y. Saberi, S.M. Zebarjad, G.H. Akbari, 'On the role of nano-size SiC on lattice strain and grain size of Al/SiC nanocomposite', Journal of Alloys and Compounds, Volume 484, Issues 1-2, 18 September 2009, Pages 637-640.

[40] Y. Yang, J. Lan, X. Li, 'Study on bulk aluminum matrix nano-composite fabricated by ultrasonic dispersion of nano-sized SiC particles in molten aluminum alloy'. Materials Science and Engineering A, Volume 380, Issues 1-2, 25 August 2004, Pages 378-383.

[41] K. D. Woo, D. L. Zhang, 'Fabrication of Al–7wt%Si–0.4wt%Mg/SiC nanocomposite powders and bulk nanocomposites by high energy ball milling and powder metallurgy'. Current Applied Physics, Volume 4, Issues 2-4, April 2004, Pages 175-178.

[42] A. Simchi, D. Godlinski, 'Effect of SiC particles on the laser sintering of Al–7Si–0.3Mg alloy'. Scripta Materialia, Volume 59, Issue 2, July 2008, Pages 199-202.

[43] G. S. Upadhyaya, 'Some issues in sintering science and technology', Materials Chemistry and Physics, Volume 67, Issues 1-3, 15 January 2001, Pages 1-5.

[44] C. D. Turner, M. F. Ashby, 'The cold isostatic pressing of composite powders—I. Experimental investigations using model powders'. Journal of Acta Materialia, Volume 44, Issue 11, November 1996, Pages 4521-4530.

[45] M. Oghbaei, O. Mirzaee, “Microwave versus conventional sintering: A review of fundamentals, advantages and applications”, Journal of Alloys and Compounds, Volume 494, Issues 1-2, 2 April 2010, Pages 175-189.

[46] R.M. Govindarajan, N. Aravas, ‘Deformation processing of metal powders: Part I—Cold isostatic pressing’, International Journal of Mechanical Sciences, Volume 36, Issue 4, April 1994, Pages 343-357.

[47] C. Musa, R. Licheri, A. M. Locci, R.Orrù, G. Cao, M. A. Rodriguez, L. Jaworska , ‘Energy efficiency during conventional and novel sintering processes: the case of Ti–Al2O3–TiC composites’ . Journal of Cleaner Production, Volume 17, Issue 9, June 2009, Pages 877-882.

[48] C. Deng, X. Zhang, Y. Ma, D. Wang, ‘Fabrication of aluminum matrix composite reinforced with carbon nanotubes’. Rare Metals, Volume 26, Issue 5, October 2007, Pages 450-455.

[49] J. Liao, M.J. Tan, I. Sridhar, L. Yu., ‘Novel Carbon Nanotube Reinforced Aluminum Nanocomposite Assisted by Polymer-binder’. Nanotube Reinforced Metal Matrix Composites II: Processing of Nanotube Reinforced MMCs I. Houston, Texas, 2010.

[50] J. Lipecka, M. Andrzejczuk, M. Lewandowska, J. Janczak-Rusch, K. J. Kurzydłowski, ‘Evaluation of thermal stability of ultrafine grained aluminium matrix composites reinforced with carbon nanotubes’, Composites Science and Technology, Volume 71, Issue 16, 14 November 2011, Pages 1881-1885.

[51] J. K. Rana, D. Sivaprahasam, K. Seetharama Raju, V. Subramanya Sarma, ‘Microstructure and mechanical properties of nanocrystalline high strength Al–

Mg–Si (AA6061) alloy by high energy ball milling and spark plasma sintering'. Materials Science and Engineering: A, Volume 527, Issues 1-2, 15 December 2009, Pages 292-296.

[52] H. Kwon, M. Estili, K. Takagi, T. Miyazaki, A.Kawasaki, 'Combination of hot extrusion and spark plasma sintering for producing carbon nanotube reinforced aluminum matrix composites'. Carbon, Volume 47, Issue 3, March 2009, Pages 570-577.

[53] H. Kwon, A. Kawasaki, 'Extrusion of Spark Plasma Sintered Aluminum-Carbon Nanotube Composites at Various Sintering Temperatures'. Journal of Nanoscience and Nanotechnology, Volume 9, Number 11, November 2009, pages 6542-6548.

[54] P.S Gilman, J.S Benjamin - Annual review of materials science, - Annual Reviews, 1998.

[55] C. Suryanarayana, E. Ivanov, V. V. Boldyrev, 'The science and technology of mechanical alloying'. Materials Science and Engineering A, Volumes 304-306, 31 May 2001, Pages 151-158.

[56] C. Suryanarayana, 'Mechanical alloying and Milling'. Progress in Materials Science, Volume 46, Issues 1-2, January 2001, Pages 1-184.

[57] S. Scudino, M. Sakaliyska, K.B. Surreddi, J. Eckert, 'Mechanical alloying and milling of Al–Mg alloys', Journal of Alloys and Compounds, Volume 483, Issues 1-2, 26 August 2009, Pages 2-7.

[58] D.L. Zhang, 'Processing of advanced materials using high-energy mechanical milling'. Progress in Materials Science, Volume 49, Issues 3-4, 2004, Pages 537-560.

[59] A Calka, A.P Radlinski, 'Universal high performance ball-milling device and its application for mechanical alloying', Materials Science and Engineering: A, Volume 134, 25 March 1991, Pages 1350-1353.

[60] L Lü, M.O Lai –'Mechanical Alloying' textbook, by Kluwer Academic Publishers, 1998.

[61] N. Al-Aqeeli, G. Mendoza-Suarez, A. Labrie, R.A.L. Drew. 'Phase evolution of Mg–Al–Zr nanophase alloys prepared by mechanical alloying', Journal of Alloys and Compounds, Volume 400, Issues 1-2, 1 September 2005, Pages 96-99.

[62] S.G Epstein, J.G Kaufman –'Aluminum and its alloys', Mechanical Engineers' handbook, 1998.

[63] J.R. Davis, J. R. Davis & Associates 'Aluminum and aluminum alloys' ASM International. Handbook Committee, 1993.

[64] J. U. Ejiofor, R. G. Reddy, 'Characterization of pressure-assisted sintered Al–Si composites'. Materials Science and Engineering A, Volume 259, Issue 2, 31 January 1999, Pages 314-323.

[65] G. A. Edwards, K. Stiller, G. L. Dunlop, M. J. Couper, 'The precipitation sequence in Al–Mg–Si alloys'. Acta Materialia, Volume 46, Issue 11, 1 July 1998, Pages 3893-3904.

[66] M. Cai, D. P. Field, G. W. Lorimer, 'A systematic comparison of static and dynamic ageing of two Al–Mg–Si alloys'. Materials Science and Engineering A, Volume 373, Issues 1-2, 25 May 2004, Pages 65-71.

[67] E.M. Ruiz-Navas, J.B. Fogagnolo, F. Velasco, J.M. Ruiz-Prieto, L. Froyen, 'One step production of aluminium matrix composite powders by mechanical alloying'.

Composites Part A: Applied Science and Manufacturing, Volume 37, Issue 11, November 2006, Pages 2114-2120.

[68] J. B. Fogagnolo, M. H. Robert, E. M. Ruiz-Navas and J. M. Torralba, '6061 Al reinforced with zirconium diboride particles processed by conventional powder metallurgy and mechanical alloying', Journal of Materials, 2004 – Springer.

[69] J. B. Fogagnolo, E. M. Ruiz-Navas, M. H. Robert, J. M. Torralba, '6061 Al reinforced with silicon nitride particles processed by mechanical milling'. Scripta Materialia, Volume 47, Issue 4, 20 August 2002, Pages 243-248.

[70] H. S. Lee, J. S. Yeo, S. H. Hong, D. J. Yoon, K. H. Na, 'The fabrication process and mechanical properties of SiCp/Al–Si metal matrix composites for automobile air-conditioner compressor pistons'. Journal of Materials Processing Technology, Volume 113, Issues 1-3, 15 June 2001, Pages 202-208.

[71] G. E. Kiourtsidis, Stefanos M. Skolianos, George A. Litsardakis, 'Aging response of aluminium alloy 2024/silicon carbide particles (SiCp) composites'. Materials Science and Engineering A, Volume 382, Issues 1-2, 25 September 2004, Pages 351-361.

[72] S.J. Hong, H.M. Kim, D. Huh, C. Suryanarayana, B. S. Chun, 'Effect of clustering on the mechanical properties of SiC particulate-reinforced aluminum alloy 2024 metal matrix composites'. Materials Science and Engineering A, Volume 347, Issues 1-2, 25 April 2003, Pages 198-204.

[73] A.K.Tak Lau, D. Hui, 'The revolutionary creation of new advanced materials—carbon nanotube composites', Composites Part B: Engineering, Volume 33, Issue 4, June 2002, Pages 263-277.

[74] J. Robertson, 'Realistic applications of CNTs'. Materials Today, Volume 7, Issue 10, October 2004, Pages 46-52.

[75] R. George, K.T. Kashyap, R. Rahul, S. Yamdagni, 'Strengthening in carbon nanotube/aluminium (CNT/Al) composites', Scripta Materialia, Volume 53, Issue 10, November 2005, Pages 1159-1163.

[76] L. Suk-Joong Kang, 'Sintering: densification, grain growth, and microstructure' textbook, 1 review, 2005.

[77] J.R. Groza, C. Suryanarayana, (ed), 'Powder Consolidation in Non-equilibrium Processing of Materials', Pergamon, Oxford, UK, 1999, pp. 345-372.

[78] J.R. Groza, 'Nanocrystalline Powder Consolidation Methods in Nanostructured Materials', Second ed., ed. C.C. Koch, William Andrew Publishing, Norwich, NY, 2007, pp. 173-233.

[79] C. Suryanarayana, T. Klassen, E. Ivanov, "Synthesis of Nanocomposites and Amorphous Alloys by Mechanical Alloying", Journal of Material Science, volume 46 (2011) pp6301-6315.

[80] J. R. Groza, A. Zavaliangos, 'Sintering activation by external electrical field'. Materials Science and Engineering A, Volume 287, Issue 2, 15 August 2000, Pages 171-177.

[81] M. Belmonte, J. González-Julián, P. Miranzo, M.I. Osendi, 'Spark plasma sintering: A powerful tool to develop new silicon nitride-based materials'. Journal of the European Ceramic Society, Volume 30, Issue 14, October 2010, Pages 2937-2946.

[82] T. Schubert, J. Schmidt, T. Weißgärber, B. Kieback, 'Spark plasma sintering and hot extrusion of aluminium alloy powder'. International Powder Metallurgy Congress and Exhibition (EURO PM), 12.-14.10.2009, Copenhagen, Denmark Shrewsbury: EPMA, 2009, pp.363-368.

[83] J. Z Liao, M.J Tan, I. Sridha, 'Spark plasma sintered multi-wall carbon nanotube reinforced aluminum matrix composites', Materials & Design, Volume 31, Supplement 1, June 2010, Pages S96-S100.

[84] Y. Shunsuke, K. Hokuto , S. Hiroki, M. Yutaka , K. Masaki, T. Takayuki. 'Fabrication and Thermal Evaluation of Carbon Nanotube/Aluminium composite by Spark Plasma Sintering Method'. Journal of the Japan Society of Powder and Powder Metallurgy Volume 53 issue: 12, 2006 pages 965-970.

[85] C. Suryanarayana, M. Grant Norton, 'X-Ray Diffraction: A Practical Approach', Plenum Press, New York, 1998.

[86] Z. Razavi Hesabi, A. Simchi, S.M. Seyed Reihani, 'effect of nanoscaled reinforcement particles on the structural evolution of aluminum powder during mechanical milling', powder metallurgy, vol 50, 2009, pages 151-157.

[87] K.S. Foo, W.M. Banks, A.J. Craven, A. Hendry, 'Interface characterization of an SiC particulate/6061 aluminium alloy composite', Composites, Volume 25, Issue 7, 1994, Pages 677-683.

[88] T. Schubert, J. Schmidt, T. Weißgärber, B. Kieback, Spark Plasma Sintering and hot extrusion of Aluminum alloy', Euro PM 2009-Non-ferrous materials-Processing.

[89] M Sherif El-Eskandarany, ‘Mechanical solid state mixing for synthesizing of SiC_p/Al-nanocomposites ‘Journal of Alloys and Compounds, Volume 279, Issue 2, 2 October 1998,Pages263-271.

[90] D. Poirier, R. Gauvin, R. A.L. Drew,’Structural characterization of a mechanically milled carbon nanotube/aluminum mixture’, Composites Part A: Applied Science and Manufacturing, Volume 40, Issue 9, September 2009, Pages 1482-1489.

VITA

NAME:	Kachalla Abdullahi Gujba
DATE OF BIRTH:	31, March 1983
PLACE OF BIRTH:	Maiduguri, Nigeria.
EMAIL:	a_gujba@yahoo.com
EDUCATIONAL QUALIFICATIONS:	**M. Sc.** ***(Mechanical Engineering)*** ***Specializing in Materials and Manufacturing*** March, 2012 King Fahd University of Petroleum and Minerals, Dhahran, Saudi Arabia. **B. Eng** ***(Mechanical Engineering)*** February, 2008 Bayero University, Kano State. Nigeria.